PROCEEDINGS OF ICSF-1

FIRST INTERNATIONAL CONFERENCE ON SCOUR OF FOUNDATIONS

NOVEMBER 17-20, 2002
TEXAS A&M UNIVERSITY
COLLEGE STATION, TEXAS, USA

SPONSORED BY
Main Sponsors:
International Society for Soil Mechanics and Geotechnical Engineering
Texas Transportation Institute

Gold Level Sponsors:
Federal Highway Administration
National Science Foundation

Silver Level Sponsors:
ADSC, The International Association of Foundation Drilling
American Society of Civil Engineers (ASCE)
Coasts, Oceans, Ports, and Rivers Institute of ASCE
Environmental & Water Resources Institute of ASCE
Geo-Institute of ASCE
Structural Engineering Institute of ASCE
Texas A&M University Department of Civil Engineering
Transportation Research Board (TRB)

ADDITIONAL COPIES OF THIS BOOK CAN BE OBTAINED FROM

Texas Transportation Institute
Publications Dept.
Tel: (979) 845-4853
Fax: (979) 862-3703
Email: sales@ttimail.tamu.edu
Internet: http://tti.tamu.edu/product/

CONFERENCE COMMITTEES

Chairman of the Conference: Jean-Louis Briaud
Vice-Chairman of the Conference: Hamn-Ching Chen
Editors of the Proceedings: Hamn-Ching Chen and Jean-Louis Briaud

National Advisory Committee:

George Annandale, Larry Arneson, Jean-Louis Briaud, Hamn-Ching Chen, Tom Dahl, Stan Davis, Jerry DiMaggio, Dave Froelich, Daryl Greer, Larry Harrison, Robert Henthorne, Carlton Ho, Rollin Hotchkiss, Beatrice Hunt, Peggy Johnson, Sterling Jones, Ed Kent, Peter Lagasse, Melinda Luna, Shawn McClemore, William Moore, Jorge E. Pagan-Ortiz, Gary Parker, Art Parola, Richard Phillips, Everett Richardson, Max Sheppard, Peter Smith, Steve Smith, David Stolpa, Phil Thompson, Mehmet Tumay

International Advisory Committee:

Laila Abed, Marco Falcon Ascanio, A. (Tony) Bracegirdle, Jean-Louis Briaud, Yee-Meng Chiew, Michael Heibaum, Sangseom Jeong, Hellgi Johannesson, Sterling Jones, Soo-Sam Kim, Boleslaw A. Klosinski, Raul A. Lopardo, Bruce Melville, Zlatko Mihalinec, Yahia E-A. Mohamedzein, Gaton Laporte Molina, A.V.S.R. Murty, Jorge E. Pagan-Ortiz, L. Rakoczi, Everett V. Richardson, A.M.M. Saffiullah, Makoto Shimamura, Testsuro Tsujimoto, Dirceu de Alencar Velloso, Narimantas Zdankus

Organizing Committee:

Michelle Benoit, Jamie Blakeney, Jean-Louis Briaud, Hamn-Ching Chen, Billy Edge, Richard Gehle, Harlow Landphair, Ya Li, Kathy Montemayor, Prahoro Nurtjahyo, Tobey Nutt, Josh Reinbolt, Susan Robertson, Jun Wang

Technical Program Committee:

Jean-Louis Briaud, Hamn-Ching Chen, Michael Heibaum, Bruce Melville, Jorge Pagan, Art Parola, Everett Richardson, Stephen Wright

Prediction Event Committee:

Jean-Louis Briaud, Kuang-An Chang, Hamn-Ching Chen, Jerry DiMaggio, Al DiMillio, Sterling Jones, Ya Li, Dave Mueller, Jorge Pagan, Jun Wang

PREFACE

Texas A&M University
September 16, 2002

Many people have contributed to making this conference a success. The teamwork that led to this event and to the proceedings will remain a very bright moment in my career. I would like to single out one person however for his tremendous contribution to this conference. Thank you Professor Chen for being such a great teammate and for your very demanding role as the main person responsible for the proceedings. You are definitely the MVP of this conference. I would also like to thank the reviewers for taking the time to review a large number of manuscripts in a relatively short period of time: Brian Barkdoll, Liang Cheng, Yee-Meng Chiew, Chen Onn Chin, Sung-Uk Choi, Keith E. Dennett, Duowen Ding, Robert Ettema, Oktay Guven, Willi H. Hager, Faruque Mia, Michael H. Heibaum, Sangseom Jeong, Yafei Jia, Peggy A. Johnson, J. Sterling Jones, Paul Kirshen, Peter Lagasse, Ya Li, Siow-Yong Lim, Richard May, Bruce Melville, David S. Mueller, Tatsuaki Nakato, Prahoro Nurtjahyo, Kunihiro Ogihara, Michael W. O'Neill, James D. Schall, D. Max Sheppard, Makoto Shimamura, Nels J. Sultan, B.Mutlu Sumer, Jun Wang. Richard Gehle and Josh Reinbolt were very helpful in assembling the proceedings electronically and in the details of the conference organization.

Our sponsors were numerous and very helpful: The International Society for Soil Mechanics and Geotechnical Engineering (Kenji Ishihara, William Van Impe), The Texas Transportation Institute (Herbert Richardson, Dennis Christiansen), The Federal Highway Administration (Sterling Jones, Al DiMillio, Jorge Pagan, Jerry DiMaggio), The National Science Foundation (Cliff Astill, Rick Fragaszy), ADSC: The International Association of Foundation Drilling (Scot Litke), American Society of Civil Engineers (ASCE), The Geo-Institute of ASCE (Carol Bowers, Gail Sor), The Environmental & Water Resources Institute of ASCE (Bryan Parsons), The Coasts, Oceans, Ports, and Rivers Institute of ASCE (Patricia Brown), The Structural Engineering Institute of ASCE (Jim Rossberg), The Transportation Research Board: TRB (Jay Jayaprakash), Texas A&M University Department of Civil Engineering (John Niedzwecki).

And then there was all the help from the various committees: International Advisory Committee, National Advisory Committee, Technical Program Committee, Prediction Event Committee, Organizing Committee. You can find the complete list of committee members within the previous page.

The Prediction Event was also a major undertaking. The Federal Highway Administration and the Texas A&M University Department of Civil Engineering were the two main sponsors with help from the USGS and several DOTs: many thanks to Sterling Jones, Dave Mueller, K. Van Wilson, Paul H. Rydlund, Richard J. Huizinga. At Texas A&M University, the flume tests were performed by Ya Li and Jun Wang with the cooperation of John Reed and Bob Randall.

I also wish to thank my wife Janet who was such a great support during all the time spent on the preparation of this conference.

Jean-Louis Briaud

Chairman of ICSF-1

First International Conference on Scour of Foundations ICSF-1
Texas A&M University, November 17 –20, 2002

Final Program

SUNDAY, NOVEMBER 17, 2002

9:00 a.m.-12:00 Noon	**ISSMGE TC-33 – Geotechnics of Soil Erosion Committee Meeting**
12:00 Noon-1:30 p.m.	**Lunch** – on your own
1:30 p.m.-3:00 p.m.	**Short Course:** Scour of Foundations **Organizers:** *J. E. Pagan*, (USA); S. Jones (USA); *J-L. Briaud*, (USA)
3:00 p.m.-3:30 p.m.	**Break**
3:30 p.m.-5:00 p.m.	**Short Course:** Scour of Foundations **Organizers:** *J. E. Pagan*, (USA); S. Jones (USA); *J-L. Briaud*, (USA)
5:30 p.m.-8:00 p.m.	**Reception in the Exhibits Hall - Registration**

MONDAY, NOVEMBER 18, 2002

7:00 a.m.-8:00 a.m.	**Breakfast and Registration in Exhibits Hall**
8:00 a.m.-8:30 a.m.	**WELCOME – Grand Ballroom** H. H. Richardson, Director, Texas Transportation Institute J. M. Niedzwecki, Head, Department of Civil Engineering J-L. Briaud, Chairman, ICSF-1, Acknowledgements
8:30 a.m.-10:00 a.m.	**SESSION (1): PLENARY SESSION I – Grand ballroom** **Session Chairs:** M. Tumay, P. Smith. **Invited Lecture 1.1:** *Scour Protection and Repair by Filtering Geosynthetic Containers.* M. H. Heibaum (Germany). **Invited Lecture 1.2:** Numerical Simulation of Scour Around Complex Piers in Cohesive Soil. *H-C. Chen* (USA). **Invited Lecture 1.3:** Unconventional Interpretation of Local Scour Downstream a Large Dam Stilling Basin. R. A. Lopardo (Argentina), J. M. Casado, M. C. Lopardo.
10:00 a.m.-10:30 a.m.	**Break in the Exhibits Hall**
10:30 a.m.-12:00 Noon	**Concurrent Sessions**
	SESSION (2): SCOUR PREDICTIONS I – Ballroom 1 **Session Chairs:** J. Audibert, C. Weber. **Invited Lecture 2.1:** *Indirect Methods of Measuring Shear Stress in the Bottom of a Scour Hole*. J. S. Jones (USA). **Presentation 2.2:** Shear Stress Approach to Pier Scour Predictions. Y. Li (USA), J-L. Briaud, H-C. Chen, P. Nurtjahyo, J. Wang. **Presentation 2.3:** A Review of Predictive Methods for General Scour. R. Bettess (UK). **Presentation 2.4:** Prediction of Local Scour Below Offshore Pipelines – A Review. L. Cheng (Australia). **Presentation 2.5:** Comparison of General Scour Prediction Equations for River Crossings. C. Lauchlan (UK), R. May.

SESSION (3): SCOUR MEASUREMENTS I – Ballroom 2
Session Chairs: C. Monk, N. Jaynes.
Invited Lecture 3.1*:* Local Scour Around Structures in Tidal Flows. R. W. P. May (UK), M. Escarameia.
Presentation 3.2*:* Movement of Bridge Pier by Water Flow Under Flood Condition. K. Ogihara (Japan), H. Muraishi, S. Masahiko, D. Nakajima.
Presentation 3.3: 3-Dimensional Measured and Simulated Flow for Scour Near Spur Dikes. R. Kuhnle (USA), Y. Jia, C. Alonso.
Presentation 3.4: Scour Experiments on Dike Angle, Porosity, and Hook for a Thin Dike. E. Martinez (USA), R. Ettema, A. Lachhab.
Presentation 3.5: Shallow Water Effect on Pier Scour in Clays. Y. Li (USA), J-L. Briaud, H-C. Chen, P. Nurtjahyo, J. Wang.

12:00 Noon-1:30 p.m. **Lunch** – **Oakwood Ballroom** (provided)

1:30 p.m.-3:00 p.m. **Concurrent Sessions**

SESSION (4): SCOUR PREDICTIONS II – Ballroom 1
Session Chairs: P. D'Odorico, D. Stolpa.
Invited Lecture 4.1: *Effect of Suspended Fine Sediment on Local Scour.* M. Sheppard (USA).
Presentation 4.2: *Numerical Simulations of 3-D Flows Around Bridge Piers.* S-U. Choi (Korea), W. Yang.
Presentation 4.3: *3-D Numerical Model for Wave-Induced Dynamic Behavior of Sand Beds at Bridge Piers*. F. Mia (Japan), H. Nago, S. Maeno.
Presentation 4.4: *Pier Scour at Woodrow Wilson Bridge and SRICOS Method.* K. Kwak (Korea), J-L. Briaud, Y. Cao, M-K. Chung, B. Hunt, S. Davis.
Presentation 4.5: *Bed Shear Stress Around Rectangular Pier: Numerical Approach*. P. Nurtjahyo (USA) H-C. Chen, J-L. Briaud, Y. Li, J. Wang.

SESSION (5): SCOUR MEASUREMENTS II – Ballroom 2
Session Chairs: W. Edge, R. Melek.
Invited Lecture 5.1: *Flume Experiments on Abutment Scour: Confronting Complexities in Process and Similitude.* R. Ettema (USA).
Presentation 5.2: *Scouring Downstream of Sluice Gate*. S-Y. Lim (Singapore), G. Yu.
Presentation 5.3: *Development of the New Inspection Method on Scour Condition Around Existing Bridge Foundations.* J. Fukui (Japan), M. Otuka.
Presentation 5.4: *Experimental Study on Toe Scour of Seawall Covered with Armor Units Due to Waves*. T. Sakakiyama (Japan), R. Kajima.
Presentation 5.5: *Scour Around Rubble-Mound Breakwater Head of Cheju Outer Port*. H. Kim, (Korea), B. C. Oh, B-S. Jung, S-Z Youn.

3:00 p.m.-3:30 p.m. **Break in the Exhibits Hall**

3:30 p.m.-5:00 p.m. **Concurrent Sessions**

SESSION (6): SCOUR PREDICTIONS III – Ballroom 1
Session Chairs: K. A. Chang, P. Nurtjahyo
Invited Lecture 6.1: *Analysis of Pier Scour Predictions and Real-Time Field Measurements*. D. S. Mueller (USA), C. R. Wagner.
Presentation 6.2: *Future Hydrographs and Scour Risk Analysis.* J-L. Briaud (USA), P. D'Odorico, E. J. Jeon
Presentation 6.3: *Database Program for Highway Bridge-Scour Data.* K. Farrag (USA), M. Morvant.
Presentation 6.4: *Nondimensional Analysis of Clear-Water Scour at Bridge*

Contractions in Cohesive Soils. O. Guven (USA), J. G. Melville, J. E. Curry.
Presentation 6.5: *FE Analysis of Coastal Cliff Erosion due to Ocean Wave Assailing*. K. Yasuhara (Japan), S. Murakami, Y. Kanno, Z. Wu.

SESSION (7): GEOTECHNICAL ASPECTS I - Ballroom 2
Session Chairs: C. Aubeny, X. Long.
Invited Lecture 7.1: *Theoretical and Practice Aspects of Rock Scour Prediction*. G. W. Annandale (USA), E. Bollaert, A. Schleiss.
Presentation 7.2: *Erosion Function Apparatus Overview and Discussion of Influence Factors on Cohesive Soil Erosion Rate in EFA Test*. Y. Cao (USA), J. Wang, J-L. Briaud, H-C. Chen, Y. Li, P. Nurtjahyo.
Presentation 7.3: *Identification of Dispersive Clays in Gaza Strip Area*; *and Filter Effects on Dam Safety*. M. A. Awad (Palestine).
Presentation 7.4: *Effects of Cohesion on Bridge Scour*. A. Molinas (USA), S. J. Jones.
Presentation 7.5: *Scour Around Submarine Pipeline in Clayey Soil.* S. Neelamani (India), A. Vijaya kumar, S. Narasimha Rao.

5:30 p.m.-6:30 p.m. **2001 TERZAGHI LECTURE – Grand Ballroom**
Session Chairs: P. Jeanjean, A. Niederoda.
Geotechnical Solutions for the Offshore: Synergy of Research and Practice S. Lacasse, (Norway)

7:00 p.m.-9:00 p.m. **Reception in the new Texas A&M University Hydraulic Laboratory**
(Buses leave every 10 minutes starting at 6:45 p.m.)

7:00 p.m.-10:00 p.m. **Committee Meetings – Mockingbird rooms**

TUESDAY, NOVEMBER 19, 2002

7:00 a.m.-8:00 a.m. **Breakfast and Registration in Exhibits Hall**

8:30 a.m.-10:00 a.m. **SESSION (8): PLENARY SESSION II – Grand Ballroom**
Session Chairs: S. Wright, B. Hunt.
Invited Lecture 8.1: Survey of Bridge Damages Due to a Heavy Rain in Northern Part of Kanto Region, Japan. J. Fukui (Japan), M. Nishitani.
Invited Lecture 8.2: The SRICOS-EFA Method**.** J-L. Briaud (USA).
Invited Lecture 8.3: *Failure Mechanisms of Riprap Layer Around Bridge Piers.* Y-M. Chiew (Singapore).

10:00 a.m.-10:30 a.m. **Break in the Exhibits Hall**

10:30 a.m.-12:00 Noon **Concurrent Sessions**

SESSION (9): COUNTERMEASURES I – Ballroom 1
Session Chairs: H. Landphair, W. Wang.
Invited Lecture 9.1: *Scour Protection Around Gravity Based Structures Using Small Size Rock*. K. J. Bos (Netherlands), H. J. Verheij, G. Kant, A. C. H. Kruisbrink.
Presentation 9.2: *Riprap as Permanent Scour Protection Around Bridge Piers*. C. D. Anglin (Canada), F. Itamunoala, G. Millen.
Presentation 9.3: *Riprap at Rectangular Bridge Piers Under Oblique Incident Flow*. J. A. Sainz (Spain), R. Salgado.
Presentation 9.4: *Countermeasure Construction Using Jet Grouting Methods to Combat Foundation Scour.* D. W. Boehm (USA).

Presentation 9.5: *Field Evaluation and Countermeasure Selection for Scour Critical Bridges in the Commonwealth of Kentucky*. K. J. Schaefer (USA), R. W. Gardner.

SESSION (10): GEOTECHNICAL ASPECTS II – Ballroom 2
Session Chairs: G. Biscontin, H. Hu.
Invited Lecture: 10.1. *GIS-Based Bridge Scour Prioritization.* C. L. Ho (USA), J. M. Di Stasi, P. Rees.
Presentation 10.2: *Erodibility Tests of Shale-Rock Samples Taken from Bridge Pier Construction Site on the Mississippi River.* T. Nakato (USA).
Presentation 10.3: *The Driving Force on Soil Grains and Its Effect on Scouring the Channel of Foundation.* L. Zhang (USA), D. Ding, W. Zhou.
Presentation 10.4: *Depth of Mobile Layer Under Severe Wave Conditions: Liquefaction Effect.* S. Sassa. (Japan).
Presentation 10.5: *Essence of Silt Factor for Scour Calculation Around Bridge Foundation.* R.K. Dhiman,(India), D. K. Mohapatra.

12:00 Noon-1:30 p.m. **Lunch** – **Oakwood Ballroom** (provided)

1:30 p.m.-3:00 p.m. **Concurrent Sessions**

SESSION (11): COUNTERMEASURES II – Ballroom 1
Session Chairs: D. Laefer, J. B. Seo.
Invited Lecture 11.1: *Impact of the Federal Highway Administration's Scour Evaluation Program in the United States of North America's Highway Bridges.* J. E. Pagan-Ortiz (USA).
Presentation 11.2: *Evaluation of Strategies to Control Erosion along U.S. Highway 50 Between Carson City and Lake Tahoe.* K. Dennett (USA), P. Fricthel, R. Siddharthan, A. Soltani.
Presentation 11.3: *Optimisation of Scour Protection Measures.* G. B. H. Spaan (Netherlands), M. H. Lindo, G. Kant.
Presentation 11.4: *Design and Construction of Bridge Scour Countermeasures Along the Salt River, Phoenix, Arizona*. D. L. Richards (USA).
Presentation: 11.5.

SESSION (12): ABUTMENTS AND EMBANKMENTS – Ballroom 2
Session Chairs: T. Dahl, S. Hilbrich.
Invited Lecture 12.1: *Abutment Scour Countermeasures: A Review* .B. Barkdoll (USA), R. Ettema, R. Kuhnle, B. Melville, T. Parchure, A. Parola, C. Alonso.
Presentation 12.2: *Countermeasures for Scour at Spill-Through Bridge Abutments.* B. Melville (New Zealand), S. Coleman, D. Hoe.
Presentation 12.3: *Hugo Reservoir Embankment Depression Study.* J. B. Nevels, Jr. (USA).
Presentation 12.4: *Pier and Abutment Scour-New Laboratory Data.* W. H. Hager (Switzerland), J. Unger, G. Oliveto.
Presentation 12.5: *Flow and Scouring in Main Channel due to Abutments.* G. Yu (Singapore), S-Y. Lim, S-K. Tan.

3:00 p.m.-3:30 p.m. **Break in the Exhibits Hall**

3:30 p.m.-5:00 p.m. **Concurrent Sessions**

SESSION (13): COUNTERMEASURES III – Ballroom 1
Session Chairs: S. Dunlap, X. Zhang.

Invited Lecture 13.1: *Treating Channel Instability at Bridges*. P. A. Johnson (USA).
Presentation 13.2: *Scour Hazard Mitigation for Tick Canyon Wash Bridge.* M. S. Islam (USA), J. Zha, A. Abghari.
Presentation 13.3: *Final Stages of Butte City Bridge Erosion Control Project.* S. K. Mishra (USA), W. B. Lindsey.
Presentation 13.4: Riprap Protection Around Bridge Piers in a Degrading Channel. *Y- M. Chiew* (Singapore).
Presentation 13.5: *Scour at a Submerged Rock Dike, Willapa Bay, Washington.* N. Sultan (USA). R. Phillips, H. Bermudez.

SESSION (14): PIER SCOUR – Ballroom 2
Session Chairs: S. Davis, J. Wang.
Invited Lecture 14.1: *3-D Numerical Modeling of Flow and Scour Around a Pile.* A. Roulund (Denmark), B. M. Sumer, J. Fredsoe, J. Michelsen.
Presentation 14.2: *New Approach to Scour Evaluation of Complex Bridge Piers.* E. V. Richardson (USA), J. S. Jones, D. M. Sheppard.
Presentation 14.3: *Time Rate of Local Scour at a Circular Pile.* W. Miller, Jr. (USA), D. M. Sheppard.
Presentation 14.4: *A Case Study of the Possible Effects of Long-Term Climate Change on Bridge Scour.* P. Kirshen (USA), L. Edgers, J. Edelmann, M. Percher, B. Bettencourt, E. Lewandowski.
Presentation 14.5: *Analysis of Pile Groups Considering Riverbed Scouring.* S. Jeong (Korea), J. Won, J. Suh.

5:30 p.m.-6:30 p.m. — **2002 BUCHANAN LECTURE – Grand Ballroom**
Session Chair: J-L. Briaud.
"The World Trade Center: Construction, Destruction, Reconstruction. A. Aronowitz, (USA)

7:00 p.m.-9:00p.m. — **Reception at the George Bush Presidential Library and Museum**
(Buses leave every 10 minutes starting at 6:45 p.m.)

WEDNESDAY, November 20, 2002

7:00 a.m.-8:00 a.m. — **Breakfast and Registration in Exhibits Hall**

8:30 a.m.-10:00 a.m. — **SESSION (15): PLENARY SESSION III – Grand Ballroom**
Session Chairs: A. Kosicki, H. Johanesson.
Invited Lecture 15.1: On the Challenges of Scour Prediction. G. Hoffmans (Netherlands), H. Verheij.
Invited Lecture 15.2: A Geotechnical Perspective: Design and Construction of Highway Bridge Foundations for Scour. C. E. Dumas (USA), J. Krolack.
Invited Lecture 15.3: Local Scour Depths at Bridge Foundations: New Zealand Methodology. B. Melville (New Zealand).

10:00 a.m.-10:30 a.m. — **Break in the Exhibits Hall**

10:30 a.m.-12:00 Noon — **Concurrent Sessions**

SESSION (16): SCOUR PROBLEMS I – Ballroom 1
Session Chairs: M. Luna, E. McDonald.
Invited Lecture 16.1: *Study on the Disasters of Bridge and Bed Protection Works During the Passage of Typhoon Herb*. C. Lin (Taiwan), T-C. Ho, P-H. Chiu, K-A. Chang.

Presentation 16.2: *Damages of the Roads-Bridges by Erosion and Remedial Measures in Albania*. L. Bozo (Albania), Y. Muceku.
Presentation 16.3: *Bridge Pier Scour in Bouldery Bed – Indian Scenario.* R. Singh (India), K. K. Razdan, R. K. Dhiman.
Presentation 16.4: *Scour Monitoring of Railway Bridge Piers via Inclination Detection.* N. Kobayashi (Japan), S. Kitsunai, M. Shimamura.
Presentation 16.5: *Non-Destructive Testing to Determine Unknown Pile Lengths Under Existing Bridges*. F. Rausche (USA), M. Huessin, M. Bixler.

SESSION (17): SCOUR MONITORING – Ballroom 2
Session Chairs: S. Smith, K. Y. Rhee.
Invited Lecture 17.1: *Instruments to Measure and Monitor Bridge Scour.* E. V. Richardson (USA).
Presentation 17.2: *Development and Implementation of a Scour Monitoring Program for Selected Bridges Crossing the Trukee River.* K. E. Dennett (USA), P. Fritchel, R. Siddharthan, A. Soltani.
Presentation 17.3: *Seismic Methods to Identify Scour Depth Around Deep Bridge Foundations.* E. J. Mercado (USA), E. B. Davies, J. A. McDonald, M. W. O'Neill.
Presentation 17.4: *Portable Scour Monitoring Research.* J. D. Schall (USA), G. R. Price.
Presentation 17.5: *Active Scour Monitor Instrumentation in the California Transportation System*. S. Ng (USA).

12:00 Noon-1:30 p.m. **Lunch** – **Oakwood Ballroom** (provided)

1:30 p.m.-3:00 p.m. **Concurrent Sessions**

SESSION (18): SCOUR PROBLEMS II – Ballroom 1
Session Chairs: R. Whitehouse, H. Shi.
Invited Lecture 18.1: *Determination of Unknown Bridge Foundation Depths with NDE Methods*. L. D. Olson (USA).
Presentation 18.2: *Scour of Railway Embankment Foundation Located on Sea-Cliff in Japan***.** H. Suzuki (Japan), M. Shimamura.
Presentation 18.3: *Design and Construction of Scour Foundations for Electric Power Transmission Line Structures.* P. M. Kandaris (USA), R. E. Kondziolka, J. P. Adams.
Presentation 18.4: *Propeller Induced Scour.* C-O. Chin (Singapore), W. Li.
Presentation 18.5: *Confederation Bridge – New Scour Design Methodology for Complex Materials.* R. B. Nairn (Canada), C. D. Anglin.

SESSION (19): CASE HISTORIES – Ballroom 2
Session Chairs: L. Arneson, Z. Lu.
Invited Lecture 19.1: *A Methodology for Predicting Channel Migration NCHRP Project No. 24-16.* P. Lagasse (USA), W. Spitz, L. Zevenbergen.
Presentation 19.2: *Predicting Meander Migration: Evaluation of Some Existing Techniques*. J-L. Briaud (USA), H-C. Chen, S. Park.
Presentation 19.3: *Collapse and Erosion of Khon Kaen Loess with Treatment Option.* P. Punrattanasin (Thailand), A. Subjarassang, O. Kusakabe, T. Nishimura.
Presentation 19.4: *Analysis of Contraction and Abutment Scour at Two Sites in Minnesota.* C. R. Wagner (USA), D. S. Mueller.
Presentation 19.5: *Factors Affecting Stream and Foundation Stability at Existing Bridges in New Jersey.* S. M. Baig (USA), J. J. Zarriello, M. A. Khan.

3:00 p.m.-3:30 p.m.	**Break in the Exhibits Hall**
3:30 p.m.-4:00 p.m.	**SESSION (20): PREDICTION EVENT – Grand Ballroom** **Session Chairs:** J. Benn, Y. Li. **Presentation: 20.1.** *Results of the FHWA Prediction Event.* J-L. Briaud (USA)
4:00 p.m. – 5:00 p.m.	**SESSION (21): *FUTURE SCOUR NEEDS. PANEL DISCUSSION* – Grand Ballroom** **Moderator:** J-L. Briaud (USA). **Panelists:** B. Melville (New Zealand). S. Jones (USA). J. Fukui (Japan). R. Whitehouse (UK). G. Hoffmans (Netherlands). C. Dumas (USA).
5:00 p.m.-9:00 p.m.	**Closing Ceremony – Reception at Janet and Jean-Louis Briaud's House** (3013 Coronado Drive, College Station, T: 979-693-3969).

TABLE OF CONTENTS

Page

VOLUME I

PLENARY

"Scour Protection and Repair by Filtering Geosynthetic Containers."
M. H. Heibaum **(Invited Lecture)** 1

"Numerical Simulation of Scour Around Complex Piers in Cohesive Soil."
H-C. Chen **(Invited Lecture)** 14

"Unconventional Interpretation of Local Scour Downstream a Large Dam Stilling Basin."
R. A. Lopardo, J. M. Casado, M. C. Lopardo **(Invited Lecture)** 34

"Survey of Bridge Damages Due to a Heavy Rain in Northern Part of Kanto Region, Japan."
J. Fukui, M. Nishitani **(Invited Lecture)** 47

"The SRICOS-EFA Method."
J-L. Briaud **(Invited Lecture)** 57

"Failure Mechanisms of Riprap Layer Around Bridge Piers."
Y- M. Chiew **(Invited Lecture)** 70

"On the Challenges of Scour Prediction."
G. Hoffmans, H. J. Verheij **(Invited Lecture)** 92

"A Geotechnical Perspective: Design and Construction of Highway Bridge Foundations for Scour." C. E. Dumas, J. Krolack **(Invited Lecture)** 112

"Local Scour Depths at Bridge Foundations: New Zealand Methodology."
B. Melville **(Invited Lecture)** 120

SCOUR PREDICTION

"Indirect Methods of Measuring Shear Stress in the Bottom of a Scour Hole."
J. S. Jones **(Invited Lecture)** 140

"Shear Stress Approach to Pier Scour Predictions."
Y. Li, J-L. Briaud, H-C. Chen, P. Nurtjahyo, J. Wang 156

"A Review of Predictive Methods for General Scour."
R. Bettess 162

"Prediction of Local Scour Below Offshore Pipelines – A Review."
L. Cheng 175

"Comparison of General Scour Prediction Equations for River Crossings."
C. Lauchlan, R. W. P. May 184

"Effect of Suspended Fine Sediment on Local Scour."
D. M. Sheppard **(Invited Lecture)** 198

"Numerical Simulations of 3-D Flows Around Bridge Piers."
S-U. Choi, W. Yang 206

"3-D Numerical Model for Wave-Induced Dynamic Behavior of Sand Beds at Bridge Piers."
F. Mia, H. Nago, S. Maeno 218

"Pier Scour at Woodrow Wilson Bridge and SRICOS Method."
K. Kwak, J-L. Briaud, Y. Cao, M-K. Chung, B. Hunt, S. Davis 227

"Bed Shear Stress Around Rectangular Pier: Numerical Approach."
P. Nurtjahyo, H-C. Chen, J-L. Briaud, Y. Li, J. Wang 242

"Analysis of Pier Scour Predictions and Real-Time Field Measurements."
D. S. Mueller, C. R. Wagner **(Invited Lecture)** 257

"Future Hydrographs and Scour Risk Analysis."
J-L. Briaud, P. D'Odorico, E. J. Jeon 272

"Database Program for Highway Bridge-Scour Data."
K. Farrag, M. Morvant 283

"Nondimensional Analysis of Clear-Water Scour at Bridge Contractions in Cohesive Soils."
O. Guven, J. G. Melville, J. E. Curry 292

"FE Analysis of Coastal Cliff Erosion due to Ocean Wave Assailing."
K. Yasuhara, S. Murakami, Y. Kanno, Z. Wu 307

SCOUR MEASUREMENTS

"Local Scour Around Structures in Tidal Flows."
R. W. P. May, M. Escarameia **(Invited Lecture)** 320

"Movement of Bridge Pier by Water Flow Under Flood Condition."
K. Ogihara, H. Muraishi, S. Masahiko, D. Nakajima 337

"3-Dimensional Measured and Simulated Flow for Scour Near Spur Dikes."
R. Kuhnle, Y. Jia, C. Alonso 349

"Scour Experiments on Dike Angle, Porosity, and Hook for a Thin Dike."
E. Martinez, R. Ettema, A. Lachhab 364

"Shallow Water Effect on Pier Scour in Clays."
Y. Li, J-L. Briaud, H-C. Chen, P. Nurtjahyo, J. Wang 373

"Flume Experiments on Abutment Scour: Confronting Complexities in Process and Similitude."
R. Ettema **(Invited Lecture)** 383

"Scouring Downstream of Sluice Gate."
S-Y. Lim, G. Yu 395

"Development of the New Inspection Method on Scour Condition Around Existing Bridge Foundations." J. Fukui, M. Otuka 410

"Experimental Study on Toe Scour of Seawall Covered with Armor Units Due to Waves."
T. Sakakiyama, R. Kajima 421

"Scour Around Rubble-Mound Breakwater Head of Cheju Outer Port."
H. Kim, B. C. Oh, B-S. Jung, S-Z Youn 437

GEOTECHNICAL ASPECTS

"Theoretical and Practice Aspects of Rock Scour Prediction."
G. W. Annandale, E. Bollaert, A. Schleiss **(Invited Lecture)** 449

"Erosion Function Apparatus Overview and Discussion of Influence Factors on Cohesive Soil Erosion Rate in EFA Test."
Y. Cao, J. Wang J-L. Briaud, H-C. Chen, Y. Li, P. Nurtjahyo 459

"Identification of Dispersive Clays in Gaza Strip Area; and Filter Effects on Dam Safety."
M. A. Awad 471

"Effects of Cohesion on Bridge Scour."
A. Molinas, S. J. Jones 485

"Scour Around Submarine Pipeline in Clayey Soil."
S. Neelamani, A. Vijaya kumar, S. Narasimha Rao 500

"GIS-Based Bridge Scour Prioritization."
C. L. Ho, J. M. Di Stasi, P. Rees **(Invited Lecture)** 516

"Erodibility Tests of Shale-Rock Samples Taken from Bridge Pier Construction Site on the Mississippi River." T. Nakato 528

"The Driving Force on Soil Grains and Its Effect on Scouring the Channel of Foundation."
L. Zhang, D. Ding, W. Zhou 540

"Depth of Mobile Layer Under Severe Wave Conditions: Liquefaction Effect."
S. Sassa. 546

"Essence of Silt Factor for Scour Calculation Around Bridge Foundation."
R. K. Dhiman, D. K. Mohapatra 560

VOLUME II

COUNTERMEASURES

"Scour Protection Around Gravity Based Structures Using Small Size Rock."
K. J. Bos, H. J. Verheij, G. Kant, A. C. H. Kruisbrink **(Invited Lecture)** 567

"Riprap as Permanent Scour Protection Around Bridge Piers."
C. D. Anglin, F. Itamunoala, G. Millen 582

"Riprap at Rectangular Bridge Piers Under Oblique Incident Flow."
J. A. Sainz, R. Salgado 597

"Countermeasure Construction Using Jet Grouting Methods to Combat Foundation Scour."
D. W. Boehm 609

"Field Evaluation and Countermeasure Selection for Scour Critical Bridges in the Commonwealth of Kentucky."
K. J. Schaefer, R. W. Gardner 623

"Impact of the Federal Highway Administration's Scour Evaluation Program in the United States of North America's Highway Bridges."
J. E. Pagan-Ortiz **(Invited Lecture)** 636

"Evaluation of Strategies to Control Erosion along U.S. Highway 50 Between Carson City and Lake Tahoe."
K. E. Dennett, P. Fricthel, R. Siddharthan, A. Soltani 642

"Optimisation of Scour Protection Measures."
G. B. H. Spaan, M. H. Lindo, G. Kant 656

"Design and Construction of Bridge Scour Countermeasures Along the Salt River, Phoenix, Arizona." D. L. Richards 670

"Treating Channel Instability at Bridges."
P. A. Johnson **(Invited Lecture)** 678

"Scour Hazard Mitigation for Tick Canyon Wash Bridge."
M. S. Islam, J. Zha, A. Abghari 684

"Final Stages of Butte City Bridge Erosion Control Project."
S. K. Mishra, W. B. Lindsey 699

"Riprap Protection Around Bridge Piers in a Degrading Channel."
Y-M. Chiew 707

"Scour at a Submerged Rock Dike, Willapa Bay, Washington."
N. Sultan, R. Phillips, H. Bermudez 719

ABUTMENTS AND EMBANKMENTS

"Abutment Scour Countermeasures: A Review."
B. Barkdoll, R. Ettema, R. Kuhnle, B. Melville, T. Parchure, A. Parola, C. Alonso
(Invited Lecture) 734

"Countermeasures for Scour at Spill-Through Bridge Abutments."
B. Melville, S. Coleman, D. Hoe 749

"Hugo Reservoir Embankment Depression Study."
J. B. Nevels, Jr. 764

"Pier and Abutment Scour-New Laboratory Data."
W. H. Hager, J. Unger, G. Oliveto 774

"Flow and Scouring in Main Channel due to Abutments."
G. Yu, S-Y. Lim, S-K. Tan 785

PIER SCOUR

"3-D Numerical Modeling of Flow and Scour Around a Pile."
A. Roulund, B. M. Sumer, J. Fredsoe, J. Michelsen **(Invited Lecture)** 795

"New Approach to Scour Evaluation of Complex Bridge Piers."
E. V. Richardson, J. S. Jones, D. M. Sheppard 810

"Time Rate of Local Scour at a Circular Pile."
W. Miller, Jr., D. M. Sheppard 827

"A Case Study of the Possible Effects of Long-Term Climate Change on Bridge Scour."
P. Kirshen, L. Edgers, J. Edelmann, M. Percher, B. Bettencourt, E. Lewandowski 842

"Analysis of Pile Groups Considering Riverbed Scouring."
S. Jeong, J. Won, J. Suh 854

SCOUR PROBLEMS

"Study on the Disasters of Bridge and Bed Protection Works During the Passage of Typhoon Herb." C. Lin, T-C. Ho, P-H. Chiu, K-A. Chang **(Invited Lecture)** 869

"Damages of the Roads-Bridges by Erosion and Remedial Measures in Albania."
L. Bozo, Y. Muceku 884

"Bridge Pier Scour in Bouldery Bed – Indian Scenario."
R. Singh, K. K. Razdan, R. K. Dhiman 896

"Scour Monitoring of Bridge Piers via Inclination Detection."
N. Kobayashi, S. Kitsunai, M. Shimamura 910

"Non-Destructive Testing to Determine Unknown Pile Lengths Under Existing Bridges."
F. Rausche, M. Huessin, M. Bixler 918

"Determination of Unknown Bridge Foundation Depths with NDE Methods."
L. D. Olson **(Invited Lecture)** 929

"Scour of Railway Embankment Foundation Located on Sea-Cliff in Japan."
H. Suzuki, M. Shimamura 945

"Design and Construction of Scour Foundations for Electric Power Transmission Line Structures." P. M. Kandaris, R. E. Kondziolka, J. P. Adams 954

"Propeller Induced Scour."
C-O. Chin, W. Li 968

"Confederation Bridge – New Scour Design Methodology for Complex Materials."
R. B. Nairn, C. D. Anglin 978

SCOUR MONTORING

"Instruments to Measure and Monitor Bridge Scour."
E. V. Richardson **(Invited Lecture)** 993

"Development and Implementation of a Scour Monitoring Program for Selected Bridges Crossing the Trukee River."
K. E. Dennett, P. Fritchel, R. Siddharthan, A. Soltani 1008

"Seismic Methods to Identify Scour Depth Around Deep Bridge Foundations."
E. J. Mercado, E. B. Davies, J. A. McDonald, M. W. O'Neill 1019

"Portable Scour Monitoring Research."
J. D. Schall, G. R. Price 1032

"Active Scour Monitor Instrumentation in the California Transportation System."
S. Ng 1042

CASE HISTORIES

"A Methodology for Predicting Channel Migration NCHRP Project No. 24-16."
P. Lagasse, W. Spitz, L. Zevenbergen **(Invited Lecture)** 1051

"Predicting Meander Migration: Evaluation of Some Existing Techniques."
J-L. Briaud, H-C. Chen, S. Park 1061

"Collapse and Erosion of Khon Kaen Loess with Treatment Option."
P. Punrattanasi, A. Subjarassang, O. Kusakabe, T. Nishimura 1081

"Analysis of Contraction and Abutment Scour at Two Sites in Minnesota."
C. R. Wagner, D. S. Mueller 1096

"Factors Affecting Stream and Foundation Stability at Existing Bridges in New Jersey."
S. M. Baig, J. J. Zarriello, M. A. Khan 1111

VOLUME III
PREDICTION EVENT

PREDICTION REQUEST

"Prediction Request for ICSF-1"
Prediction Event Committee 1127

PREDICTION PAPERS

"Pier Scour Prediction for Mississippi River Bridge / Pier 11 for the 08-03-93 flood event / Bridge Case 7." Guillermo Ferrando, Carlos Cian 1152

"Pier Scour Prediction for Mississippi River Bridge / Pier 17L for the 05-01-91 flood event / Bridge Case 8" Guillermo Ferrando, Carlos Cian 1155

"On the Prediction of the Maximum Depth of a Scour Hole Around Cylindrical Bridge Piers in Non Cohesive Soils" Oscar Link, Ulrich Zanke 1160

"Contribution Prediction Van Oord ACZ" T. Piepers 1166

"Prediction of Local Scour of Non-Cohesive Sediments Around Bridge Piers Using FVM-Based CCHE2D Model" Weiming Wu, Sam S. Y. Wang 1176

"Numerical Simulation of Local Scouring Around a Cylindrical Pier" Yafei Jia, Yichun Xu, Sam S. Y. Wang 1181

FLUME TESTS RESULTS

"Flume Tests Results" Ya Li , Jun Wang, Wei Wang, Jean-Louis Briaud , Hamn-Ching Chen 1188

COMPARISON BETWEEN PREDICTIONS AND MEASUREMENTS

"Comparison Between Predictions and Measurements" Ya Li, Jun Wang, Wei Wang, Jean-Louis Briaud, Hamn-Ching Chen 1208

ICSF-1

First International Conference on Scour of Foundations
November 17-20, 2002
Texas A&M University
College Station, TX 77843-3136, USA

PREDICTION REQUEST

FOR ICSF-1

(http://tti.tamu.edu/conferences/scour/)

Acknowledgements

The committee in charge of this prediction event is composed of:

Briaud, Jean-Louis (Chair)
Chang, Kuang-An
Chen, H.-C.
DiMaggio, Jerry
DiMillio, Al
Jones, Sterling
Li, Ya
Mueller, Dave
Nurtjahyo, Prahoro
Pagan, Jorge
Wang, Jun
Wang, Wei

Many organizations have contributed directly or indirectly to make this prediction event possible. They are all thanked for their support.

Federal Highway Administration
United States Geological Survey
National Science Foundation
Texas Transportation Institute
Texas A&M University Dpt. of Civil Engineering
International Society for Soil Mechanics and Geotechnical Engineering
American Society of Civil Engineers (ASCE)
The Geo-Institute of ASCE
The Environmental & Water Resources Institute of ASCE
The Structural Engineering Institute of ASCE
The Coasts, Oceans, Ports, and Rivers Institute of ASCE

Other individuals have worked diligently with the committee and made significant time contributions. They are thanked for their support.

K. Van Wilson
John Reed
Paul H. Rydlund
Richard J. Huizinga

1. Introduction

A prediction event is being organized at the occasion of the First International Conference on Scour of Foundations (ICSF-1). There are two parts to this prediction request: flume tests prediction (6 cases) and bridge sites prediction (2 bridge sites). You are not required to predict all cases but predictions must be sent in writing according to the enclosed format (Attachment IV) before July 15, 2002. Comparisons between the measurements and the predictions will be presented at the conference and collated in a separate volume available at the conference.

The flume tests prediction includes six cases. These flume tests will be performed during July and August 2002. The bridge sites prediction includes two full-scale bridges. For all the prediction cases, the hydrograph is given as well as available soil properties and bridge pier geometry.

2. Flume Tests Predictions

There are 6 flume test results to be predicted. The flume test parameters are listed in Attachment I (circular pier diameter, water velocity, water depth, flume width), in Attachment II (geotechnical soil properties), and in Attachment III (erosion soil properties).

- **Flume Case 1**

  Description: 160 mm diameter circular pier placed in a clean sand deposit and subjected to a constant velocity over a period of one day.
  Request: Please predict the maximum depth of the scour hole in flume test 1 after 1 day of scouring.

- **Flume Case 2**

  Description: 160 mm diameter circular pier placed in a clean sand deposit and subjected to a multi-velocity hydrograph over a period of 4 days.
  Request: Please predict the maximum depth of the scour hole in flume test 2 after 4 days of scouring

- **Flume Case 3**

  Description: 160 mm diameter circular pier placed in a clay deposit and subjected to a constant velocity over a period of 30 days.
  Request: Please predict the maximum depth of the scour hole in flume test 3 after 30 days of scouring

- **Flume Case 4**

  Description: 160 mm diameter circular pier placed in a in a uniform clay deposit and subjected to a multi-velocity hydrograph over a period of 4 days.

Request: Please predict the maximum depth of the scour hole in flume test 4 after 4 days of scouring.

- **Flume Case 5**

  Description: 160 mm diameter circular pier placed in a sand over clay layered soil and subjected to a constant velocity flow over a period of 10 days.
  Request: Please predict the maximum depth of the scour hole in flume test 5 after 10 days of scouring.

- **Flume Case 6**

  Description: 160 mm diameter circular pier placed in a clay over sand layered soil and subjected to a constant velocity flow over a period of 10 days.
  Request: Please predict the maximum depth of the scour hole in flume test 6 after 10 days of scouring.

3. Bridge Sites Predictions

- **Bridge Case 7**

  Request: Please predict the pier scour depth at pier 11 due to the 8/3/93 flood event. Describe the prediction methodology used. Specify additional data you would require to make a more accurate estimate. Give your best estimation of the cost for obtaining the additional data. More detailed information for this prediction is presented in Attachment V.

- **Bridge Case 8**

  Request: Please predict the pier scour depth at pier 17L due to the 5/1/91 flood event. Describe the prediction methodology used. Also, please **predict the pier scour depth that would be expected at pier 17L over the next 50 years. Assume there will be at least one 500-year flood during that period.** Describe the prediction methodology used. Specify additional data you would require to make a more accurate estimate. Give your best estimation of the cost for obtaining the additional data. More detailed information for this prediction is presented in Attachment VI.

4. Requested Format

The participants are requested to send their predictions in the form of a short paper following the ASCE Journal of Geotechnical Engineering Guidelines. An example of this format is attached in Attachment IV. The paper must include the table below, it must be on 216 mm x 279 mm paper, the text must be single-spaced, the margins must be 25 mm all around, references must be given for any method used, the total number of

pages must be less than or equal to 5 including figures, tables and references. Please give your answer in SI units, give the paper a title with the name of the authors and their address, give an explanation of how the predictions were reached, add any other useful comments. The summary must be presented in a table similar to the following one.

Flume Tests Prediction

Test description	Maximum depth of scour hole when the flume test stops
Flume case 1: 160 mm diameter circular pier placed in clean sand deposit and subjected to a constant velocity over a period of one day.	
Flume case 2: 160 mm diameter circular pier placed in a clean sand deposit and subjected to a multi-velocity hydrograph over a period of 4 days.	
Flume case 3: 160 mm diameter circular pier placed in clay deposit and subjected to a constant velocity over a period of 30 days.	
Flume case 4: 160 mm diameter circular pier placed in a in a uniform clay deposit and subjected to a multi-velocity hydrograph over a period of 4 days.	
Flume case 5: 160 mm diameter circular pier placed in a sand over clay layered soil and subjected to a constant velocity flow over a period of 10 days.	
Flume case 6: 160 mm diameter circular pier placed in a clay over sand layered soil and subjected to a constant velocity flow over a period of 10 days.	

Bridge Sites Prediction

Description	Maximum depth of scour hole
Bridge site case 7, 8-3-93 flood	
Bridge site case 8, 5-1-91 flood	
Bridge site case 8, 50 years prediction	

Attachment I: Flume Test Parameters

Test No.	*Test Type*	*Soil Type*	*Soil Layer*	*Velocity*	*Hydrograph*	*Time (day)*
1	Sand and constant velocity	Sand	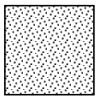	V=0.35m/s	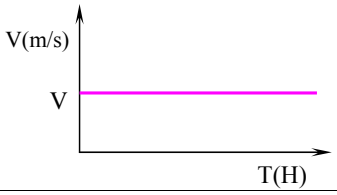	1
2	Sand and multi-velocity	Sand	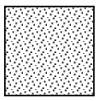	V1=0.35m/s V2=0.25m/s	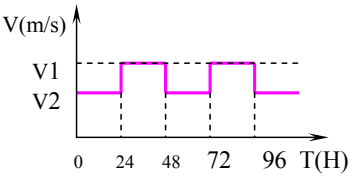	4
3	Clay and constant velocity	Clay		V=0.35m/s	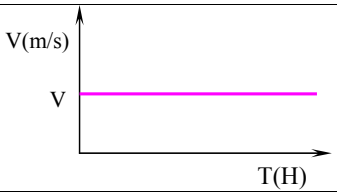	30
4	Clay and multi-velocity	Clay		V1=0.35m/s V2=0.25m/s	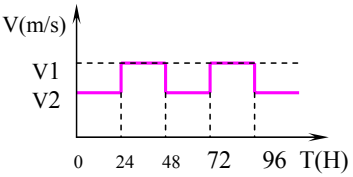	4

5	Sand over clay and constant velocity	Top: sand Bottom: clay	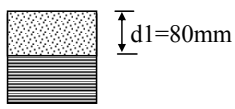	V=0.35m/s	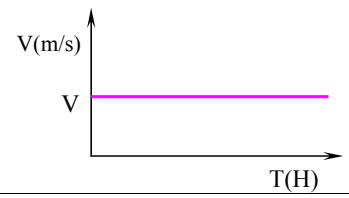	10
6	Clay over sand and constant velocity	Top: clay Bottom: sand	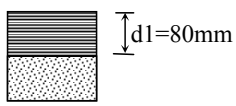	V=0.35m/s	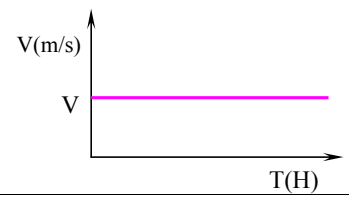	10

Note:

- In each flume test, one circular pier will be installed at the center of the flume. The circular pier will be a PVC pipe with an outside diameter equal to 160 mm.
- The water depth will be measured in line with the pier and 2 meters upstream of the pier. For all flume tests, the water depth will be kept constant and equal to 375mm.
- The flow velocity, V, given in the table is the depth average velocity of the flow at a location in line with the pier and 2 meters upstream of the pier.
- All flume tests will be conducted in a 1.5 m wide concrete flume.

Attachment II: Geotechnical Soil Properties for Flume Predictions

Part I: Porcelain Clay for Flume Test Predictions

Table 1: Geotechnical Properties of Porcelain Clay

Test No.	*Properties*	*Values*
1	Liquid Limit, %	33%
2	Plastic Limit, %	17%
3	Plastic Index (PI), %	16%
4	Specific Gravity	2.7
5	Water Content, %	24.2%
6	Mini-Vane Shear Strength, KPa	23.3

Table 2: Hydrometer Test of Porcelain Clay

No.	*D (mm)*	*P(%)*
1	0.019722	74.65
2	0.014979	70.20
3	0.011895	64.48
4	0.008565	59.72
5	0.005853	53.05
6	0.00454	52.73
7	0.003449	46.06
8	0.002346	40.66
9	0.001832	37.16
10	0.001583	34.31
11	0.001125	31.76
12	0.000925	28.91
13	0.00054	25.73

Where:

D: Diameter of particle

P: Percentage of soil remaining in suspension at the level at which the hydrometer measures the liquid density.

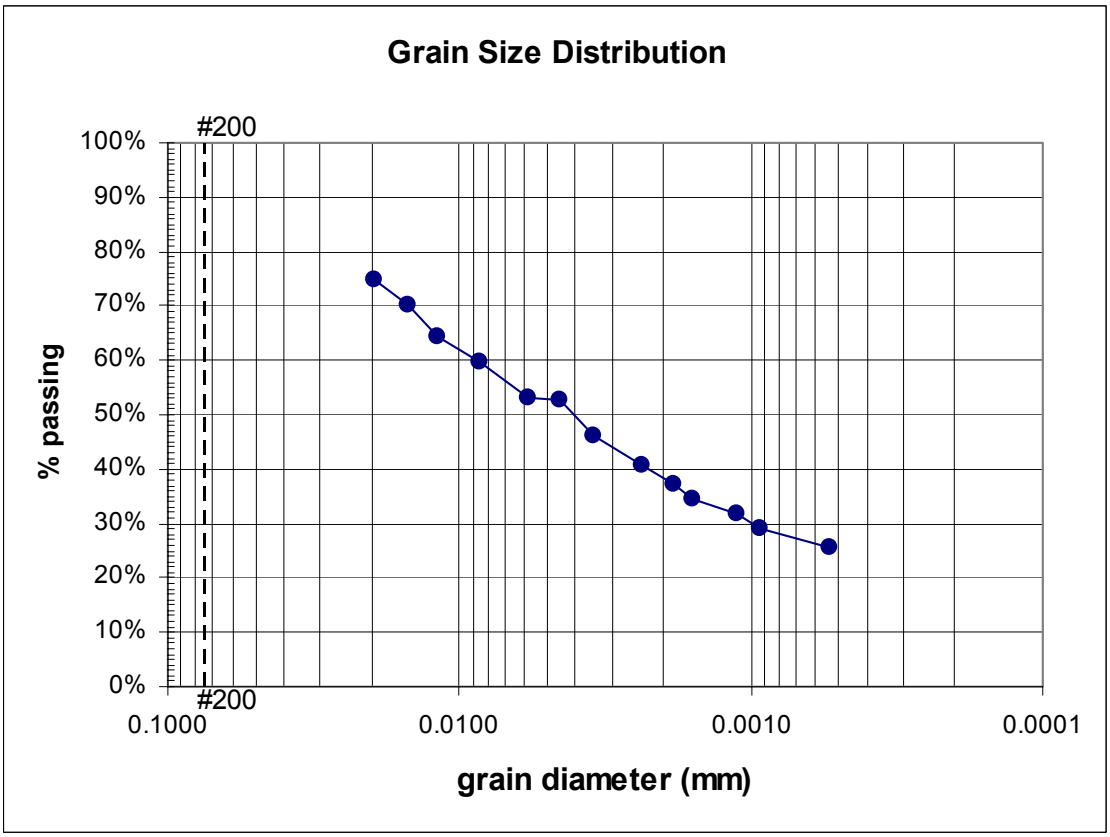

Fig 1: Grain Size Distribution of Porcelain Clay by Hydrometer Test

Part II: Mortar Sand for Flume Test Predictions

Table 3: Sieve Analysis of Mortar Sand

Sieve No.	*Size of sieve (mm)*	*Percent Passing(%)*
10	2.00	99.6
20	0.85	97.2
40	0.425	78.0
60	0.25	35.0
100	0.15	7.0
200	0.075	0.4

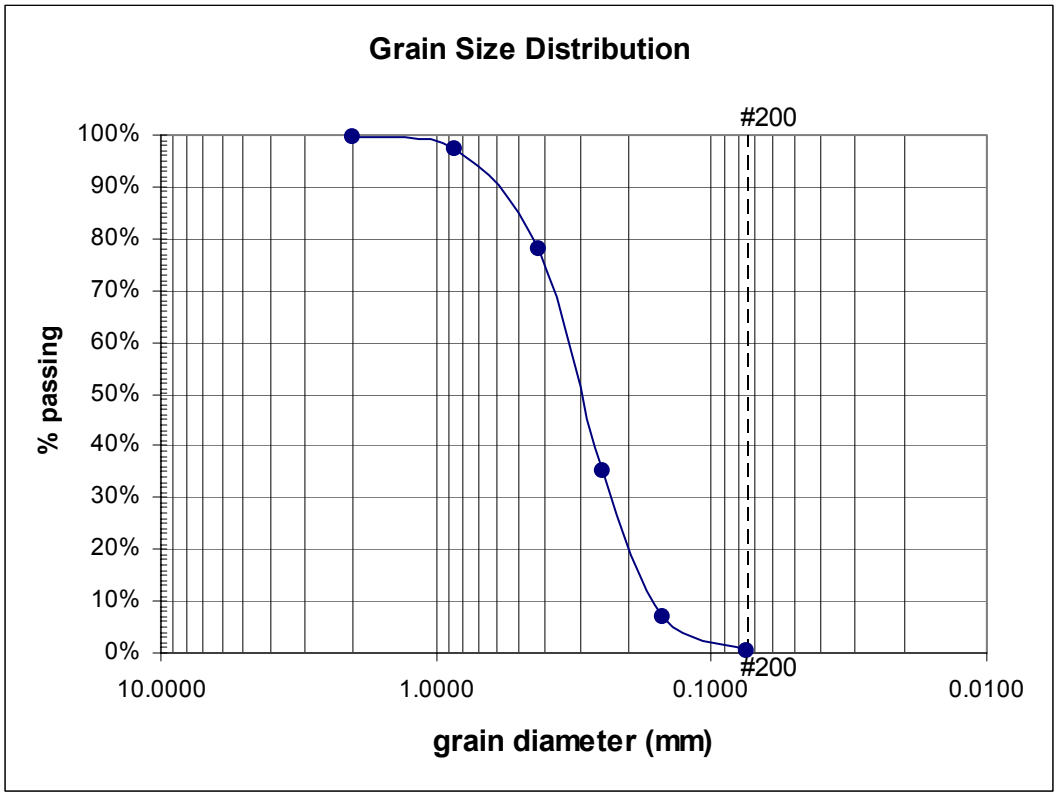

Fig 2: Grain Size Distribution of Mortar Sand by Sieve Analysis

Note:

- ASTM standard test procedures were followed to determine the soil properties of the porcelain clay and mortar sand for the flume predictions.

Attachment III: EFA (Erosion Function Apparatus) Test Results for Soils for Flume Predictions

(http://tti.tamu.edu/geotech/scour)

Part I: Porcelain Clay for Flume Test Predictions

Velocity (m/s)	*Scour Rate (mm/hr)*	*Shear Stress (N/m^2)*
0.351	0.20	0.403
0.451	0.89	0.624
0.459	1.11	0.644
0.542	2.32	0.861
0.681	2.76	1.286
0.692	2.82	1.322
1.018	5.65	2.596
1.426	8.50	4.684
2.08	18.31	9.69
2.74	39.90	16.01

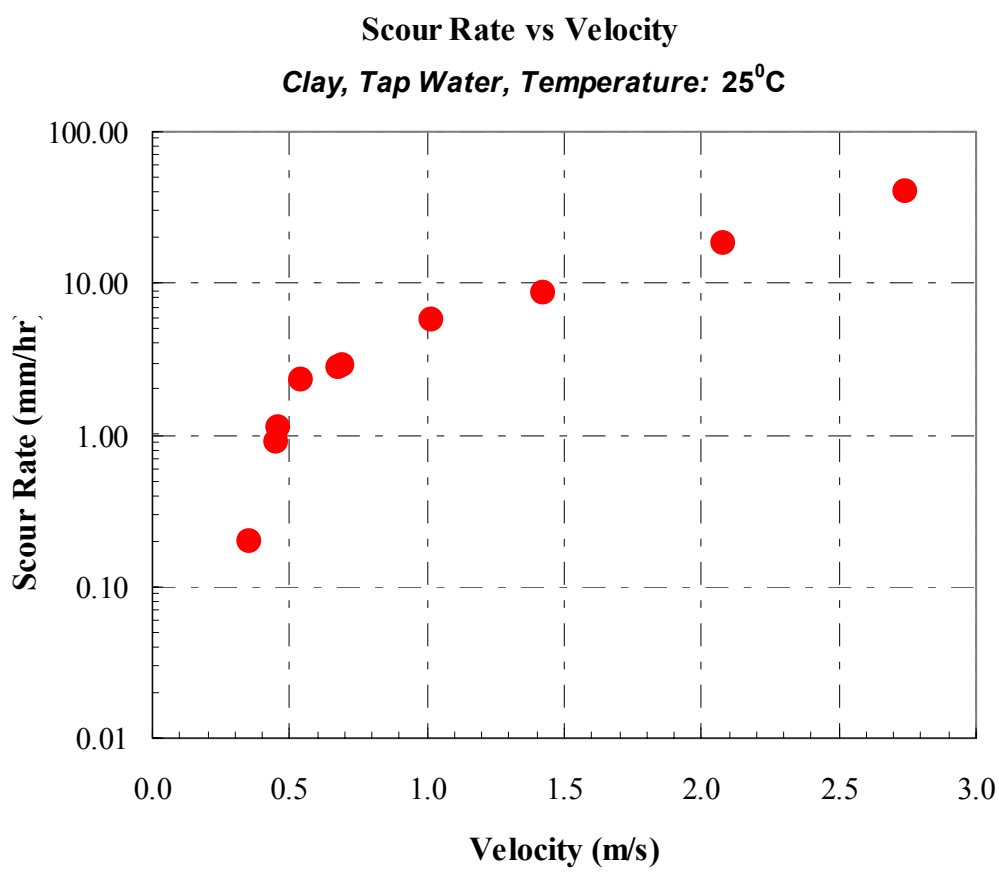

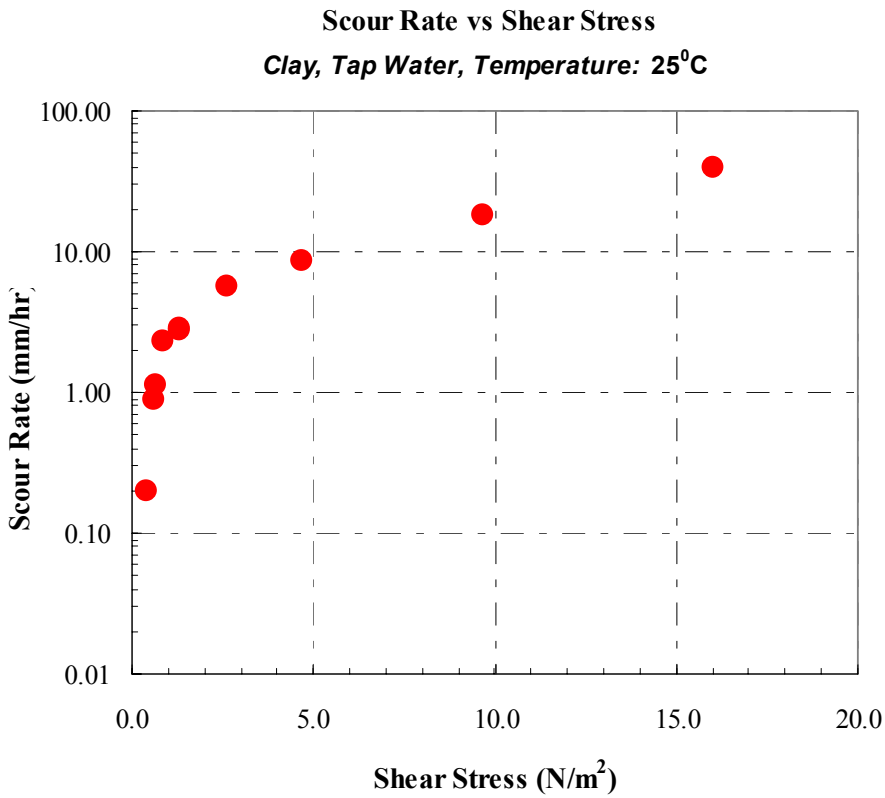

Note:

- A summary description of the EFA can be found at the following website: http://tti.tamu.edu/geotech/scour
- ***Scour Rate:*** Vertical length of soil eroded by flowing water per unit time
- ***Velocity:*** Average velocity of the water flowing over the soil sample in the rectangular pipe (50.8mm × 101.6 mm)
- ***Shear Stress:*** Shear stress at soil-water interface corresponding to the water velocity; the shear stress is calculated by using Moody Chart.

Part II: Mortar Sand Flume Test Predictions

Velocity (m/s)	*Scour Rate (mm/hr)*	*Shear Stress (N/m^2)*
0.146	0	0.087
0.177	0.05	0.121
0.189	0.19	0.136
0.204	0.79	0.156
0.244	4.79	0.213
0.387	486.49	0.479
0.659	2200	1.21
0.740	3000	1.49

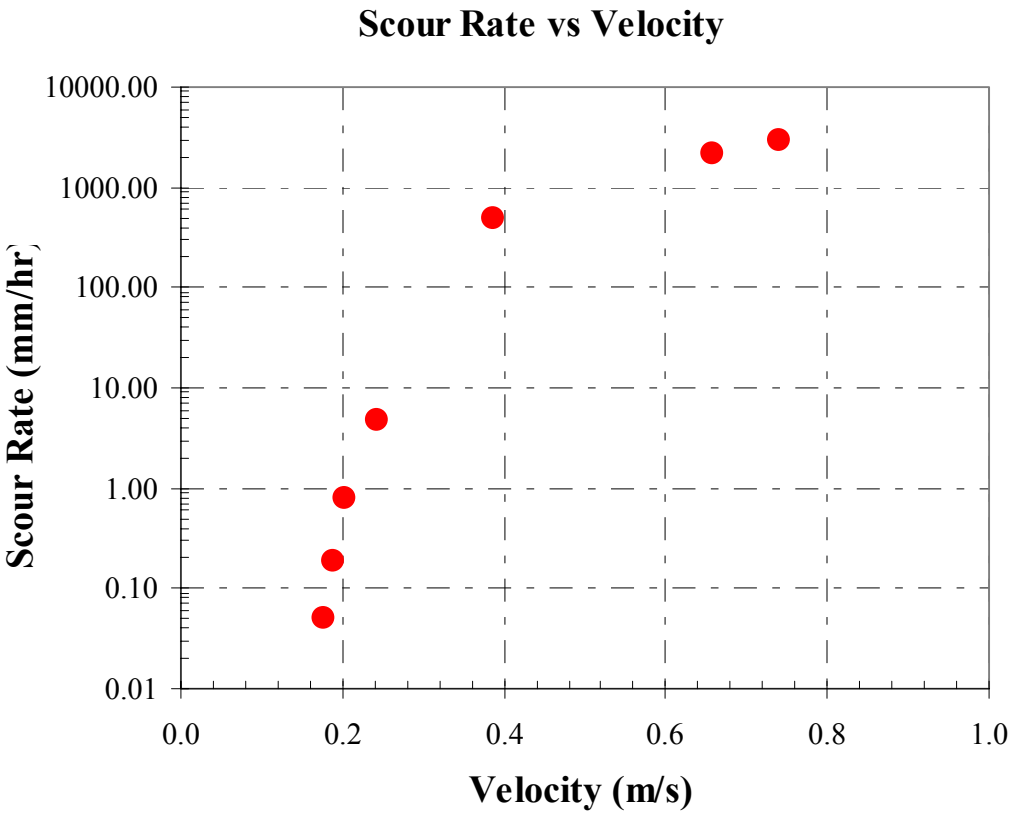

Sand, Tap Water, Temperature:

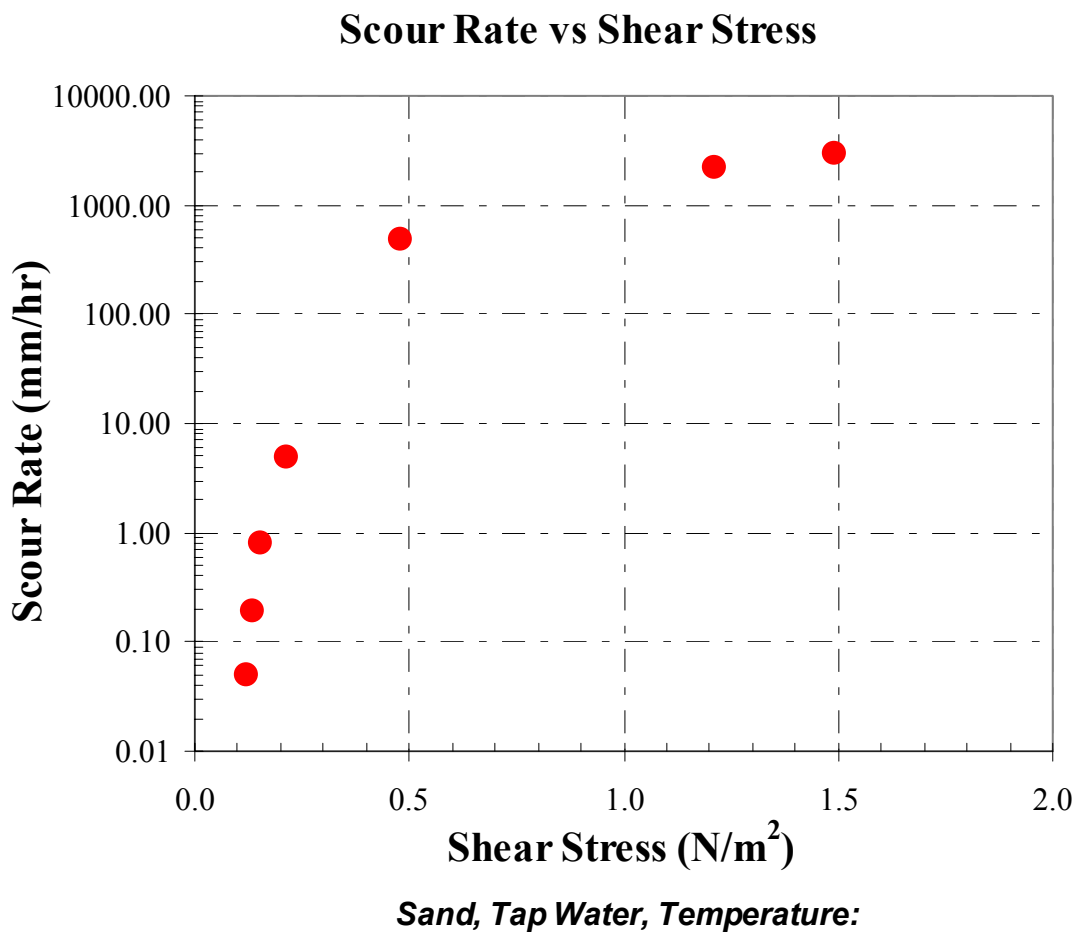

Note:

- A summary description of the EFA can be found at the following website: http://tti.tamu.edu/geotech/scour
- ***Scour Rate:*** Vertical length of soil eroded by flowing water per unit time
- ***Velocity:*** Average velocity of the water flowing over the soil sample in the rectangular pipe (50.8mm × 101.6 mm)
- ***Shear Stress:*** Shear stress at soil-water interface corresponding to the water velocity; the shear stress is calculated by using Moody Chart.

Attachment IV: example format for the prediction response.

Double click on the icon

Acrobat Document

Attachment V: Bridge Sites Prediction: Bridge Case 7

Double click on the icon

"Bridge Case 7.doc"

Attachment VI: Bridge Sites Prediction: Bridge Case 8

Double click on the icon

"Bridge Case 8.doc"

Attachment V: Bridge Case 7
Pier Scour Prediction for Mississippi River Bridge

Request:

Predict pier scour at pier 11 for the 8/3/93 flood event. Describe the prediction methodology used. Specify additional data you would require to make a more accurate estimate. Give your best estimate of the cost for obtaining the additional data.

Site Description:

The USGS has operated a discharge gaging station at this site since 1942 and river stage records have been recorded at this site since 1891. The datum of the gage is 103.95 m above NGVD 1929 datum (MSL). Periodic bed-material samples and daily suspended-sediment samples were obtained at the gage during the flood. The Mississippi River drainage area at this site is 1,835,266 sq. km. The Mississippi River flows at the eastern edge of its flood plain in the study reach. The bank at this side rises steeply at slopes of 0.1 to 0.7 m/m from the main channel to about 85.34 m above normal river levels. The main channel is fairly straight in the study reach. There is a gradual bend to the left about 4023.36 m upstream, a very gradual bed to the right at the bridge, and a gradual bend left about 2 miles downstream. The main channel is about 518.16 m wide at the bridge and averages about 670.56 m wide over a 6437.38-meter reach centered at the bridge. The annual average daily discharge at this site is 5626.56 m^3.

Stream Data

Drainage Area (sq m): 1835265
Slope in Vicinity (m/m): 0.0003
Flow Impact: Straight
Channel Evolution: Unknown
Armoring: None
Valley Setting: Moderate
Floodplain Width: Wide
Natural Levees: Unknown
Sinuosity: Sinuous
Braiding: None
Stream Width Variability: Equiwidth

Debris Frequency: Rare
Debris Effect: None
Stream Size: Wide
Flow Habit: Perennial
Bed Material: Sand
Apparent Incision: None
Channel Boundary: Alluvial
Banks Tree Cover: Low
Anabranching: None
Bars: Narrow

Flow Data

See the attached Excel file "Bridgecase7Hydrograph.xls" for the daily flow hydrograph for the 1993 flood year for this site.

Double click on the icon

BridgeCase7Hydrograph.xls

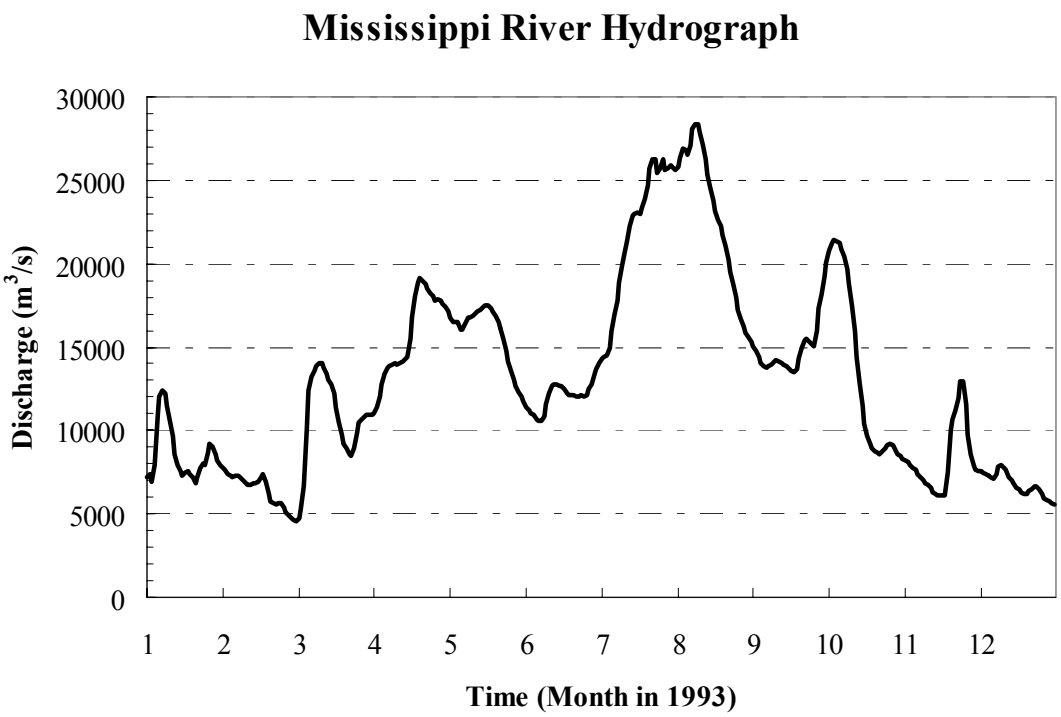

Bridge Data

Length (m): 861.36
Width (m): 6.71
Number of Spans: 13
Vertical Configuration: Curvilinear

Flow and Bed Elevations

Date	Q (m^3/s)	W.S. Elevation (m)	Reference Bed in Vicinity of Pier 11		Bed Material approaching pier			
			Depth (m)	Bed Elevation (m)		D_{84} (mm)	D_{50} (mm)	D_{16} (mm)
8/3/93	26561.2	118.43	22.52	95.89	sand	4.1	1.08	0.65
8/12/93	24522.4	117.77	22.37	95.40	sand	4.1	1.08	0.65
9/13/93	13592.1	113.61	16.70	96.91	sand	4.1	1.08	0.65

Pier Scour at Pier 11

Date	Approach flow depth (m)	Approach average velocity (m/s)	Skew angle (°)	Sediment Transport	Debris	Bed Form
8/3/93	22.52	2.429	4	Live bed	Insignificant	Unknown
8/12/93	22.37	2.000	4	Live bed	Insignificant	Dune
9/13/93	16.70	1.838	11	Live bed	Insignificant	Dune

Description of Pier 11

Pier 11 has a rectangular caisson footing 16.00 m long by 7.32 m wide with its base at elevation 78.03 m and extending up to elevation 99.06 m. From the top of the caisson a solid, round nosed section 14.78 m long by 5.49 m wide rises to elevation 109.73 m. The nose of the pier is circular with a 2.74 m radius. Two tapered columns extend from elevation 109.73 m to the bridge deck (elevation 134.14 m). The columns are connected by a continuous, 1.07 m wide web from elevation 109.73 m to 116.59 m. The columns are tapered and measure 4.572 m wide at their base (elevation 109.73 m), and 3.35 m feet wide at elevation 122.83 m. The columns have a stepped, square face. See sketch below.

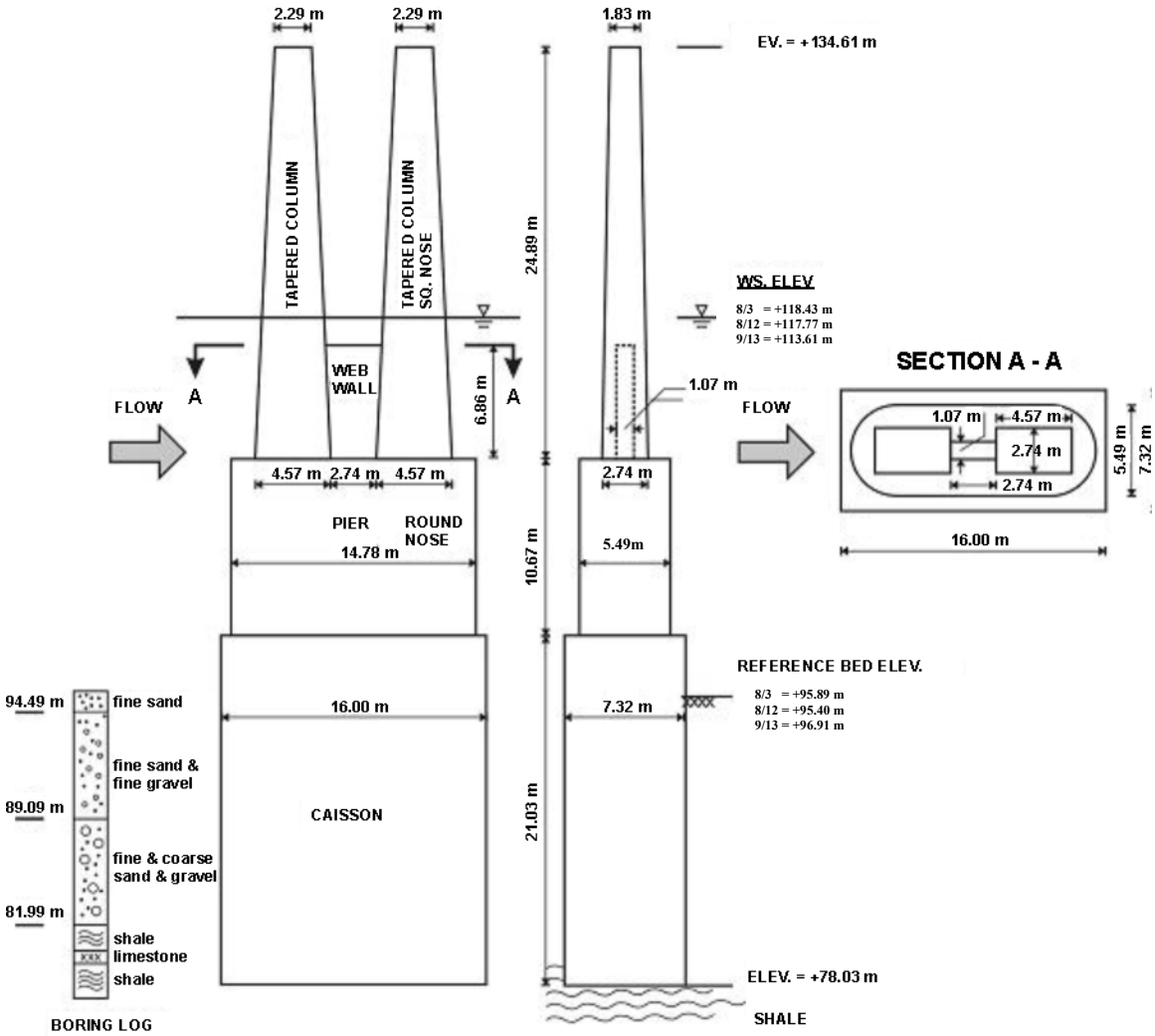

PIER 11 OVER MISSISSIPPI RIVER

Attachment VI: Bridge Case 8
Pier Scour Prediction for Pearl River Bridge

Request:

Predict the pier scour depth at pier 17L due to the 5/1/91 flood event. Describe the prediction methodology used. **Predict the pier scour depth that would be expected at pier 17L over the next 50 years. Assume there will be at least one 500-year flood during that period.** Describe the prediction methodology used. Specify additional data you would require to make a more accurate estimate. Give your best estimation of the cost for obtaining the additional data.

Site Description:

This is a 360-meters -long bridge. The bridge has a span arrangement of 15 spans at 12.2 m, 1 span at 27.4 m, 1 span at 36.6 m, 1 span at 27.4 m, and 7 spans at 12.2 m from right to left (west to east). The 12.2-m spans are supported by single-pile bents (2L-15L and 20L-25L), the 27.4-m spans are supported by a double-pile bent (16L & 19L) and a main pier (17L & 18L), and the 36.6-m span is supported by two main piers (17L & 18L). The main piers consist of two 31.1-m-diameter columns on a pile-supported footing. The pile bents consist of 0.41x0.41-m piles. A 22.9-m-long spur dike is located at the right (west) abutment, and a 45.7-m-long spur dike is located at the left (east) abutment. Scour data were collected during high and low flows using a fathometer. The flow velocities approaching the bridge piers were determined from velocity soundings during discharge measurements obtained at the upstream side of the bridge. Ground-penetrating radar was also used at the site in July 1992 to detect infilling of scour holes.

Stream Data

Drainage Area (m^2): 9860128447
Slope in Vicinity (m/m): 0.00019
Flow Impact: Right
Channel Evolution: Pre-modified
Armoring: None
Valley Setting: Moderate
Floodplain Width: Wide
Natural Levees: Both
Sinuosity: Meandering
Braiding: None
Stream Width Variability: Wider
Debris Frequency: Occasional
Debris Effect: Local
Stream Size: Medium
Flow Habit: Perennial
Bed Material: Sand
Apparent Incision: None
Channel Boundary: Alluvial
Banks Tree Cover: Low
Anabranching: None
Bars: Narrow

Flow Data

See the attached Excel file" BridgeCase8Hydrograph.xls" for the daily flow hydrograph for this site.

Double click on the icon

BridgeCase8Hydrograph.xls

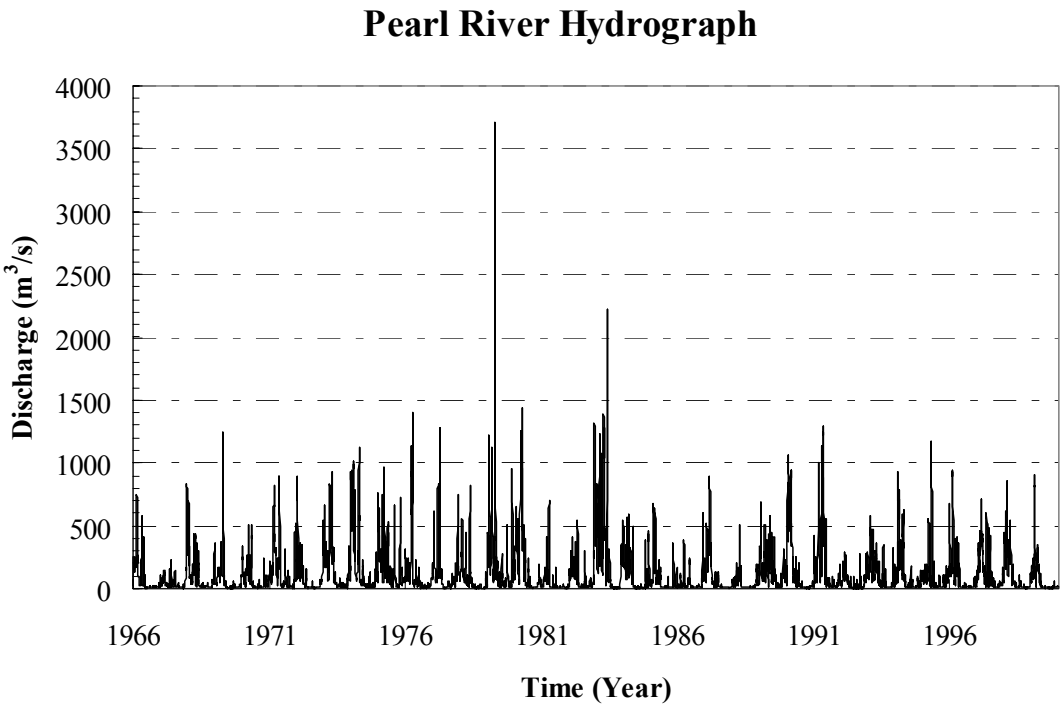

Bridge Data

Length (m): 360
Width (m): 9.8
Low Chord Elevation (m): 86
Upper Chord Elevation (m): 87
Overtopping Elevation (m): 86.5
Skew (degrees): 25
Guide Banks: Elliptical
Plans on File: Yes
Parallel Bridges Yes
Continuous Abutment: No

Distance Between Centerlines: 88
Upstream/Downstream: Upstream
Number of Spans: 21 Number of spans is actually 25.
Vertical Configuration: Curvilinear
Average Daily Traffic: 16440
Year Built: 1966
Waterway Classification: Main
Distance Between Pier Faces: 59

Manning's n Values

Right Over bank: 0.16
Main Channel: 0.038
Left Over bank: 0.12

Bed Samples

On April 28, 1993, bed samples were collected from the main channel at selected intervals along three channel cross sections. Individual samples with similar characteristics were combined for gradation analyses. The following is a brief description of the bed samples collected (grain sizes and specific gravity):

Sample	D_{95}	D_{84}	D_{50}	D_{16}	SG	Cross Section	Comment
1	2.9	1.2	0.54	0.36	2.65	1	Bed at about mid-span between bents 16-17L.
2	1.3	0.9	0.39	0.26	2.65	1	Bed in vicinity of main piers 17-18L.
3	9.5	5.5	0.39	0.26	2.65	2	Mid-channel
4	1.7	1.3	0.64	0.35	2.65	2	Left part channel
5	1.0	0.4	0.29	0.18	2.65	3	Mid-to-left part of channel

Note: The samples are non-cohesive soil.

The right part of the channel bed at cross sections 2 & 3 seemed to be mostly silty clay. Bed sample No. 1 was used for bents 15-16L and sample No. 2 was used for main piers 17-18L. For pile bents 12-14L, the material is clay with cohesion of about 11.5 Kpa and an angle of internal friction of about 27 degrees, as determined from shear-strength tests.

Soil Boring Information

The following information was for shear strength parameters of the soils near Pier 17L.

Zone	Undrained Shear Stress (Kpa)	Friction Angle (Degree)	Comment
1(sand)	0	36	
2A	119.7	0	Only one unconfined compression test.
2A (sand layer)	0	37	
2B(sand)	0	37	
2C	47.9~143.6	0	
2D	Probably >71.8	0	Only one unconfined compression test.

Flood Frequency/flow depths/velocities/shear stresses

The above information is provided as an Excel file; see: “BridgeCase8FloodAnalysis.xls”

Double click on the icon

BridgeCase8FloodAn
alysis.xls

Fordetails of the flood analysis information, please see the table right after the figure of Pier 17L.

Description of Pier 17L

Pier 17L has two 1.07-m-diameter concrete columns spaced 5.2 m apart. Columns have 3.4-m-wide by 3.05-m-long by 1.4-m-deep concrete footings (with 1.07-ft-wide connecting webs) supported by eight 0.46-m concrete piles. There are three piles at the upstream side of the footing, two in middle, and three at the downstream side. Bottom of footing elevation is 65.6 m; pile tip elevation is 65.5 m. See sketch below.

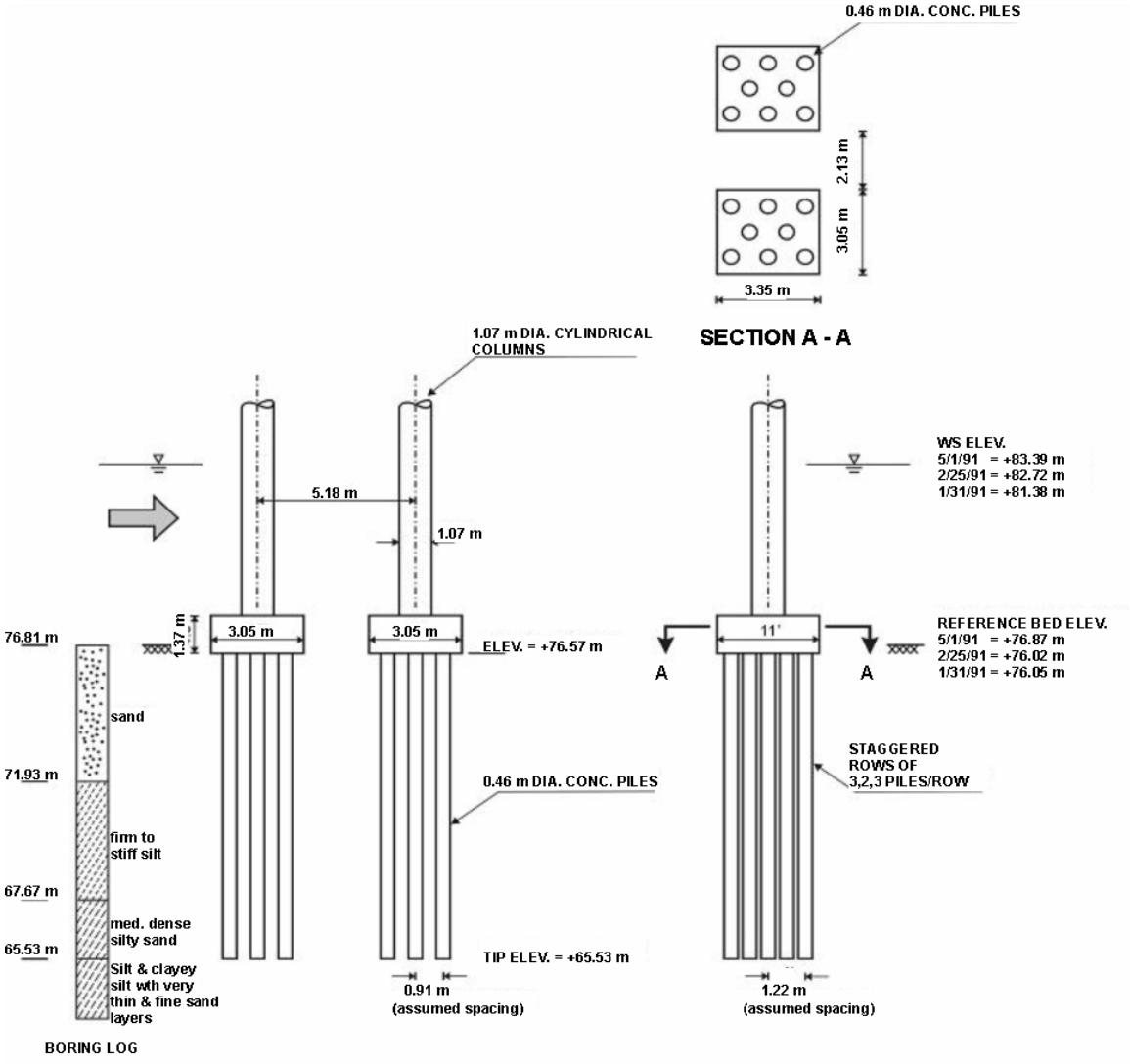

PIER 17L OVER PEARL RIVER

The following was based on WSPRO computations and field data at Pearl River

	Qtotal (m^3/s)	Qmc (m^3/s)	Stage (m)	Hf (m)	Lave (m)	Sf (m/m)	Approach Flow at upstream side of Pier 17L at station 102+31 Velocity (m/s)	Depth (m)			Channel-bed shear stress at upstream side of Pier 17L at station 102+31	Average Stream Power Approaching Pier 17L Velocity*Stress
Flood Frequency 2- to 500-year Discharges:											(Pa)	(Pa*m/s)
2-yr	758.9	736.2	82.0	0.04	387.4	0.0000944	0.9	5.7			1.60	1.41
5-yr	1240.3	1152.5	83.4	0.04	387.7	0.0001022	1.1	6.9			2.11	2.25
10-yr	1608.4	1464.0	84.2	0.04	395.0	0.0001080	1.2	7.6			2.46	2.92
25-yr	2123.8	1885.9	84.9	0.05	409.7	0.0001190	1.4	8.4			2.97	4.16
50-yr	2548.5	2228.5	85.5	0.05	418.5	0.0001238	1.5	8.9			3.28	5.00
100-yr	3001.6	2585.3	85.9	0.06	440.1	0.0001316	1.7	9.2			3.63	6.09
500-yr	4190.9	3029.9	86.9	0.12	475.5	0.0002436	1.9	9.6			6.97	13.16
Two of the largest known floods:									In BSDMS & WRIR-94-4241		0.00	
4/17/1979	3766.2	3086.6	86.6	0.11	469.4	0.0002403	1.9	9.6	Measured app. flow upstream		6.87	13.19
5/25/1983	2251.2	1987.9	85.0	0.05	410.6	0.0001262	1.5	8.4	of Pier 17L at station 102+31		3.16	4.62
Flood measurements when scour data were collected:							0.0	0.0	Velocity	Depth	0.00	
5/1/1991	1410.2	1330.9	83.4	0.05	388.0	0.0001335	1.2	6.9	1.1	6.5	2.77	3.38
2/25/1991	1042.1	985.4	82.7	0.04	387.4	0.0001101	1.0	6.3	1.0	6.7	2.09	2.16
1/31/1990	637.1	628.6	81.4	0.04	387.1	0.0001102	0.9	5.1	0.9	5.3	1.69	1.44
											0.00	
Estimates Using 1979 Bridge Section for Comparison:											0.00	
4/17/1979	3766.2	3143.2	86.6	0.12	469.392	0.0002597	2.4	12.4			9.65	23.53

The 1979 bridge section was used to show the differences in the computations of the 1979 flood based on two different sections.
In 1979, the channel at the bridge was much deeper at Pier 17L. The river channel has migrated westward through the years. One channel section can not accurately represent the historical approach velocities, depths, shear stresses, and streampower in the vicinity of Pier 17L, due mostly to the lateral movement of the channel section through time.

PREDICTION PAPERS

PIER SCOUR PREDICTION FOR MISSISSIPI RIVER BRIDGE
PIER 11 for the 08-03-93 flood event
Bridge Case 7

Authors : Civil Engineer Guillermo Ferrando and Hydroresources Engineer Carlos Cian
Santa Fe – ARGENTINA.

A - Prediction Methodology used.
To determine pier scour we used the CSU (Colorado State Univesity) equation.- The equation is:

(1) $Ys = Y_1 \; 2.0 \; K_1 K_2 K_3 K_4 \; (a/Y_1)^{0.65} \; Fr_1^{0.43}$
equation number 21 - page 36 - Publication Nº FHWA-IP-90-017. November 1995 - Circular HEC Nº18.

Where:

Ys = Scour depth; m
Y_1= Flow depth directly upstream of the pier; m
K_1= Correction factor for pier nose shape.
K_2= Correction factor for angle of attack of flow.
K_3= Correction factor for bed condition.
K_4= Correction factor for armoring by bed material size.
L = Lenght of pier; m.
a = Pier witdh; m.
Fr_1= Froude Number directly upstream of the pier; $V_1/(g\,Y_1)^{1/2}$.
V_1= Mean velocity of flow directly upstream of the pier; m/s.
g = Acceleration of gravity; 9.81 m/s^2.

There are many situations about this case.

At the first time, we have the basic formula (1) with the data of the footing, to know:
WS elevation: 118.38 m
Bed elevation: 95.86 m
Skew angle (θ) : 11º
Pier scour in condiction "Live - bed"
Bed form: Dune
Y_1= 22.52 m
We calculated the values of "a" and "L", using the following averages ponderated for the depth:

(2) $$a_{average} = \frac{3.20m \times 7.32\,m + 10.67m \times 5.49m + 8.65\,m \times (2.74m+2.42m)/2}{3.20\,m + 10.67m + 8.65\,m} = 4.63\,m$$

$a_{average}$ = 4.63 m

(3) $$L_{average} = \frac{3.20m \times 16.00m + 10.67m \times 14.78m + 11.57\,m \times 6.86m + 7.63m \times 1.79m}{22.52\,m}$$

$L_{average}$= 13.41 m

V1 = 2.429 m/s

Froude number:
$Fr_1 = 2.429 / (9.81 \times 22.52)^{½} = 0.163$

K_1.-The correction factor K_1 for pier nose shape should be determined for angles of attack up to 5 degrees.- For greater angles, K_2 dominates and K_1 is considered as 1. Then K_1= 1.

K_2 can be calculated using the following equation: $K_2 = (\cos\theta + L / a \sin\theta)^{0.65}$
$K_2 = (\cos 11º + 13.41/4.63 \times \text{sen } 11º)^{0.65} = 1.32$

K_3 = 1.1, because the data is dune.

K_4.- The correction factor result from recent research for FHWA by Molinas at CSU. This factor decreases scour depths for armoring of the scour hole for bed material that have a D_{50} equal to or larger than 0.06m ($D_{50} \geq 0.06$m).- For this case D_{50} = 0.0006m, then K_4= 1.0

Other data used are:
WS elevation: 118.38 m
Bed elevation: 95.86 m
Skew angle (θ) : 11º
Pier scour in condition "Live - bed"
Bed form: Dune

Equation 21:
$Ys_1 = 22.52 \times 2.0 \times 1.0 \times 1.32 \times 1.1 \times 1.0 \times (4.63 / 22.52)^{0.65} \times (0.163)^{0.43}$

Then : **Ys_1 = 10.72 m.-**

We calculated the one second value of scour depth based in recommendations of the publication Nº FHWA-IP-90-017 – November 1995, Hydraulic Engineering Circular Nº 18, pages 39 and 40, we used for prediction pier scour the followings sketch:

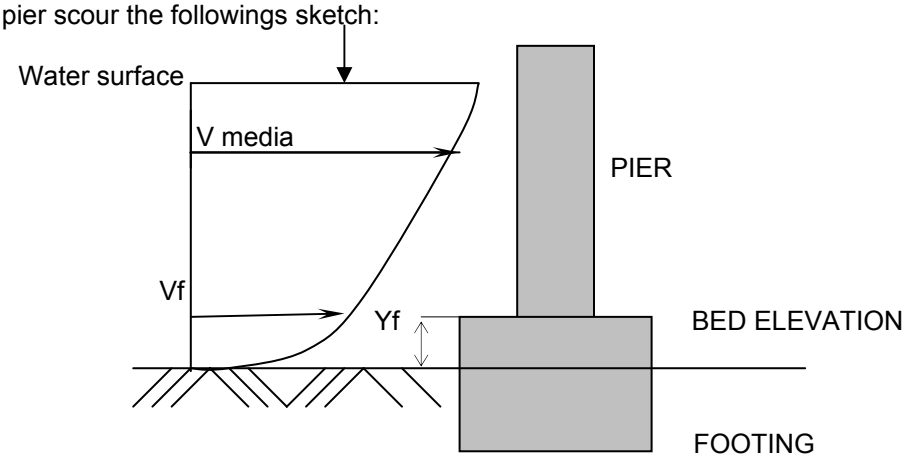

The formula is:
(4) $V_f = V_1 \times [\ln(10.93 \times Yf / D_{84} + 1) / \ln(10.93 \times Y1 / D_{84} + 1)]$
Where :
V_1 = 2.249 m/s
Y_1 = 22.52 m
D_{84} = 0.0013 m
Y_f = 3.20 m

Then V_f = 2.04 m/s

The Froude number is:
$Fr_f = 2.04 / (9.81 \times 3.20)^{1/2} = 0.364$

And $K_2 = (\cos 11º + 13.41m/4.63m \times \sin 11º)^{0.65} = 1.321$

K_3 = 1.1, adopted of table for small dunes.

K_4= 1.0

Applied the CSU equation with this data we obtain:

$$Ys_1 = 3.20m \times 2.0 \times 1 \times 1.321 \times 1.1 \times 1 \times (4.63m/3.20m)^{0.65} \times (0.364)^{0.43}$$

Then : **Ys_2 = 7.66 m.-**

Note: during the data investigation, whe knowed (internet) that in 1993 the meassured scour at the pile 11 in this bridge was 7.10m (23.3 ft) – *BSDMS Summary Report–Site 57 Mississippi River at S.R.51/150 at Chester*, wich very similar to Ys_2 calculated in this paper.

The HEC-18 has recomended to adopt the bigger within both results (page 39).

According with HEC-18, for PREDICTION EVENT we adopt the value **Ys_1 = 10.72m.**

B - Additional data.
We had considered that the data was enough for this case.-

C – Best estimate of the cost for obtaining the additional data.
Is not necessary additional cost.-

IC Guillermo Ferrando
IRH Carlos Cian
11/07/2002.

PIER SCOUR PREDICTION FOR MISSISSIPI RIVER BRIDGE
PIER 17L for the 05-01-91 flood event
Bridge Case 8

Authors : Civil Engineer Guillermo Ferrando and Hydroresources Engineer Carlos Cian
Santa Fe – ARGENTINA.

A - Prediction Methodology used.
To determine pier scour we used the CSU (Colorado State Univesity) equation.- The equation is:

(1) $Ys = Y_1 \; 2.0 \; K_1 K_2 K_3 K_4 \; (a/Y_1)^{0.65} \; Fr_1^{0.43}$
equation number 21 - page 36 - Publication Nº FHWA-IP-90-017. November 1995 - Circular HEC Nº18.

Where:

Ys = Scour depth; m
Y_1= Flow depth directly upstream of the pier; m
K_1= Correction factor for pier nose shape.
K_2= Correction factor for angle of attack of flow.
K_3= Correction factor for bed condition.
K_4= Correction factor for armoring by bed material size.
L = Lenght of pier; m.
a = Pier witdh; m.
Fr_1= Froude Number directly upstream of the pier; $V_1/(g\,Y_1)^{1/2}$.
V_1= Mean velocity of flow directly upstream of the pier; m/s.
g = Acceleration of gravity; 9.81 m/s^2.

B- Computation scour depth due to event 5/1/91

We calculated scour depth based in recommendations of the publication Nº FHWA-IP-90-017 – November 1995, Hydraulic Engineering Circular Nº 18, pages 40 and 43.- For prediction pier scour , we considered recomendation for situations about this case:

At the first time, we have the basic formula (1), with the data of the pier 17L over Pearl River, and:
WS elevation: 83.39 m
Bed elevation: 76.87 m
Depth: 6.52 m
Skew angle (θ) : 25º
Debris effect: Local
Pier scour in condiction "Live - bed"
Y_1= 6.52 m
V_1= 1.10 m/S
F_{R1}= 0.134

1) Computation of scour caused by the exposed pile group.

K_1= Correction factor for pier nose shape = 1 (calculated for angle of attack up to 5 degrees)

K_2= Correction factor for angle of attack of flow.

According with HEC-18, we considered equivalent pier:

SECCTION A-A PIER 17L PEARL RIVER PIER EQUIVALENT

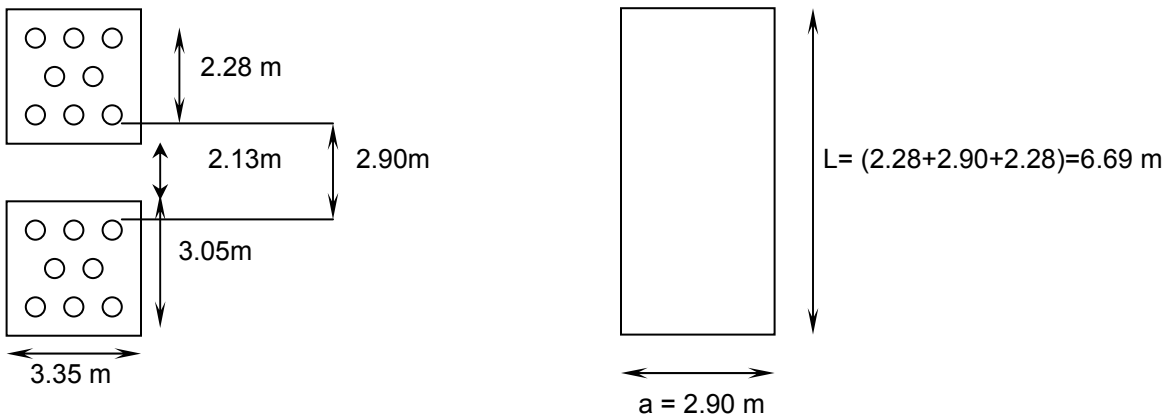

$K_2 = (\cos\theta + L / a \sin\theta)^{0.65}$

$K_2 = (\cos 25^o + 6.69/2.90 \times \sin 25^o)^{0.65} = 1.52$

K_3= Correction factor for bed condition.- Adopted K_3= 1.1
K_4= Correction factor for armoring by bed material size. K_4= 1

Equation (1):
$Ys_1 = 6.52 \times 2.0 \times 1.0 \times 1.52 \times 1.1 \times 1.0 \times (2.90 / 6.52)^{0.65} \times (0.134)^{0.43}$

Then : **Ys_1 = 5.42 m.**

2) Computation of scour caused by Pile cap.

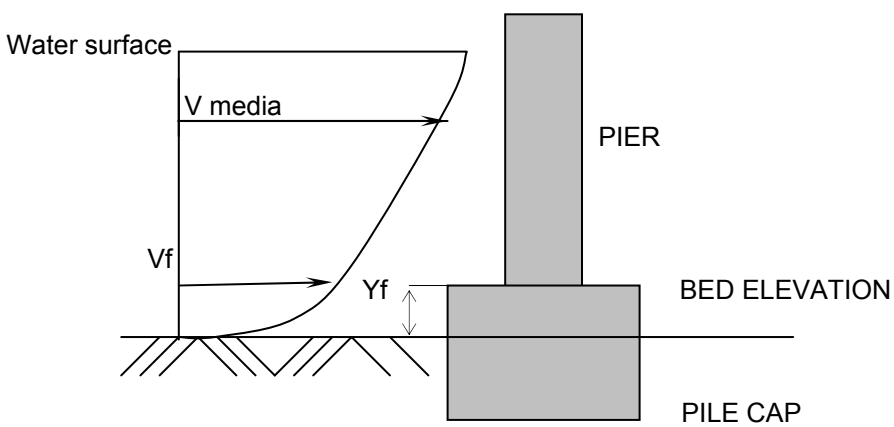

The formula is:
(4) $V_f = V_1 \times [\ln(10.93 \times Yf / D_{84} + 1) / \ln(10.93 \times Y1 / D_{84} + 1)]$
Where :
V_1 = 1.10 m/s
Y_1 = 6.52 m
D_{84} = 0.0009 m
Y_f = 1.07 m

Then V_f = 0.92 m/s
The Froude number is:
$Fr_f = 0.92 / (9.81 \times 1.07)^{1/2} = 0.284$

According with HEC-18, we considered equivalent pier:

SECCTION A-A PIER 17L PEARL RIVER PIER EQUIVALENT

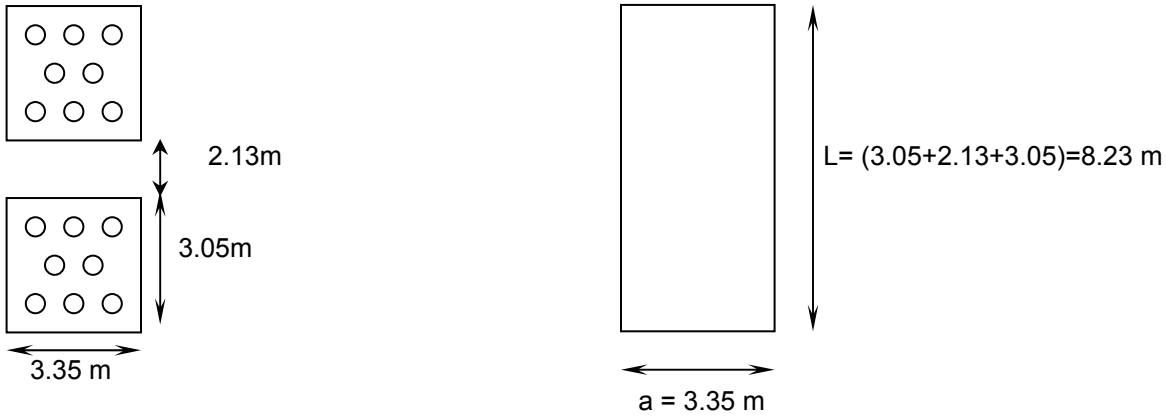

And K_2= (Cos 25º + 8.23m/3.35m x Sin 25º) $^{0.65}$ = 1.54

K_3= Correction factor for bed condition.- Adopted K_3= 1.1
K_4= Correction factor for armoring by bed material size. K_4= 1

Equation (1):
Ys_1 = 1.07 x 2.0 x 1.0 x 1.54 x 1.1 x 1.0 x (3.35 / 1.07) $^{0.65}$ x (0.284) $^{0.43}$

Then : **Ys_2 = 4.43 m.**

3) Computation of scour caused by Pier partially submerged in the flow.

According with sketch pier 17L Pearl River we considered:

K_1= Correction factor for pier nose shape = 1 (calculated for angle of attack up to 5 degrees)

According with HEC-18, we considered equivalent pier:

SECCTION A-A PIER 17L PEARL RIVER PIER EQUIVALENT

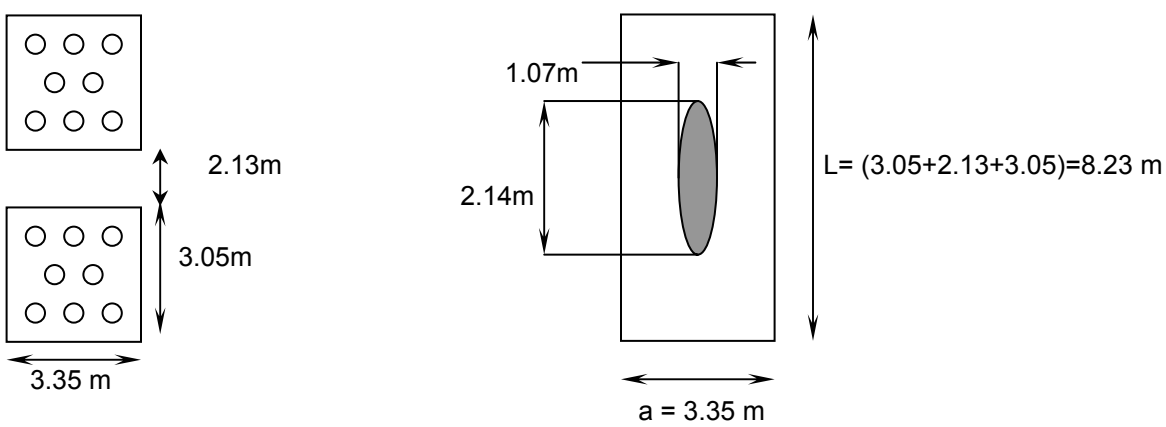

And K_2= (Cos 25º + 8.23m/3.35m x Sin 25º) $^{0.65}$ = 1.54 for pile cap
And K_2= (Cos 25º + 2.14m/1.07m x Sin 25º) $^{0.65}$ = 1.44 for pier

Then $K_{2\ average} = \dfrac{1.54 \times 1.07m + 1.44 \times 5.45\ m}{6.52\ m} = 1.46$

$a_{average} = \dfrac{3.35m \times 1.07m + 1.07m \times 5.45\ m}{6.52\ m} = 1.45\ m$

K_3= Correction factor for bed condition.- Adopted K_3= 1.1
K_4= Correction factor for armoring by bed material size. K_4= 1

Equation (1):
F_{R1}= 0.134
$Ys_1 = 6.52 \times 2.0 \times 1.0 \times 1.46 \times 1.1 \times 1.0 \times (1.45 / 6.52)^{0.65} \times (0.134)^{0.43}$

Then : **Ys_3 = 3.32 m.**

Scour depth results obtained event 5/1/91:

Scour caused by the exposed pile group: ..... Ys_1 = 5.42 m
Scour caused by Pile cap: ..... Ys_2 = 4.43 m
Scour caused by Pier partially submerged in the flow.... Ys_3 = 3.32 m

The scour depth for event 5/1/91 according with HEC-18 is: **Ys = 5.42 m.**

C- Computation scour depth expected at pier 17L over the next 50 years
Data:
Skew angle (θ) : 25º
Debris effect: Local
Pier scour in condiction "Live - bed"
Y_1= 8.90 m
V_1= 1.50 m/S
F_{R1}= 0.160

Computation of scour caused by the exposed pile group.
K_1= Correction factor for pier nose shape = 1 (calculated for angle of attack up to 5 degrees)

According with HEC-18, we considered equivalent pier:

SECCTION A-A PIER 17L PEARL RIVER

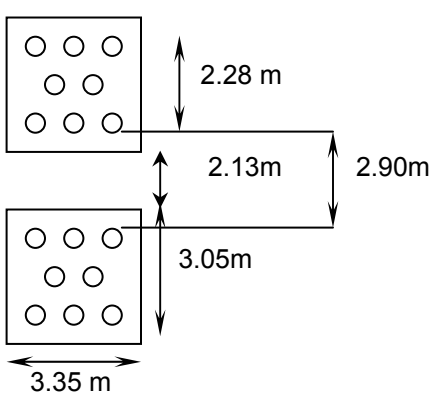

PIER EQUIVALENT

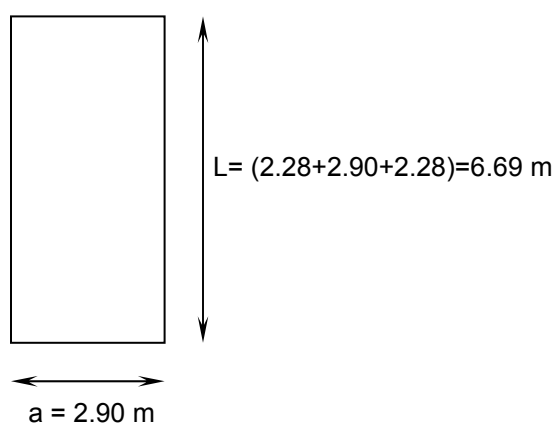

$K_2 = (\cos\theta + L / a \sin\theta)^{0.65}$
$K_2 = (\cos 25º + 6.69/2.90 \times \sin 25º)^{0.65} = 1.52$

K_3= Correction factor for bed condition.- Adopted K_3= 1.1

K_4= Correction factor for armoring by bed material size. K_4= 1

Equation (1):
$Ys_1 = 8.90 \times 2.0 \times 1.0 \times 1.52 \times 1.1 \times 1.0 \times (2.90 / 8.90)^{0.65} \times (0.160)^{0.43}$

Then : **$Ys_{50\ years}$ = 6.52 m.**

D - Computation scour depth expected at pier 17L for 500 year flood

Data:
Skew angle (θ) : 25º
Debris effect: Local
Pier scour in condiction "Live - bed"
Y_1= 9.60 m
V_1= 1.90 m/S
F_{R1}= 0.195

Computation of scour caused by the exposed pile group.
K_1= Correction factor for pier nose shape = 1 (calculated for angle of attack up to 5 degrees)

According with HEC-18, we considered equivalent pier:

SECCTION A-A PIER 17L PEARL RIVER

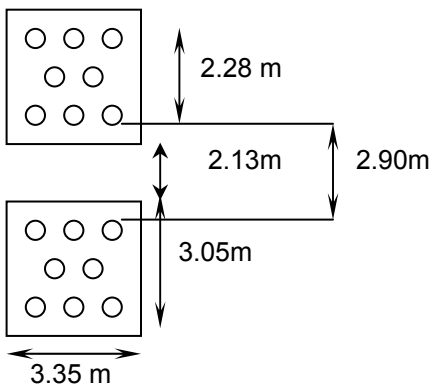

PIER EQUIVALENT

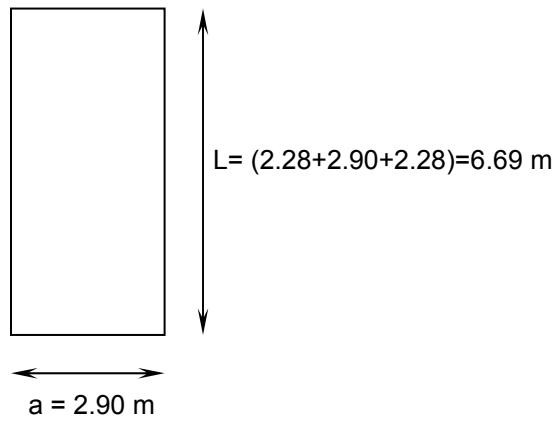

$K_2 = (\cos\theta + L / a \sin\theta)^{0.65}$
$K_2 = (\cos 25º + 6.69/2.90 \times \sin 25º)^{0.65} = 1.52$

K_3= Correction factor for bed condition.- Adopted K_3= 1.1
K_4= Correction factor for armoring by bed material size. K_4= 1

Equation (1):
$Ys_1 = 9.60 \times 2.0 \times 1.0 \times 1.52 \times 1.1 \times 1.0 \times (2.90 / 9.60)^{0.65} \times (0.195)^{0.43}$

Then : **$Ys_{500\ years}$ = 7.30 m.**

E - Additional data.
We had considered that the data was enough for this case.-

F – Best estimate of the cost for obtaining the additional data.
Is not necessary additional cost.-

IC Guillermo Ferrando
IRH Carlos Cian
11/07/2002.

ON THE PREDICTION OF THE MAXIMUM DEPTH OF A SCOUR HOLE AROUND CYLINDRICAL BRIDGE PIERS IN NON COHESIVE SOILS

By

Oscar Link[1] and Ulrich Zanke[2]

ABSTRACT

The requested predictions for the maximum depth of scour in non cohesive soil around bridge piers are calculated by using a semiempirical approach. The presented method was derived from the continuity equation of mass and a balance of the acting forces during scouring in a non-cohesive sediment bed. As part of the results, the calculated evolution of the maximum scour depth with time is also shown.

INTRODUCTION

In this paper we present a method to estimate the maximum depth of scour around a bridge pier and apply it to solve the cases 1, 2, 7 and 8 of the prediction event in which only non cohesive sediments are expected to be eroded. The method is based on equations similar to others of wide application like those proposed by Breusers et al (1977), Jain and Fischer (1980), Richardson (1987) cited in Yammaz and Cicekdag (2001) also known as CSU-equation, or Melville and Sutherland (1988). Our methodology is based on an equation derived by Zanke (1982a) and differs from the above mentioned methods in the fact that the maximum depth of scour is time dependent. Melville and Chiew (1999) derived an equation using dimensional analysis which also incorporates time as a variable. Nevertheless, these authors assumed an exponential law for the erosion rate and adjusted their parameters. Such a mathematical form had been previously suggested by other authors (see Hoffmans and Verheij, 1997) but the suggestions were only based on the fact that the observed scour depth was well correlated. Ting et al (2001) presented laboratory measurements of scour-depth-versus-time curves and fitted them with an hyperbola. These experiments were conducted on sand and clay mounted piers.

Zanke (1978a) proposed a general formula for sediment transport estimation. It is based on the forces acting on the soil particles and dimensional analysis. Under the assumption that the variation of the volume of a three dimensional scour hole is proportional to that of the scour surface perpendicular to the horizontal plane and directed to the pier, it is posible to solve three dimensional scour cases, such as scour around bridge piers, as the general bidimensional case. Zanke (1982a) rearranged his primitive function for bedload estimation into a general equation for the prediction of the maximum scour of depth around bridge piers. The resulting dimensionless parameters were determined based on laboratory measurements (Zanke 1982a) and on the data of Ettema (1980) cited in Zanke (1982b). A summary of the mathematical derivation of Zanke´s equation is given below. In this work, we implement an algorithm to calculate scour depth under unsteady flows. This is also briefly explained.

METHOD

It is well known that the variation of the solid discharge, Q_s, per unit of area, A, equals the variation of the scour depth, z, per unit of time, t. If the specific solid discharge per unit of width is q_s, then

$$\frac{\partial Q_s}{\partial A} = \frac{\partial Q_s}{\partial x \partial y} = \frac{\partial q_s}{\partial x} = \frac{\partial z}{\partial t} \tag{1}$$

$$t \approx \frac{A_l}{q_s} \tag{2}$$

[1] Postgraduate student.

[2] Professor.

Institute for Hydraulic and Water Resources Engineering, Darmstadt University of Technology. Rundeturmstraße 1, 64283 Darmstadt, Germany. E-mail: link@hrz2.hrz.tu-darmstadt.de

Where x means the principal direction of flow and A_l the scoured surface along the x direction. Zanke (1978b) corroborated Mosony's results (cited in Zanke 1982b) for a bidimensional scour case. They showed that the scoured surface is proportional to the second power of the scour depth, $A_l \approx z^2$. Measurements of bridge piers scour by Dargahi (1990) also confirm these results. The relationship used herein is

$$t \approx \frac{z^2}{q_s} \tag{3}$$

The specific solid discharge is then calculated by Zanke's bed-load transport formula (Zanke, 1978a), which was derived based on the fact that horizontal forces acting on soil particles, F_H tend to increment the bed-load when a critical trend is exceeded while vertical forces due to submerged weight , F_V tend to reduce it:

$$q_s \approx \left(\frac{F_H}{F_V}\right)^{\alpha} \tag{4}$$

$$q_s \approx \left(\frac{V^2 - V_{cr}^2}{w^2}\right)^{\alpha} \tag{5}$$

Where V is the velocity of flow, V_{cr} is the sediment entrainment velocity, w is the settling velocity of sediment particles in water and α is a coefficient. For cases in which flow depth exceeds 35 cm, and assuming a typical natural sand porosity of 30%, Zanke (1978a) proposed

$$q_s = 1.4 * 10^{-7} \left(V^2 - V_{cr}^2\right)^2 \left(\frac{D_*}{w}\right)^4 \nu \tag{6}$$

Where ν is the fluid cinematic viscocity, $D_* = \Delta g d_s^3 / \nu^2$ the sedimentologic diameter, $\Delta = \left(\rho_s - \rho_f\right)/\rho_f$ the relative density between the solid particles and the fluid, g the gravitational acceleration and d_s the representative sediment diameter.

The turbulence intensity in a scour hole due to the presence of a bridge pier is different to the case of an undisturbed flow. Based on Ettema's experimental data cited in Zanke (1982b), the latter related the flow velocity, V with an effective velocity, V_{ef} in front of the pier as follows

$$V_{ef} = \frac{V\omega}{1 + \frac{z}{b}} \tag{7}$$

Where ω represents an effective velocity increase due to the increment of turbulence caused by secondary flows. The term 1+z/b, where b is the pier diameter, is derived from the mass continuity condition. From eq. (3) follows

$$t \approx \frac{z^2}{q_s} \quad , \; V<V_{cr} \tag{8}$$

$$t \approx \frac{z^2}{q_s - q_0} \quad , \; V>V_{cr} \tag{9}$$

Where q_0 is the sediment specific discharge entering into the scour hole from the upstream bed-load. Following Eqs. (6) – (9), Zanke (1982b) proposed the following equation, valid for $0.4<V/V_{cr}<8.8$

$$t = \frac{1{,}94 z^2}{\left(\frac{D_*}{w}\right)^4 \nu \left\{ \left[\left(\left(\frac{V\omega}{1+\frac{z}{b}} \right)^2 - V_{cr}^2 \right) \frac{V}{V_{cr}} \right]^2 - \left(V^2 - V_{cr}^2 \right)^2 \right\}} \tag{10}$$

The settling velocity of sediment particles in water, w and the sediment entrainment velocity, V_{cr} are calculated by Zanke's equations (Zanke, 1977b and Zanke, 1977a, respectively):

$$w = \frac{11\nu}{d_s}\left(\sqrt{1+0.01D_*^3} - 1\right) \tag{11}$$

$$V_{cr} = 1{,}4\left(2\sqrt{g\Delta d_s} + 10{,}5\frac{\nu}{d_s}\right) \qquad , h > 0.35m \tag{12}$$

Since the equilibrium depth of scour is reached when time tends to infinity, from Eqs. (8)-(10) it follows that

$$\frac{z}{b} = \left(\frac{V}{V_{cr}}\omega - 1\right) \qquad , V<V_{cr} \tag{13}$$

$$\frac{z}{b} = \left(\frac{\omega}{\left(\frac{V_{cr}}{V} + \frac{V_{cr}^2}{V^2} - \frac{V_{cr}^3}{V^3}\right)^{0.5}} - 1\right) \qquad , V>V_{cr} \tag{14}$$

Because the erosion capacity or scour rate of a given flow is time dependent, i.e.:$\partial z/\partial t \neq$ constant, different scour depths will develop under the action of identical discharges depending upon initial geometrical conditions, $z_{t=0}$. Therefore, the initial depth of scour should be considered in depth scour computations.

The time evolution of the maximum scour depth caused by an unsteady flow can be treated as a succesion of different constant discharges flowing over the bed during given periods. It is neccesary to determine an equivalent initial time at which the new discharges start to erode. This equivalent initial time represents the period that a new discharge needs to erode the actual or initial scour depth. Figure 1 shows a flow diagram for the computation of scour depth under unsteady flow. The equivalent initial time is called t_{dummy}.

To automatise the presented methodology we approximated Ettema's data (Ettema, 1980 cited in Zanke, 1982b) by a polynom of order six with a correlation coefficient, r^2=0.999. This regression is valid in the range of the original data, 0.01< z/b < 2.5.

RESULTS

As mentioned before, we only solved those cases without cohesive soils, i.e. cases 1, 2, 7 and 8 of the prediction event. The predictions are summarized in Table 1. In the cases 1 and 2, we assumed a particle density of 2.65 t/m^3.

In the flume case 1 the scour depth at the end of the first day is estimated to be about 64% of the equilibrium depth scour, which should be about 0.24 m after 3.67 years subjected to the given conditions. In the second case, it is estimated that the resulting scour depth should take only about 2.15 days to develop, when subjected to a constant velocity of to 0.35 m/s, and about 36 days when subjected to a constant velocity of 0.25 m/s. Figure 2 shows the calculated time evolution of the maximum depth of scour for cases 1 and 2.

To calculate the scour depth of both Bridge site cases, we made a spline interpolation of the given hydrograph, in order to obtain hourly discharges. We correlated discharge with velocity and depth data by fitting a potential curve as proposed by Leopold and Madock (1992, pp. 215). The correlation coefficients for the cases 7 and 8 were r^2=0.992 and r^2=0.994 respectively. Because the fitted values varied in a wide range, the regression allowed us the estimation of the hourly velocities without need of extrapolation.

Figure 3 shows the prediction of the maximum scour depth in the bridge site case 7 during the 8.3.93 flood. In the calculations, we assumed that at the beginning of the flood there was no scour depth.
The prediction of the maximum scour depth in the bridge site case 8 during the 5.1.91 flood is showed in figure 4. It is possible that this flood did not cause any erosion, since other important flood events had taken place before. We considered two cases: (a) the bridge presents no scour depth, z =0 during the summer and (b) the bridge presents no scour depth, z =0, at the beginning of the 5.1.91 flood. Quiet a different evolution of the scour depth in time resulted for cases (a) and (b), but the same maximum depth of scour after the 5.1.91 flood. In both situations it was z =1.76m.
To predict the scour depth after the next 50 years, we based on the idea of bankfull discharge as they are supposed to have a 1 to 5 years recurrence interval and they occur most of the time. Mathematically, the probability of excedance of a given discharge is equal to the inverse of its recurrence interval. A discharge with T=5 will be probably exceeded during the 1/5 of the time. For the present case, it means about 10 years.
We first calculated how long a discharge needs to be exceeded so that the equilibrium scour depth is reached. Under the given conditions, bankfull discharges will probably cause the equilibrium scour if they are exceeded during about 4 years, not necessarily uninterrupted. It is expected that under bankfull conditions the velocities range between about 0.85 and 1.1 m/s.
A discharge with the magnitude of the 500-year's one should take about 10 days to cause the equilibrium depth. The given hydrograph shows that floods take usually longer than 10 days to develop their rising and recession stages. In consequence, if within the next 50 years there is at least one 500-year flood we estimate that equilibrium scour depth associated with this extrem discharge will develop, z = 2.52 m.

Table 1- Predictions

Test description	Maximum depth of scour hole (m)
Flume case 1	0.15
Flume case 2	0.17
Bridge site case 7, 8-3-93 flood	10.06
Bridge site case 8, 5-1-91 flood	1.76
Bridge site case 8, 50 years prediction	2.52

DISCUSSION AND FINAL REMARKS

In this paper we estimate the maximum depth of a scour hole around bridge piers in non cohesive soils based on Zanke's attempt (Zanke, 1982a). The equations used herein, are not valid for cohesive soils. Following the results obtained by Ting et al. (2001) it is expected that similar equilibrium scour depth will develop on cohesive and non cohesive soils. Nevertheless, the rate of scouring is much slower in clay than in sand.
Our predictions are valid for single cylindrical piers in a sediment bed. The bridge site cases 7 and 8, include groups of two in line piles mounted on rectangular caissons. Breusers and Raudkivi (1991, pp. 85-86) indicate that, depending on the relative spacing between the piles, the expected scour depth at the front pile increases about 10-20% under the conditions given in the aforementioned cases (relative spacing of about 4). On the other hand, a foundation caisson should provide scour protection. Chabert and Engeldinger (1956) and Shen and Schneider (1970) cited in Breusers et al. (1977) investigated the effect of a circular caisson having a diameter three times the diameter of the pier and a variant of the caisson system in which the caisson is sourrounded by a vertical lip (cut-of sheet-pile) respectively. Their results showed that scours were reduced up to 35-50% of that reached with the pier alone. We estimate that the afore mentioned effects tend to cancel each other under the given conditions and therefore our bridge site case predictions should provide a reasonable estimate of the asked scour depth.
As all known sediment transport predictions are less exact, we assume our results of the time dependent scour elevation to be more insecure in time than in elevation.

ACKNOWLEDGEMENTS

The financial support provided by the Deutscher Akademischer Austauschdienst (DAAD) is greatly acknowledged.

REFERENCES

1. Breusers, H., Nicollet, G., Shen, H., 1977, “Local Scour around Cylindrical Piers”. J. of Hydraulic Research, Vol 15, No. 3.
2. Breusers, H., Raudkivi, A., 1991, “Scouring“. A.A. Balkema Rotterdam. pp. 143.
3. Dargahi, B., 1990, “Controlling Mechanism of Local Scouring”. J. of Hydraulic Engineering, Vol 116, No. 10.
4. Hoffmans, G, Verheij, H.,1997, “Scour Manual”. A.A. Balkema Rotterdam. pp. 205.
5. Jain, S., Fischer, E., 1980, „Scour Around Bridge Piers at High Velocities”. J. of the Hydraulics Division, Vol 106, No. HY11.
6. Leopold, L., Wolman, M. and Miller, J., 1992, “Fluvial Processes in Geomorphology”. Dover Publications, New York. pp. 522.
7. Melville, B. ,Chiew, Y., 1999, “Time scale for Local Scour at Bridge Piers”. J. of Hydraulic Engineering, Vol 125, No. 1.
8. Melville, B., Sutherland, A., 1988, „Design Method for Local Scour at Bridge Piers“. J. of Hydraulic Engineering, Vol 114, No. 10.
9. Ting, F., Briaud, J., Chen, H., Gaudavalli, R., Perugu, S., Wei, G., 2001, “Flume Tests for Scour in Clay at Circular Piers”. J. of Hydraulic Engineering, Vol 127, No. 11.
10. Yammaz, A., Cicekdag, O., 2001, “Composite Reliability Model for Local Scour Around Cylindrical Bridge Piers”. Can. J. Civ. Eng. 28: 520-535.
11. Zanke, U., 1977, “Neuer Ansatz zur Berechnung des Transportbeginns von Sedimenten unter Strömungseinfluß”. Mitteilungen des Franzius-Instituts. Universität Hannover. Heft 46. pp. 157-178.
12. Zanke, U., 1977, “Berechnung der Sinkgeschwindigkeiten von Sedimenten”. Mitteilungen des Franzius-Instituts. Universität Hannover. Heft 46. pp. 230-261.
13. Zanke, U., 1978, “Zusammenhänge zwischen Strömung und Sedimenttransport. Teil 1”. Mitteilungen des Franzius-Instituts. Universität Hannover. Heft 47. pp. 214-345
14. Zanke, U., 1978, “Zusammenhänge zwischen Strömung und Sedimenttransport. Teil 2”. Mitteilungen des Franzius-Instituts. Universität Hannover. Heft 48. pp. 1-96.
15. Zanke, U., 1982, “Kolke am Pfeiler in richtungskonstanter Strömung und unter Welleneinfluß”. Mitteilungen des Franzius-Instituts. Universität Hannover. Heft 54. pp. 381-416.
16. Zanke, U., 1982, “Grundlagen der Sedimentbewegung“. Springer Verlag. pp. 402.

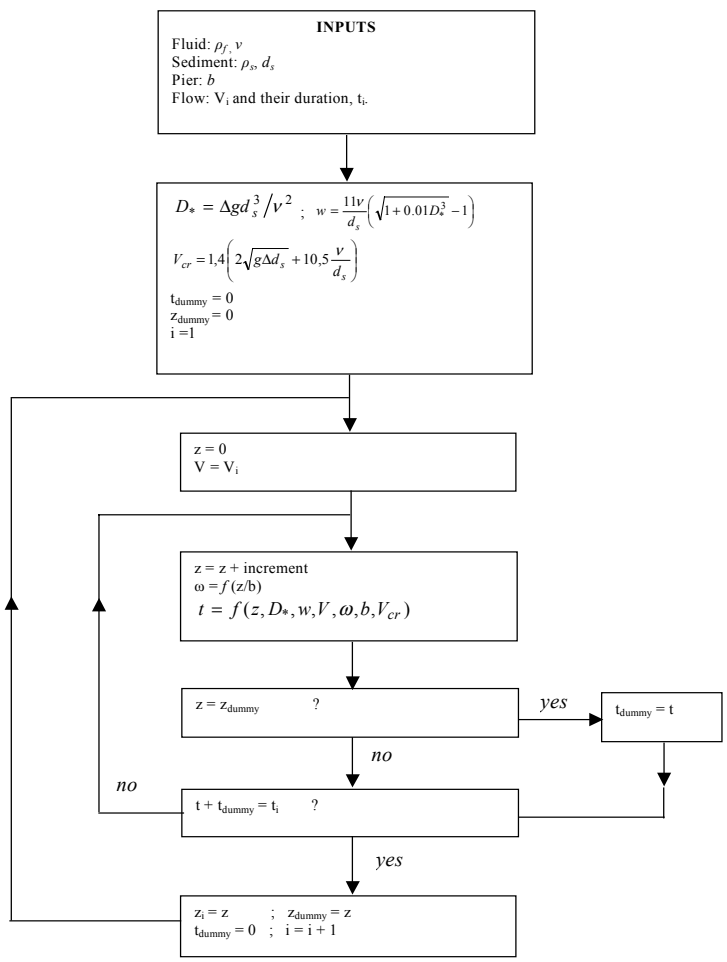

Fig. 1- Flow diagram for the computation of scour depth around a bridge pier under unsteady discharge.

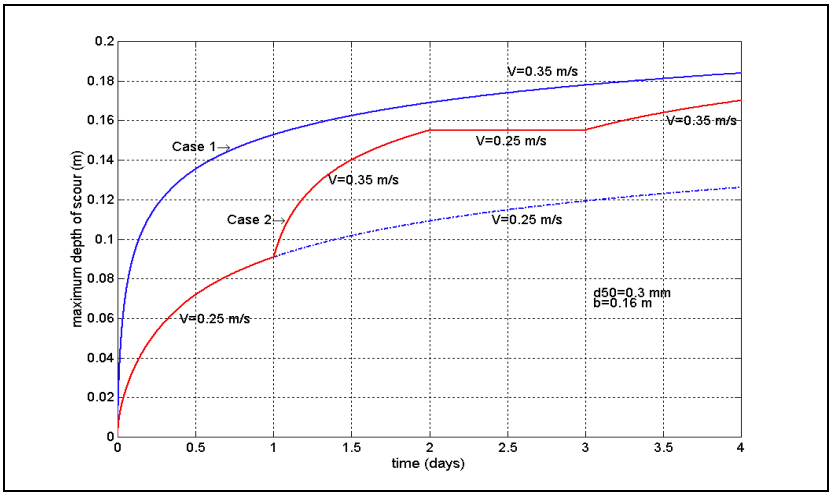

Fig. 2– Time dependence of the maximum depth of scour, for cases 1 and 2.

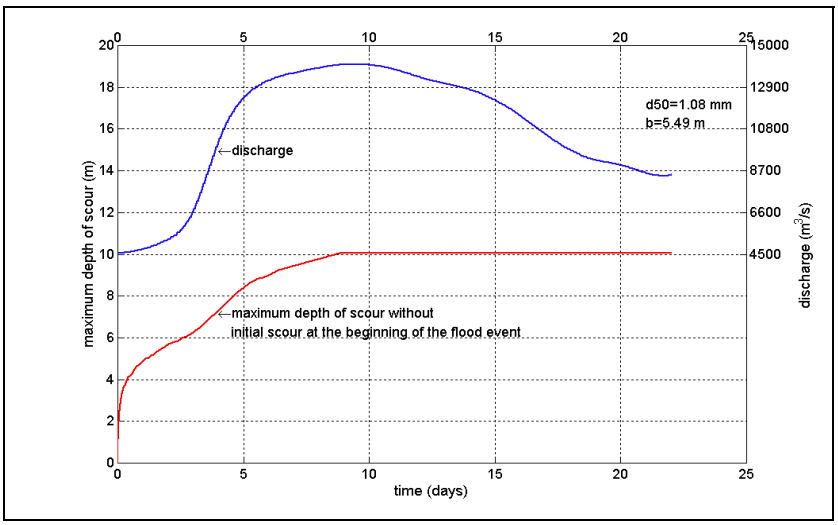

Fig. 3- Solution of the bridge site case 7, assuming no scour at the beginning of the flood event. Additionally, discharge is also plotted.

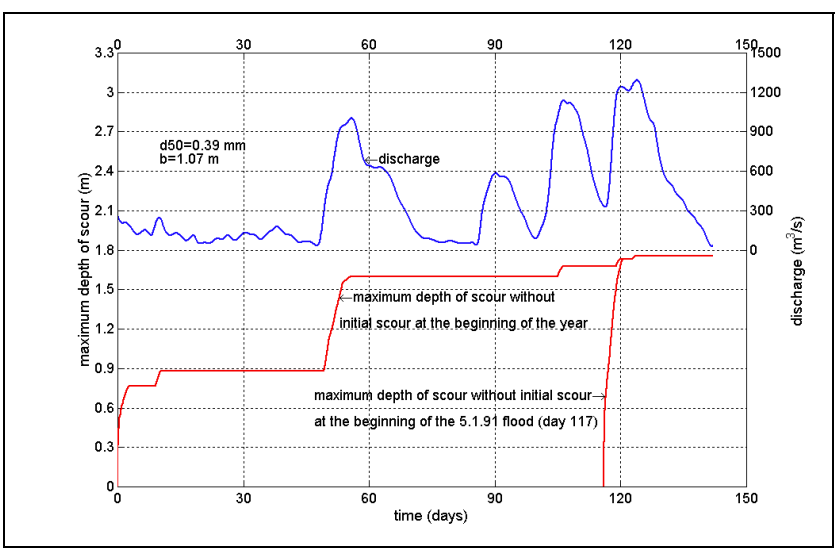

Fig. 4 - Solution of the bridge site case 8 without initial scour at the beginning of the flood event and without initial scour at the beginning of the year. Additionally, discharge is also plotted.

1 INTRODUCTION

This note deals with the prediction of scour in a total of 8 cases consisting of 6 flume test predictions and 2 actual case studies. The Committee of the First International Conference on Scour of Foundations has delivered the cases to the participants of this conference to be held on November 17-19, 2002.

Van Oord ACZ is pleased to contribute to the understanding and prediction of scour of foundations.

2 FLUME TEST PREDICTIONS

2.1 SOIL PROPERTIES AND FLOW DATA

Information provided by the Committee of the ICSF-1 on the soils used in the flume test predictions has been summarised in Table 1 and 2. The relevant flow data as used in the experiments is listed in Table 3.

Table 1: Soil properties porcelain clay

w_L	w_P	w_N	PI	LI	ρ_s	d_{50}	s_u
[%]	[%]	[%]	[%]	[%]	[kg/m^3]	[μm]	[kPa]
33	17	24.2	16	35	2700	3	23.3

w_L liquid limit
w_P plastic limit
w_N water content
PI: Plasticity Index
LI: Liquidity Index

Table 2: Soil properties mortar sand

ρ_s	d_{50}
[kg/m^3]	[μm]
2600	300

Table 3: Flow data

Water temperature	Flow depth	Flow width	Diameter pile
[°]	[m]	[m]	[m]
25	0.375	2	0.160

2.2 METHODOLOGY

The first step in the scour calculations consists of the assessment of the critical mean velocity U_0, which can then be used to determine the calculation method. For the fume test predictions, the approach to the scour prediction by Breussers[1] and Teramoto[2] has been used. These methods are valid for a pile or pier diameter b versus flow depth h_0 ratio of $b/h_0 < 1$.

2.2.1 Critical velocity

Based on the character of the soil, (1) non-cohesive and (2) cohesive, a distinction in methodology has to made the assessment of the critical velocity:

(1) Non-cohesive soils

According to Shields[3], critical mobility factor Ψ_c is equal to:

$$\psi_c = \frac{u^2{}_{*,c}}{\Delta g d_{50}} \qquad [1]$$

In which:

$u_{*,c}$=	critical bed-shear velocity	[m/s]
g =	acceleration of gravity	[m/s^2]
Δ =	relative density (=$\rho_{solid}/\rho_{water}$ – 1)	[-]
d_{50} =	median grain size	[m]

For a uniform flow on a hydraulically rough surface the mean critical velocity equals

$$U_c = u_{*,c}\frac{C}{\sqrt{g}} \qquad [2]$$

Where the Chézy coefficient is given by

$$C = \frac{\sqrt{g}}{\kappa}\ln\left(\frac{12h_0}{k_s}\right) \qquad [3]$$

In which:

U_c =	mean critical velocity	[m/s]
κ =	constant of Karman = 0.4	[-]
h_0 =	flow depth	[m]
k_s =	equivalent roughness of Nikuradse. Rough flow, k_s=3d_{50} and in case of a smooth flow, k_s=2d_{50}	[m]

If the width B of the flow is large in comparison to the flow depth h_0, the first equation can be rewritten as:

$$U_c = 2.5\sqrt{\psi_c \Delta g d_{50}}\ \ln\left(\frac{12h_0}{k_s}\right) \qquad [4]$$

With the use of the sedimentological diameter D_* (Van Rijn[4]) equation 4 can be solved by using the relation between Ψ and D_* listed in Table 4.

$$D_* = d_{50}\left(\frac{\Delta g}{\upsilon}\right)^{1/3} \ with\ \ \upsilon = \frac{40.10^{-6}}{20+T} \qquad [5]$$

In which:	ν =	kinematic viscosity	[m^2/s]
	T =	water temperature	[°]

Table 4: Relation of sedimentological diameter D_* with critical mobility factor Ψ_c

Relation	In case of
$\Psi_c=0.24D_*^{-1}$	$D_* \leq 4$
$\Psi_c=0.14D_*^{-0.64}$	$4 < D_* \leq 10$
$\Psi_c=0.04D_*^{-0.10}$	$10 < D_* \leq 20$
$\Psi_c=0.013D_*^{0.29}$	$20 < D_* \leq 150$
$\Psi_c=0.055$	$D_* > 150$

(2) Cohesive soils

Based on the work of Mirtskhoulava[5], the mean critical velocity for cohesive soils equals:

$$U_c = \log\left(\frac{8.8h_0}{0.004}\right)\sqrt{\frac{0.4}{\rho_{water}}\left(0.004g\left(\rho_{solid}-\rho_{water}\right)+0.021C_0\right)} \qquad [6]$$

In which:	C_0 =	cohesion	[N/m^2]
	ρ_{solid} =	density solid material	[kg/m^3]
	ρ_{water} =	density water	[kg/m^3]

2.2.2 Scour calculation

The time dependent relation for clear water scour can be calculated using the equations developed by Teramoto and Breussers. Both methods are valid for slender bridge piers in which the pier diameter b versus flow water depth h_0 ratio (b/h_0) < 1.

Teramoto

$$y_m = 0.072h_0\left(\frac{u_*}{u_{*,c}}\right)^{2.75}\left(\frac{Fr^2U_0t}{h_0}\right)^{0.364} \quad with\ Fr = \frac{U_0}{\sqrt{gh_0}} \qquad [7]$$

In which:	Fr =	Froude number	[-]
	U_0=	depth average flow velocity	[m/s]
	$u_{*,c}$=	critical bed-shear velocity	[m/s]
	g =	acceleration of gravity`	[m/s^2]
	h_0 =	water flow depth	[m]
	t =	time	[s]
	y_m=	maximum scour depth at time	[m]

This equation is only valid for situations where the flow velocity is relatively small, ergo $U_0/U_c < 1$.

Breussers

The following relation, providing that the equilibrium scour depth exceeds the diameter of the bridge pier can describe the maximum scour depth.

$$y_m = y_{m,e}\left(1 - e^{\ln\left(1-\frac{b}{y_{m,e}}\right)\left(\frac{t}{t_1}\right)^{\gamma}}\right) \qquad [8]$$

In which:

y_m=	maximum scour depth at time t	[m]
$y_{m,e}$=	maximum scour depth in equilibrium phase	[m]
t =	time	[s]
t_1=	characteristic time at which y_m = b	[s]
b =	width of pier	[m]
γ =	Coefficient between 0.2 and 0.4	[-]

The characteristic time can be written as:

$$t_1 = 29.2\frac{b}{\sqrt{2U_0}}\left(\frac{\sqrt{\Delta g d_{50}}}{\sqrt{2U_0 - U_c}}\right)^3\left(\frac{b}{d_{50}}\right)^{1.9} \qquad [9]$$

In which:

U_0=	depth average flow velocity	[m/s/
U_c =	mean critical velocity	[m/s]
g =	acceleration of gravity	[m/s^2]
Δ =	relative density (=$\rho_{solid}/\rho_{water}$ –1)	[-]
d_{50} =	median grain size	[m]

The relation of the ratio U_0/U_c with the equilibrium scour depth can be described for the following three conditions:

1. $\frac{U_o}{U_c} \leq 0.5$

   No scouring will occur.

2. $0.5 < \frac{U_o}{U_c} < 1$

   The equilibrium scour depth $y_{m,e}$ can be described with:

$$y_{m,e} = 2K_i b\left(\frac{2U_0}{U_c} - 1\right)\tanh\left(\frac{h_0}{b}\right) \qquad [10]$$

In which: K_i = Correction factor for pier shape, bed gradation, flow direction and pier group. This factor is in case of the flume tests equal to 1 [-].

3. $\frac{U_o}{U_c} > 1$

The equilibrium scour depth can be described with:

$$y_{m,e} = 1.5 K_i b \tanh(\frac{h_0}{b}) \qquad [11]$$

2.3 CALCULATION RESULTS

The calculation results have been summarised in Table 5. The scour has also been calculated using the SRICOS method as described by Briaud, Chen and Ting[6].

From the results it can be deduced that the “conventional methods” of Breussers and Teramoto are in the same order as the results obtained with the SRICOS method.

Table 5: Results scour depth predictions of flume tests

Test description	**Maximum depth of scour hole when the flume test stops [mm]**		
	Breussers	**Teramoto**	**Sricos**
Flume case 1: 160 mm diameter circular pier placed in clean sand deposit and subjected to a constant velocity over a period of one day.	230	N/A Approach velocity is too high	190
Flume case 2: 160 mm diameter circular pier placed in a clean sand deposit and subjected to a multi-velocity hydrograph over a period of 4 days.	233	N/A Approach velocity is too high	191
Flume case 3: 160 mm diameter circular pier placed in clay deposit and subjected to a constant velocity over a period of 30 days.	N/A Approach velocity is too low	38	182.6
Flume case 4: 160 mm diameter circular pier placed in a uniform clay deposit and subjected to a multi-velocity hydrograph over a period of 4 days.	N/A Approach velocity is too low	14.3	109.2
Flume case 5: 160 mm diameter circular pier placed in a sand over clay layered soil and subjected to a constant velocity flow over a period of 10 days.	Combined: first Breussers and than Teramoto 105.6		233.3
Flume case 6: 160 mm diameter circular pier placed in a clay over sand layered soil and subjected to a constant velocity flow over a period of 10 days.	N/A Approach velocity is too low	25.6	281

3 BRIDGE SITES PREDICTION

3.1 CASE 7: MISSISSIPPI RIVER BRIDGE

3.1.1 Soil and flow properties

The soil and flow properties during the 8/3/93-flood event have been summarised in the Tables 6 and 7.

Table 6: Soil properties sand riverbed Mississippi

ρ_s	d_{84}	d_{50}	d_{16}
[kg/m^3]	[μm]	[μm]	[μm]
2600	1300	600	300

Table 7: Flow data

Date	Water temperature	Approach depth	Approach velocity	Skew angle	Sediment Transport	Flow width	Width pile
[-]	[°]	[m]	[m/s]	[°]	[-]	[m]	[m]
8/3/93	15	22.52	2.429	11	Life bed	518	7.32
8/12/93	15	22.37	2.000	4	Life bed	518	7.32
9/13/93	15	16.70	1.838	4	Life bed	518	7.32

3.1.2 Calculation method

For life bed scour, the equilibrium scour depth $y_{m,e}$ can be described according to Breussers:

$$y_{m,e} = 1.35 K_i b^{0.7} h_0^{0.3} \qquad [12]$$

In which:
- b = width of pier [m]
- h_0 = water flow depth [m]
- K_i = correction factor for pier shape, bed gradation, flow direction and pier group [-]

The factor K_i consists of four different correction factors:

$$K_i = K_s K_\omega K_g K_{gr} \qquad [13]$$

In which:
- K_s = pier shape factor [-]
- K_ω = factor for orientation of pier to the flow [-]
- K_g = factor for the influence of groups an piers [-]
- K_{gr} = factor for the influence of the bed material grading [-]

Pier shape
The pier shape factor K_s can be deduced from Table 8 after Laursen & Toch[7]., Neill[8] and Dietz[9].

Table 8: Pier shape factor K_s

Form of cross section	K_s
Horizontal	
Lengticular	0.7 to 0.8
Elliptic	0.6 to 0.8
Circular	1.0
Rectangular	1.0 to 1.2
Vertical	
Pyramid	0.76
Inverted pyramid	1.2

The pier shape factor K_s equals 0.75 for this type of lengticular pier.

Orientation
The relation of skew angle and flow can be expressed as the factor K_ω and has been described by Froehlich[9]:

$$K_\omega = \left(\cos\omega + \frac{L_p}{b} \sin\omega \right)^{0.62} \qquad [14]$$

In which: ω = skew angle [°]
L_p= length of pier [m]
b = width of pier [m]

With a skew angle of 11 degrees, the factor K_ω is equal to 1.23.

Gradation bed material
The influence of the bed gradation has been investigated by Vanoni[9] and can be expressed as the (graphical) relation of σ_g (equal to the ratio of d_{84}/d_{50}) shown in Figure 1.

Figure 1: Graphical relation K_g with ratio of d_{84}/d_{50}

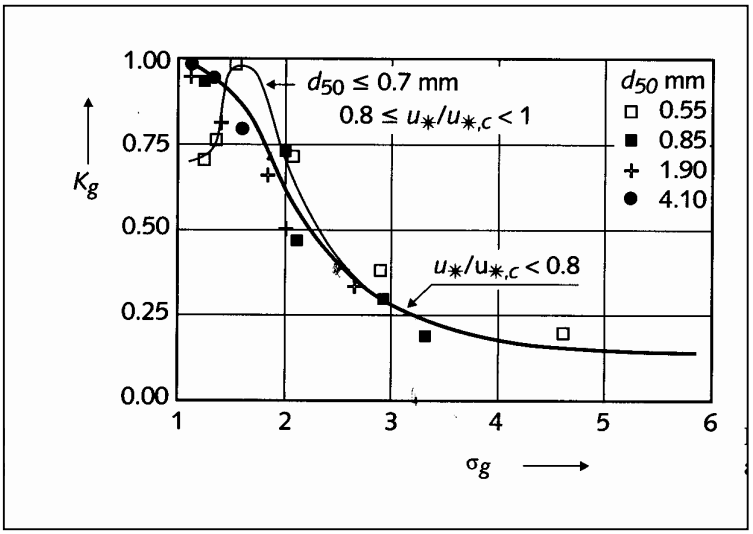

The bed material of the riverbed near pier 11 has a σ_g equal to 4.3 and thus a factor K_g of 0.18.

Group of piers

Breussers and Raudkivi[11] have described the influence of the spacing between circular piers on the scour depth. In general, if the spacing is more than 8b, in which b is the pier width, the influence can be ignored and K_{gr} = 1, see Table 10.

Table 10: Factor K_{9r} for a group of circular piers

	Configuration		Pier spacing	Front pier K_{9r}	Rear pier K_{9r}
1			[m]	[-]	[-]
	O	O	1b	1.0	0.9
			2 to 3b	1.15	0.9
			> 15b	1.0	0.8
2	O		1b	1.9	1.9
		O	5b	1.15	1.2
			> 8b	1.0	1.0
3	O	O	1b	1.9	1.9
			2 to 3b	1.2	1.2
			> 8b	1.0	1.0

The pier spacing is approximately 9 times b so that K_{gr} = 1.

3.1.3 Calculation results

The scour created by the 8/3/93-flood event is according the calculations equal to 9 m.
After the water discharge decreases, the approach velocity and water flow depth will decrease to the average approximately 1.8 m/s and 16.7 m. The scour depth according to the latter averages equals 7.3 m.

The flood-induced scour is therefore equal to 1.7 m.

Additional data required:
- None when using the above-mentioned method.

3.2 CASE 8: PEARL RIVER BRIDGE

3.2.1 Soil and flow properties

The nature of the soil samples taken from the vicinity of pier 17 can not be clearly assessed from the provided data. For the scour calculations, we assume that the riverbed in the vicinity of pier 17 consists of sand.

The soil and flow properties of the riverbed in the vicinity of pier 17 have been summarised in the Tables 10 and 11.

Table 10: Soil properties sand riverbed Pearl River

Sample	ρ_s	d_{84}	d_{50}	d_{16}	Location sample
[-]	[kg/m^3]	[μm]	[μm]	[μm]	[-]
1	2600	1200	540	360	Mid-span piers 16 and 17
2	2600	900	390	260	Vicinity of piers 17 and 18

Table 11: Flow data

Date	Approach depth	Approach Velocity	Sediment Transport	Width pile	Event
[-]	[m]	[m/s]	[-]	[m]	[-]
05/1/95	6.9	1.2	Unknown	3.35	5/1/95 flood
N/A	8.9	1.5	Unknown	3.35	50 yr flood event

3.2.2 Calculation method

The provided data leads to the assumption of a non-existing bed load implying that the equilibrium scour depth can be described according to Breussers using equation 10 and 11 depending on the critical velocity.

The critical velocity, based on the data of the 5/1/91-flood event is equal to 0.38 m/s, which implies a ratio of U_0/U_c of 4 so that equation 11 has to be used.

Since the approach flow velocity in case of a 1 to 500 year flood is even larger than the velocity measured at during the 5/1/91-flood event, equation 11 can also be used to predict the scour depth.

The K_i factor has a lower and upper limit of 0.25 and 0.20 due to the large difference in the gradation in the bed material, expressed in the parameter d_{84} and d_{50}. The K_i factor has been calculated from the following values:

Pier shape factor K_s: 0.75 (lengticular pier shape)
Orientation factor K_ω: 1.0 (skew angle =0)
Bed gradation factor K_g: 0.25 for sample1 and 0.20 for sample 2
Group factor K_{gr}: 1.3 (configuration 1 with pier spacing of 1.7b)

3.2.3 Calculation results

Based on the data mentioned above, the scour depth during the 5/1/91-floodevent equals 0.9 to 1.2 m, depending on the coarseness of the bed material. Since there is no flow data for an average situation, the extra scour induced by this flood event can not be calculated.

During a 50-year period incorporating a 1 to 500 year flood event, the maximum scour depth is equal to 1.0 to 1.3 m, depending on the coarseness of the bed material.

Additional data required:

- Average flow velocities and flow depth averages during normal conditions. Also, EFA experimental data could improve the assessment of the final scour depth.

LIST OF REFERENCES

[1] Breussers, H.N.C., G. Nicolet and H.W. Chen, 1977: *Local scour around cylindrical piers,* Journal of Hydraulic Research, IAHR, p. 211-215, Delft, Netherlands;
[2] Teramoto, S, 1973: *Study on scouring of sit on bottom type offshore structure*, Mitsubishi Heavy Industries Ltd, Japan;
[3] Shields, A, 1936: *Anwendung der Ahnlichtingsmechanik und der Turbulenzforschung auf die Geschiebebegewegung,* Mitteilungen Preussisschen Versuchtanstalt fur Wasser und Schiffbau, Berlin, Germany;
[4] Van Rijn, L.C., 1984: *Sediment transport Part I: Bed load transport, Part II: Suspend load transport, Part III: Bedforms and alluvial roughness*, Journal of Hydraulic Engineering, Delft, Netherlands;
[5] Mirtskhoulava, Ts.Ye., 1988: *Basic physics and mechanics of channel erosion*, Gidrometaoizdat, Leningrad, Russia;
[6] Briaud, J.L., Chen, H.C. Kwak, K. 2000: *The Scricos method: a summary*, provided by the Committee on the First International Conference on Scour of Foundations, Texas, USA;
[7] Laursen, E.M, and Toch, 1956: *Scour around bridge piers and abutments*, Bulletin 4, Iowa Highway Research Board, State University of Iowa, USA;
[8] Neill, C.R., 1968: *Guide to Bridge Hydraulics*, University of Toronto Press, Canada;
[9] Dietz, J.W., 1972: *Ausbildung von langen Pfeilern bei Schraganstromung am Beispiel der BAB Mainbrucke Eddersheim*, Mitteilungsblatt der BAW, Karlsruhre, Germany;
[10] Vanoni, V.A., 1977: Sedimentation Engineering, ASCE, New York, USA;
[11] Breussers, H.N.C. and Raudkivi, A.J., 1991: *Scouring*, Rotterdam, Netherlands;
[12] Hoffmans G.J.C.M. and H.J. Verheij, 1997: *Scour Manual*, A.A. Balkema, Rotterdam, Netherlands.

PREDICTION OF LOCAL SCOUR OF NON-COHESIVE SEDIMENT AROUND BRIDGE PIERS USING FVM-BASED CCHE2D MODEL

By

Weiming Wu[1] and Sam S.Y. Wang[2]

ABSTRACT

The FVM-based CCHE2D model is a depth-averaged 2-D numerical model for flow and sediment transport in open channels. It is enhanced to simulate the local scour around hydraulic structures after modifying Wu et al's (2000) sediment transport capacity formulas to account for the influences of pressure gradient and turbulence intensity on sediment movement. Preliminary tests using 34 sets of experimental data from bridge piers and spur dikes show that the measured and simulated maximum scour depths are in good agreement. The FVM-based CCHE2D model is applied to simulate the local scour around bridge piers in ICSF-1 test cases 1 and 2. The predicted maximum scour depths are 0.182m and 0.205m, respectively, with a margin of about ±20% errors.

INTRODUCTION

The local scour around hydraulic structures is a very complicated three-dimensional phenomenon, and the prediction of the scouring process is very challenging. Many empirical formulas have been established by using experimental measurements. These formulas usually are limited to providing some lumped information on the maximum scour depth, the scour volume, etc., under constant flow conditions. In order to provide more detailed information on the local scour process in more general situations, numerical modeling has been applied to this field recently. Because of the complexity of flow and sediment transport in the vicinity of hydraulic structures, a three-dimensional numerical model is usually required. However, the cost of three-dimensional modeling is still very high. Recently, we are trying to establish the local scour prediction capability in the depth-averaged 2-D numerical model, FVM-based CCHE2D. Some promising progress has been achieved. The FVM-based CCHE2D is applied to simulate the test cases proposed by the First International Conference on Scour of Foundation (ICSF-1). Introduced in this paper are the modeling techniques, model calibration and prediction results.

BRIEF DESCRIPTION OF THE FVM-BASED CCHE2D MODEL

The FVM-based CCHE2D flow model is a depth-averaged 2-D model for open-channel flows. It solves the two-dimensional depth-averaged shallow water equations by using the finite volume

[1] Research Assistant Professor, National Center for Computational Hydroscience and Engineering, The University of Mississippi, MS 38677, USA, (wuwm@ncche.olemiss.edu)
[2] F.A.P. Barnard Distinguished Professor and Director, National Center for Computational Hydroscience and Engineering, The University of Mississippi, MS 38677, (wang@ncche.olemiss.edu)

method on a non-staggered (collocated) curvilinear grid system. The SIMPLE and SIMPLEC algorithms in conjunction with Rhie and Chow's (1983) momentum interpolation technique are used to solve the pressure-velocity coupling problem. The convection terms in the governing equations can be discretized by four numerical schemes: hybrid upwind/central scheme, exponential scheme, QUICK scheme and HLPA scheme. The turbulence stresses can be determined by five turbulence models, including the depth-averaged parabolic model, mixing length model, "sub-grid" model, standard k-ε turbulence model and RNG k-ε turbulence model. The FVM-based CCHE2D flow model can simulate steady and unsteady flows in rivers and estuaries.

The FVM-based CCHE2D sediment transport model (Wu and Wang, 2002) simulates the non-equilibrium transport of nonuniform total-load sediment. The bed load and suspended load are calculated separately or jointly according to sediment transport modes. The non-cohesive sediment transport capacity is determined by four formulas: Wu et al's (2000) formula, the SEDTRA module, the modified Ackers and White's formula and the modified Engelund and Hansen's formula. The governing equations are discretized by the finite volume method in curvilinear grid, which is the same as that used in the flow model. The model has been tested in many experimental and field cases of general sediment transport under gradually-varying flow conditions.

However, the above-mentioned FVM-based CCHE2D model, which was designed for general sediment transport modeling, cannot be applied to local scour simulation. For this purpose, certain enhancements must be made. For simulating the local scour due to jet impingement and headcut migration using a three-dimensional numerical model, Wu et al's (1999) modified van Rijn's (1989) sediment transport formulas by introducing several correction factors to take into consideration the influences of the dynamic pressure gradient, downward flow, bed slope and turbulent intensity on sediment movement. Following Wu et al's approach, we modified the Wu et al's (2000) sediment transport capacity formulas implemented in the FVM-based CCHE2D model. Due to the fact that the downward flow and the vertical pressure gradient cannot be determined by a depth-averaged 2-D model, the correction factors for these two flow attributes have to be dropped. The pressure gradient in stream-wise direction is replaced by the water elevation gradient. The critical shear stress, τ_c, for the incipient motion of uniform sediment in the modified formulas is given as 0.045, which is 1.5 times of the value used in the original Wu et al's (2000) formulas. The same change can be found in other stochastic formulas, such as that proposed by van Rijn (1989).

After considering the influences of the stream-wise pressure gradient and the turbulence intensity, the effective tractive force τ_e used in the modified Wu et al's sediment transport capacity formulas is determined by

$$\tau_e = \alpha_t \max\left(\tau_b, -\frac{\pi}{6} f d \rho g \frac{\partial z_s}{\partial s}\right) \tag{1}$$

where τ_b is the bed shear stress; d is the diameter of sediment particles; g is the gravitational acceleration; z_s is the water elevation; s is along the stream-wise direction; ρ is the flow density; and f is a empirical coefficient relating to the sediment particle shape, pier shape, flow conditions, etc. The coefficient f is preliminarily calibrated as

$$f = \begin{cases} 3.4 D_*^{-0.3} f_s & D_* < 50 \\ 52.5 D_*^{-1} f_s & D_* \geq 50 \end{cases} \tag{2}$$

where $D_* = d\left[g\left(\rho_s/\rho - 1\right)/\nu^2\right]^{1/3}$; ρ_s is the sediment density; ν is the dynamic viscosity of flow; f_s is the shape factor of sediment particles, $c/\sqrt{ab}$, with *a*, *b* and *c* being the longest, the medium and the shortest diameters of sediment particles.

α_t is the correction factor to consider the influence of turbulence intensity. Assuming the instantaneous tractive force to have a normal distribution, time-averaging the instantaneous sediment transport rate and taking the ratio of the time-averaged sediment transport rates in the rapidly-varying flow and normal flow, one can obtain

$$\alpha_t = \left(\frac{\sigma}{\sigma_0}\right)\left[\int_0^\infty x^m e^{-0.5(x-p)^2} dx\right]^{1/m} \Bigg/ \left[\int_0^\infty x^m e^{-0.5(x-p_0)^2} dx\right]^{1/m} \tag{3}$$

where *m* is the power index of $\tau_e/\tau_c - 1$ in Wu et al's (2000) formulas, and hence $m = 2.2$ for the bed-load transport rate, and *m* is approximated as 2.6 for the suspended-load transport rate; $x = \left(\hat{\tau}_e - \tau_c\right)/\sigma$, $p = \left(\bar{\tau}_e - \tau_c\right)/\sigma$, and $p_0 = \left(\bar{\tau}_{e0} - \tau_c\right)/\sigma_0$. $\hat{\tau}_e$ is the instantaneous tractive force. $\bar{\tau}_e$ is the mean value of $\hat{\tau}_e$. $\bar{\tau}_{e0}$ is the bed shear stress in the approach normal flow. σ and σ_0 are the deviations of the tractive force at the rapidly-varying flow and normal uniform flow respectively. $\sigma = 0.4\rho c_{\Gamma\varepsilon} c_\mu \bar{k}$, in which $\bar{k}$ is the turbulent energy. c_μ and $c_{\Gamma\varepsilon}$ are coefficients in the k-ε turbulence model (Rodi, 1993). σ_0 is the value of σ at the upstream approach reach.

If the slope angle is larger than the submerged repose angle of sediment, a loose bed will collapse due to the gravity. This physical phenomenon has been considered in the calculation by adjusting the steeper bed slopes to the submerged repose angle of sediment according to mass conservation.

TEST OF THE FVM-BASED CCHE2D MODEL FOR LOCAL SCOUR

The FVM-based CCHE2D model with the newly modified Wu et al's sediment transport capacity formulas is tested using several groups of laboratory flume experiments, including the experiments on local scour at cylindrical piers conducted by Ettema (1980), near cylindrical piers by Ahmed (1995), around cylindrical and square piers by Yanmaz and Altinbilek (1991), and near spur dikes by Rajaratnan and Nwachukwu (1983). The total number of experimental runs simulated here is 34, including 6 on spur-dikes, 3 on square piers and 25 on cylindrical piers. The approach flow depths are in the range of 0.1m-0.6m, the approach flow velocities are in 0.2m/s-0.48m/s, and the diameters of piers or the lengths of spur dikes are in 0.057m-0.24m. The sediment is almost uniform, with size ranging 0.24mm-7.8mm. Fig. 1 shows the comparison between the measured and simulated maximum scour depths. The agreement between measurement and simulation is very good. The errors in most of the tested cases are in the range of ±20%. The development process and the final shape of the scour hole are simulated reasonably well. Those results are not shown here unfortunately because of the limit of paper length.

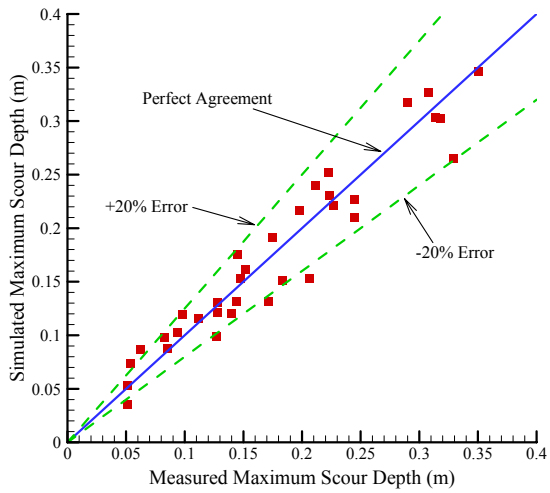

Fig. 1 Measured vs. Simulated Maximum Scour Depths around Bridge Piers and Spur Dikes

PREDICTION RESULTS FOR THE ICSF-1 TEST CASES

Because the modified Wu et al's sediment transport capacity formulas are only for non-cohesive sediment, the prediction is just made for the flume cases 1 and 2. In case 1, the diameter of the cylindrical pier is 160mm, and the width of the flume is 1.5m. The medium size of sediment particles is 0.3mm. The approach flow velocity and depth are constant during the 1-day experimental period, with values of 0.35m/s and 0.375m, respectively. In case 2, the pier diameter, the flume width and the sediment size are the same as in case 1. The experiment in case 2 lasts 4 days. The approach velocity is 0.25m/s in the first day and 0.35m/s in the second day, and then each of the two velocities repeats once in the third and forth days.

Table 1 shows the prediction results using the FVM-based CCHE2D model. The predicted maximum scour depths in cases 1 and 2 are 0.182m and 0.205m, respectively. As shown in Fig. 1, the prediction by the FVM-based CCHE2D may have about ±20% errors, which may apply to the values of the predicted maximum scour depth shown in Table 1.

Table 1 Flume Test Prediction by FVM-Based CCHE2D Model

Test description	Maximum depth of scour hole when the flume test stops
Flume case 1: 160 mm diameter circular pier placed in clean sand deposit and subjected to a constant velocity over a period of one day.	0.182 m
Flume case 2: 160 mm diameter circular pier placed in clean sand deposit and subjected to a multi-velocity hydrograph over a period of 4 days.	0.205 m

CONCLUSION

The FVM-based CCHE2D model, which is a depth-averaged 2-D numerical model for flow and sediment transport in open channels, is capable of simulating the local scour of non-cohesive sediment near hydraulic structures after modifying the Wu et al's (2000) sediment transport capacity formulas to take into consideration the influences of the pressure gradient and the turbulence intensity on sediment movement. Preliminary tests using 34 sets of flume experimental data of local scour around bridge piers and spur dikes show that the simulated maximum scour depth is very close to the measurements. The FVM-based CCHE2D model is applied to simulate the local scour around bridge piers in ICSF-1 test cases 1 and 2. The predicted maximum scour depths are 0.182m and 0.205m, respectively. According to the model calibration, the prediction using the FVM-based CCHE2D model may have about ±20% errors, which may apply to the values reported here.

The FVM-based CCHE2D model is under development, and it will be tested using a wider range of experimental and field data. It will also be enhanced to simulate the local scour of cohesive sediment near hydraulic structures.

ACKNOWLEGEMENTS

The FVM-based CCHE2D model has been developed from the Specific Cooperative Agreement No.58-6408-7-035 between the National Center for Computational Hydroscience and Engineering of the University of Mississippi and USDA Agricultural Research Service. Mr. Dalmo A. Vieira of NCCHE is acknowledged for his suggestion.

REFERENCES

1. Ahmed, F. (1995), "Flow and Erosion around Bridge Piers," PhD dissertation, University of Alberta, Canada.
2. Ettema, R. (1980), "Scour at Bridge Piers," University of Auckland, New Zealand.
3. Rajaratnan, N. and Nwachukwu, B.A. (1983), "Erosion near Groyne-Like Structures," *Journal of Hydraulic Research*, IAHR, Vol. 21, No.4, pp. 277-287.
4. Rhie, T.M. and Chow, A. (1983), "Numerical study of the turbulent flow past an isolated airfoil with trailing-edge separation," *AIAA J.,* Vol.21, pp.1525-1532.
5. Rodi, W. (1993): Turbulence Models and their Applications in Hydraulics, *IAHR Monograph,* 3rd Edition, Balkema, Rotterdam.
6. Van Rijn, L. C. (1989), "Handbook: Sediment Transport by Currents and Waves," Report H 461, Delft Hydraulics.
7. Wu, W., Wang, S.S.Y. and Jia, Y. and Robinson, K.M. (1999), "Numerical Simulation of Two-Dimensional Headcut Migration," *The 1999 International Water Resources Engineering Conference*, Seattle, USA. (on CD-ROM)
8. Wu, W., Wang, S.S.Y. and Jia, Y. (2000), "Nonuniform Sediment Transport in Alluvial Rivers," *Journal of Hydraulic Research*, IAHR, Vol. 38, No. 6, pp.427-434.
9. Wu. W. and Wang, S.S.Y. (2002), "CCHE2D Nouniform Sediment Transport Model," *The Second Federal Interagency Hydrology Modeling Conference*, Las Vegas, Nevada, USA.
10. Yanmaz, A.M. and Altinbilek, H.D. (1991), "Study of Time-Dependent Local Scour around Bridge Piers," *Journal of Hydraulic Engineering*, ASCE, Vol. 117, No. 10, pp. 1247-1268.

Numerical Simulation of Local Scouring around a Cylindrical Pier

Yafei Jia[1] Yichun, Xu[2] and Sam S.Y. Wang[3]

Abstract:

This paper reports the findings of a numerical modeling study for simulating the time-dependent scour hole development around a cylindrical pier standing on a loose bed on an open channel. In order to be able to obtain the realistic flow characteristics such as the downwash motion in front of the pier, the horseshoe vortex around pier, the vortex shadings behind the pier, etc., the CCHE3D model, developed, verified and validated by the scientists of the National Center for Computational Hydroscience and Engineering at the University of Mississippi was applied. Special features for accounting the effects of downwash, vortices and fluctuating turbulence intensity on the sediment entrainment and transport capacity have been added to the transport model. In addition, the non-equilibrium sediment transport equation has been used to further enhance the accuracy. The resulting three-dimensional turbulent flow and the enhanced sediment transport model has been applied to the simulation of the bridge pier scour development study. After calibration of the so-called site-specific parameters using physical model and field data, a validation procedure was conducted based on additional physical measurement having not been used in the calibration process. The calibrated and validated CCHE3D is then, used to perform a prediction of the maximum scour hole depth for the Case No. 1 specified by the Organization of the Prediction Event of the First International Conference on Scour of Foundations (ICSF-1). The maximum depth and geometry of the scour hole at the end of prediction time are included.

Introduction

It has been observed that in the free surface flow around an obstruction, such as a bridge pier, downwash motions, horseshoe vortices, an vortex shading are formed and the turbulence is intensified in front, around and behind the piers. In addition, a uniquely shaped scour hole on the loose bed around a pier is seen. Experimental studies have found that both the flow and the sediment transport processes during the scour hole development are highly complex.

Many measurements from physical models have shown that the depth of the scouring hole is closely related to the approaching flow condition, sediment property and the dimension of the pier (Melville, 1975 and 1984, Ettema, 1980, Knight, 1975, Kothyari, 1988, Shen and Schneider, 1969, Ahmed and Rajaratnam, 1998 and Eckerle and Langston, 1987). Some empirical functions based on fitting laboratory and field data have been derived to determinate the maximum scour depth around cylindrical piers.

[1] Research Associate Professor, National Center for Computational Hydroscience and Engineering, The University of Mississippi, MS 38677, USA. Email: jia@ncche.olemiss.edu
[2] Research Scientist, same institution, xu@ncche.olemiss.edu
[3] Frederick A.P. Barnard Professor, Director, the same institute. Email: wang@ncche.olemiss.edu

Some progresses of using numerical simulation to study the flow around a pier and scouring process have been made in recent years. Rizzetta (1993) and Richardson and Panchang (1998) computed flow fields around a bridge pier with a flat bed and in a scour hole using three-dimensional flow models. Zaghloul and McCorquodale (1975) simulated scour hole near a spur dike, vorticity and turbulence energy were introduced to add additional information and enhance sediment transport simulation in the scour hole. Olsen and Melaaen (1993) predicted local scour developing processes using a three-dimensional flow and sediment transport model. The limitation of their simulation was that the sediment transport capacity was only related to frictional shear stress, and the predicted local scour appeared only on the sides of the pier. By introducing vorticity and turbulence energy into the sediment transport capacity, Jia and Wang (1996) simulated local scouring around a spur dike. Accounted for downwash flow, vorticity and turbulence energy, Dou, et al, (1996) introduced a sediment transport capacity formula into three dimensional numerical simulation, and successfully simulated scouring around structures such as cylindrical pier, square pier and bridge abutments. Good agreements between numerical simulation and physical model measurement have been obtained.

This paper presents numerical predications of the maximum depth and the development process of the scour hole near a cylindrical pier. A modified van Rijn's formula relating the sediment transport rate to bottom shear stress and downwash flow was introduced to simulate the scour hole development and it is validated using experiment data.

Mathematic Model

Flow Model

CCHE3D is a three-dimensional numerical model for simulating turbulent free surface flows and sediemnt transport using finite element method (Wang and Hu, 1992 and Jia and Wang, 1998). The momentum and continuity equations were solved:

$$u_{i,t} + u_i u_{i,j} + \frac{p_{,i}}{\rho} - (-\overline{u_i u_j})_j + f_i = 0 \tag{1}$$

$$u_{i,i} = 0 \tag{2}$$

where u_i is velocity component in the i-direction ($i = 1,2,3$ for *x, y, z* of the Cartesian coordinate). f_i is the forcing term in the ith direction. $-\rho\overline{u_i u_j}$ are the Reynolds Stresses, ρ is the density of water. p is pressure. Free surface kinematical equation was used to determine the free surface elevation, η:

$$\eta_{,t} + u_\eta \eta_{,x} + v_\eta \eta_{,y} - w_\eta = 0 \tag{3}$$

A velocity correction method is used for solving the pressure to enforce mass conservation. The turbulent stresses, $-\rho\overline{u_i u_j}$, are calculated using the mean flow gradients through Boussinesq's eddy viscosity concept:

$$-\overline{u_i u_j} == \nu_t \left(\frac{\partial u_i}{\partial x_j} + \frac{\partial u_j}{\partial x_x}\right) - \frac{2}{3} k \delta_{ij} \tag{4}$$

where ν_t is the turbulence eddy viscosity,

$$\nu_t = C_\mu \frac{k^2}{\varepsilon} \tag{5}$$

k and ε are the turbulent kinetic energy per unit mass and its dissipation rate, governed by transport equations:

$$k_{,t} + u_i k_{,i} = (\frac{\nu_t}{\sigma_k} k_{,i})_{,i} + P - \varepsilon \tag{6}$$

$$\varepsilon_{,t} + u_i \varepsilon_{,i} = (\frac{\nu_t}{\sigma_\varepsilon} \varepsilon_{,i})_{,i} + c_{1\varepsilon} \frac{\varepsilon}{k} P - c_{2\varepsilon} \frac{\varepsilon^2}{k} \tag{7}$$

$$P = -\overline{u'_i u'_j} u_{ij} \tag{8}$$

The modification made by Speziale and Thangam (1992) to the standard k-ε model, RNG k-ε model, is adopted which requires C_μ=0.085, σ_k=0.7179, σ_ε=0.7179, $C_{2\varepsilon}$=1.68 and

$$C_{1\varepsilon} = 1.42 - \frac{\eta(1-\eta/4.38)}{1+0.015\eta^3} \tag{9}$$

Sediment Transport Model

In sediemnt transport simulation, bed load is considered to be dominant in the studied cases. Because the local scouring affected by the turbulent 3D flow, bed load transport is the non-equilibrium transport process governed by

$$\frac{\partial q_{bx}}{\partial y} + \frac{\partial q_{by}}{\partial y} + \frac{1}{L_s}(q_b - q_{*b}) = 0 \tag{10}$$

The local scour deformation around the cylindrical pier is governed by the sediment mass balance equation:

$$(1-p')\frac{\partial z_b}{\partial t} + \frac{\partial q_{bx}}{\partial y} + \frac{\partial q_{by}}{\partial y} = 0 \tag{11}$$

where z_b is bed elevation, q_{bx} and q_{by} are the sediment transport rate in x and y direction, respectively, and $q_b = \sqrt{q_{bx} + q_{by}}$, q_{b*} is sediment transport capacity under equilibrium transport condition. p' is porosity of the bed material. L_s is the so called adaptation length, related to local flow conditions and mesh size.

Sediment transport capacity is determined by modified van Rijn's formula:

$$q_{*b} = 0.053(\frac{\rho_s - \rho}{\rho} g)^{0.5} \frac{d^{1.5}}{D_*} T^{2.1} \tag{12}$$

where, ρ_s and ρ are sediments and fluid density, d is the sediment size and $D_* = d_{50}\{\frac{\rho_s - \rho}{\rho}\frac{g}{\nu^2}\}^{1/3}$. T is sediment mobility parameter:

$$T = \frac{[C_s \tau_d (u_\perp / u_{\perp,\max}) + \tau] - \tau_{cr}}{\tau_{cr}} = \frac{C_s \tau_d (u_\perp / u_{\perp,\max})}{\tau_{cr}} + \frac{\tau}{\tau_{cr}} - 1 \tag{13}$$

The first term is introduced in this study for handling local scouring process. $u_{\perp}$ is the near bed velocity component normal to bed surface. τ_d is the mean frictional shear stress around the cylinder and C_s is an empirical coefficient. It can be seen that the impact of vertical velocity or the "downwash" flow has been taken as the most significant factor for scouring. τ_d serves as a reference measuring the strength of the turbulent flow near the bed of the scouring hole. The term of $\tau / \tau_{cr} - 1$ is the same as the sediment mobility defined by van Rijn (1986). The critical shear stress, τ_{cr}, has included the effect of bed slope and the near bed flow direction.

Validation of the Flow and Sediment Transport Models

The CCHE3D model has been verified and validated by using several analytic methods, physical model and field data. Figure 1 shows the simulated flow field in a preformed scouring hole (Jia and Wang, 1999). The flow conditions of the test case were from the flume experiment of Melville and Raudkivi (1977). The figure indicates that the flow structure (horseshoe vortex) and the near bed velocity are computed realistically.

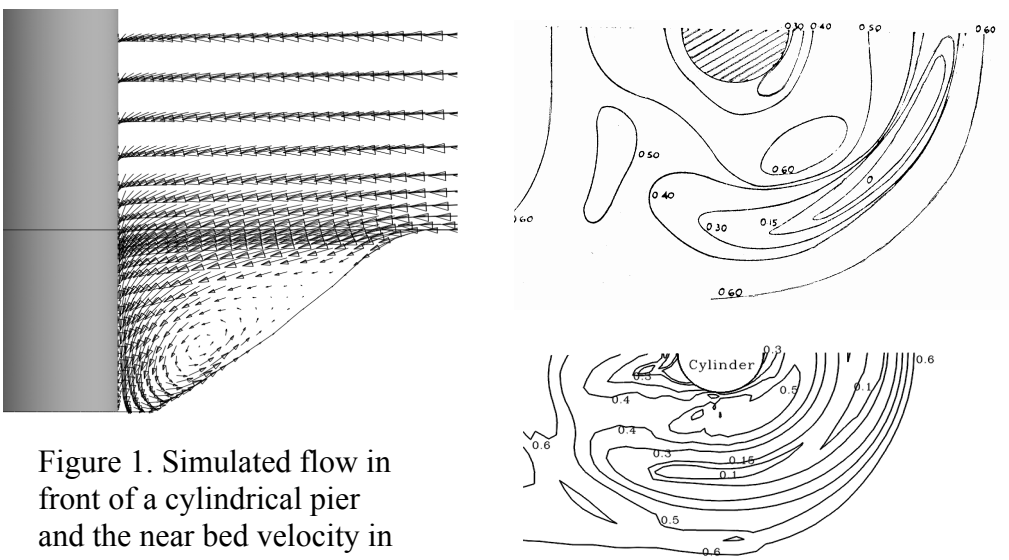

Figure 1. Simulated flow in front of a cylindrical pier and the near bed velocity in a preformed scour hole.

The aforementioned model has been tested using physical model data measured by Ettema (1980). The test cases selected have similar flow condition, cylindrical pier size and sediment size (0.38mm and 0.24mm). The case was clear water scouring with U_*/U_{*cr}=0.9. In these tests, the adaptation length L_s (=5.0) and the coefficient for entraining sediment due to the pier, C_s (=3.0) were determined.

Simulation Results

The CCHE3D model was applied to predict the flow fields and the local scouring around a cylindrical pier under clear water and live-bed scour conditions with sand bed material.

A non-uniform, body fitted mesh with 48x121 nodes were used for the domain discretization. The grid close to the pier has much higher density than those away from it. Grid spacing increases gradually in the radial direction from the pier center. The vertical grid consists of 21 levels with fine grid size near the bed and coarser one near the free surface. The vertical grid was gradually stretched as the scour hole developing. Because the bed change rate is low, the grid velocity was neglected in the computation. The hydrodynamics and the sediment transport computation were not coupled, the flow field was considered as a quasi-steady and updated as bed elevation changes.

The Case 1 of the ICSF-1 (First International Conference on Scour of Foundations) test cases was selected for simulation. The test flume is 1.5m wide with flat bed and vertical walls. A single pier was located in the middle of a straight flume. The flow and sediment conditions used in the numerical simulation are listed in Table 1.

Table 1. Flow conditions of the simulated local scouring cases.

Case	Soil type	y_1 (m)	b (m)	U (m/s)	$R_b = \frac{Ub}{\upsilon}$	$F_r = \frac{U}{\sqrt{gy_1}}$	D_{50} (m)	D_{90} (m)
1	Sand	0.375	0.16	0.35	56,000	0.1825	0.0003	0.0006

y_1 = water depth, b = diameter of the pier, U = approaching mean velocity

The erosion started from the two sides of the pier where the bed surface has the maximum bottom shear stress. The two small scouring holes gradually migrated upstream around the pier and met at the front of the pier. The two scouring holes merged into a bigger one, and its depth and size grew around the front of the pier due to the strong downwash flow. The deepening and widening of the scouring hole stimulated the downwash flow and the vortex in the hole that in turn further accelerated the scouring.

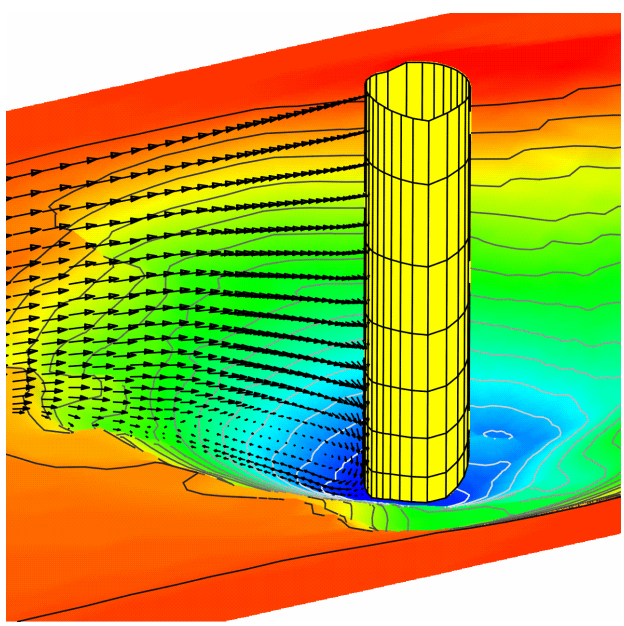

Figure 2. An oblique view: the simulated scouring hole and the three-dimensional flow structure. Case 1.

The simulation started from the flat bed and the scouring depth was recorded from time to time. Figure 2 displays the geometry of the scour hole at the scouring time approaching to 24 hours. The simulation results show that the scour hole depth was asymptotically approaching to 0.323m, when the simulation time reached to 24 hours approximately.

Conclusions

This paper presents the simulation results of local scour around a cylindrical pier, the prediction case proposed by ICSF-1, using CCHE3D model, a numerical model for simulating unsteady three-dimensional hydrodynamic, sediment transport and scour hole formation processes. The modified van Rijn's formula for predicting sediment transport capacity was introduced and validated using experimental data. The predicted maximum depth of the local scour hole for the test Case 1 was 0.323m after 1 day of scouring.

Acknowledgment

This work is a result of research supported in part by the USDA Agriculture Research Service under Specific Research Agreement No. 58-6408-7-035 (monitored by the USDA-ARS National Sedimentation Laboratory), and The University of Mississippi.

Reference

Ahmed, F. and Rajaratnam, N. (1998). "Flow around bridge piers."J. Hydr. Engrg., ASCE, 124(3), pp. 288–300

Dou, X. Jia, Y. and Wang, S.S.Y., 1996, "Numerical Simulation of Bridge Abutment Scour Development", Proceedings of and Presented at North American Water and Environment Congress in Anaheim, CA.

Eckerle and Langston, 1987, "Horseshoe Vortex Formation Around a Cylinder, Journal of Turbomachinery", Vol. 109, pp. 278-285.

Ettema, R., Melville, B. W., and Barkdoll, B. (1998), "Scale effect in pier-scour experiments." J. Hydr. Engrg., ASCE, 124(6), pp. 639-642.

Jia,Y., and Wang, S.S.Y. 1996, "A Modeling Approach to Predict Local Scour Around Spur Dike Like Structures," Proceedings of the 6th FISC, Vol. 1, pp. 90-97, Las Vegas, NV, March 1996.

Jia,Y., and Wang, S.S.Y. 1998, "Numerical Modeling of Secondary Motions of Turbulent Flows in Compound Channels", Conference of Water Resource Engineering, 1998. pp. 1038-1043.

Jia, Y., and Wang, S.S.Y. 1999 "Simulation of horse-shoe vortex around a bridge pier", Proceedings of ASCE International Conference on Water Resource Engineering, On CD-ROM.

Knight, 1975, "A Laboratory Study of Local Scour at Bridge Piers", 16th IAHR Conference, Proceeding, Vol. 2, pp. 243-250, Sao, Paulo, Brazil.

Kothyari, U.C., Garde, R.J. and Ranga Raju, K.G., 1992. "Live-bed scour around cylindrical bridge pier", J. of Hydr. Res., IAHR, 30(5), pp. 701-715.

Melville, B.M., 1975, "Local Scour at Bridge Sites", Thesis presented to the University of Auckland, at Auckland, New Zealand in 1975.

Melville, B.M., and Raudkivi, A., 1977, "Flow characteristics in local scour at bridge piers", Journal of Hydraulic Research, Vol. 15, No. 4, pp. 373-380.

Melville, B.M., 1984, "Live-Bed Scour at Bridge Piers", J. Hydr. Engrg., 110(9), pp. 1234-1247.

Olsen, N. R. B., and Melaaen, M. C.(1993). "Three-dimensional calculation of scour around cylinders." J. Hydr. Engrg., 119(9), pp. 1048–1054.

Shen, H. W., Schneider, V. R., and Karaki, S. (1969). "Local scour around bridge piers." J. Hydr. Div., ASCE, 95(6), pp. 1919–1940.

Speziale, C. G. and Thangma, S. (1992), "Analysis of a RNG Based Turbulence Model for Separated Flows", NASA, CR-189600, ICASE Rept. No. 92-3.

Richardson and Panchang, 1998, "Three Dimensional Simulation of Scour Inducing Flow at Bridge Pier", J. Hydr. Engrg., ASCE, 124(5), pp. 530-540.

Rizzetta (1993), "Numerical Simulation of Turbulent Cylinder Juncture Flow Fields", AIAA Hournal, Vol. 32, No. 6.

Van Rijn, 1986, "Mathematical Modeling of Suspended Sediment in Nonuniform Flows", J. Hydr. Engrg., vol. 112, No. 6, pp.433-455.

Wang, Sam S.Y. and Hu, K.K.1992, "Improved methodology for formulating finite-element hydrodynamic models, Finite Element in Fluids", edited by T.J. Chung, Vol. 8, Hemisphere Pubulication Cooperation, pp. 457-478.

Zaghloul, N.A., and McCorquodale, J.A. 1975, "A stable numerical model for local scour", Journal of Hydraulic Research, Vol. 13, No. 4, pp. 425-444.

Flume Tests Results

Ya Li[1], Jun Wang[1], Wei Wang[1], Jean-Louis Briaud[2], Hamn-Ching Chen[3]

Abstract: *In this paper, the 6 flume tests for the prediction event are described in detail. The flume test set up, including the flume system and measurement tools are introduced first. Then the experimental procedure is outlined. Finally, the measurements and important observations of the scour generation are presented.*

Experimental Set Up

Flume tests for the prediction event were conducted in the 1.5 m wide concrete flume in the Hydraulic Laboratory at Texas A&M University. Description of the equipment used is detailed in the following sections.

Flume and False Bottom

The in-floor concrete flume is 1.5 m wide, 30.48 m long and 3.48 m deep. Together with an upstairs flume, it forms a close system, as plotted diagrammatically in FIG 1. Water is circulated by a series of pumps and the total volume of water in the system is constant during the experiments except minor leakage and evaporation. A screen wire is placed in front of the false bottom to reduce secondary flows and turbulences created by water falling from the upper flume. The false bottom was built with plastic plates and supported by Aluminum frames, with ramps of 1:3 (vertical to horizontal) slope at both ends. The distance from the rear edge of the upstream tank to the front edge of the downstream tank is 7.6m. A trial test before the official scour tests proved that the ramp slopes were smooth enough and the soil tanks were far enough from each other, to ensure that the approaching flow to the scour areas were not modified by the existing structures. The soil tanks were 0.6 m deep, and 1.2 m long for the upstream tank and 0.6 m deep, and 1.5m long for the downstream tank.

In this flow system, the slope of the false bottom is zero, and the approaching velocity and the water depth are controlled by the pump rate. The flow cross-section area for the uniform channel is determined by the flow depth, which can be precisely justified by a mini pump (as shown in FIG 1 (4)) at the end of the tank.

Pier Model

The cylindrical piers were cut from PVC pipe with an outside diameter of 160mm. The pier was installed in the middle of the channel and a little closer to the front edge of the soil tank in the longitudinal direction.

[1] *Graduate student., Dept. of Civil Engineering, Texas A&M Univ., College Station, TX 77843*

[2] *Spencer J. Buchanan Prof., Dept. of Civil Engineering, Texas A&M Univ., College Station, TX 77843*

[3] *Professor., Dept. of Civil Engineering, Texas A&M Univ., College Station, TX 77843*

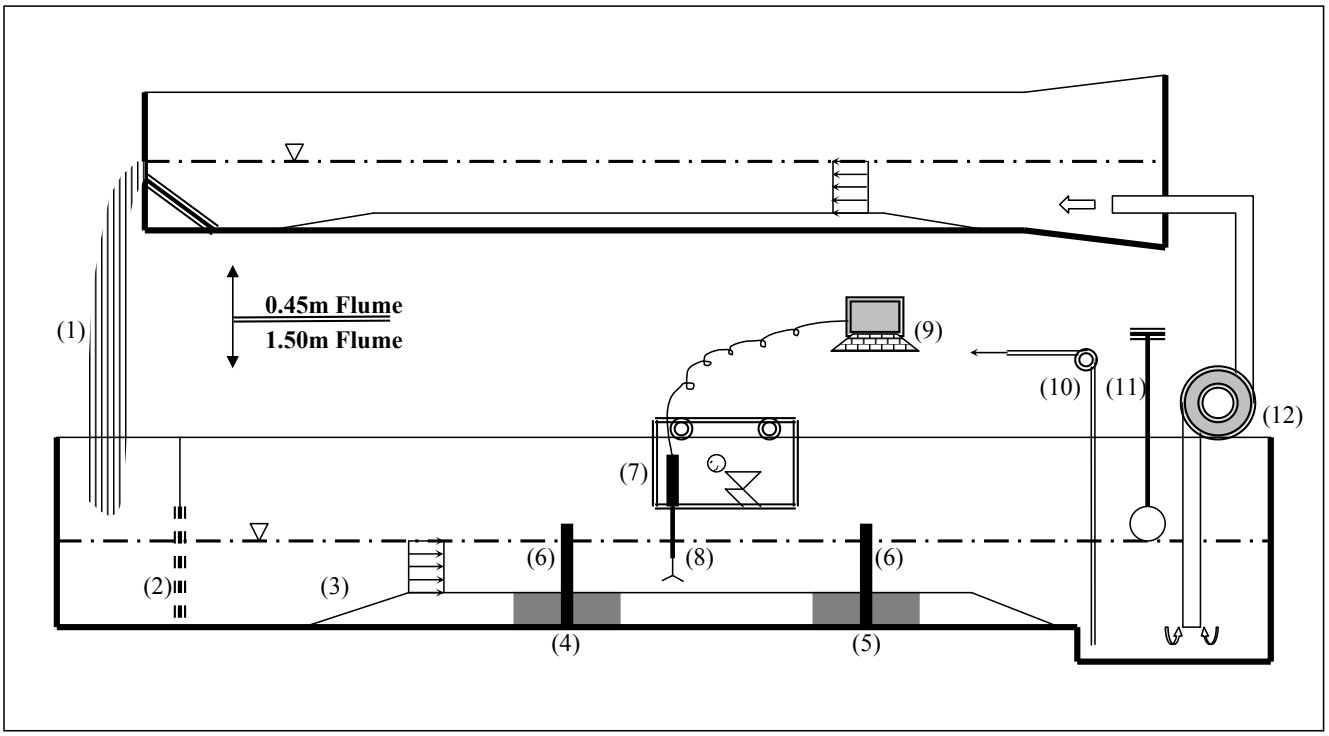

FIG 1 Diagrammatic Figure of the Flume System (not to Scale)

(1): Water Fall	(4): Soil Tank 1	(7): Movable Measurement Cage	(10): Mini Pump
(2): Screen Wire	(5): Soil Tank 2	(8): ADV and Point Gage	(11): Switch
(3): False Bottom	(6): Piers Cage	(9): Computer	(12): Pump

Equipment for Velocity Measurement

An ADV (Acoustic Doppler Velocimeter) uses acoustic sensing techniques to measure flow in a remote sensing volume so that the measured flow is undisturbed by the presence of the probe. A 2-D ADV (longitudinal direction U and vertical direction V), which is sketched in FIG 2, was used to measure the mean velocity of the flow in the tests. It had a velocity range of ±2.5m/s and a resolution of 0.1mm/s.

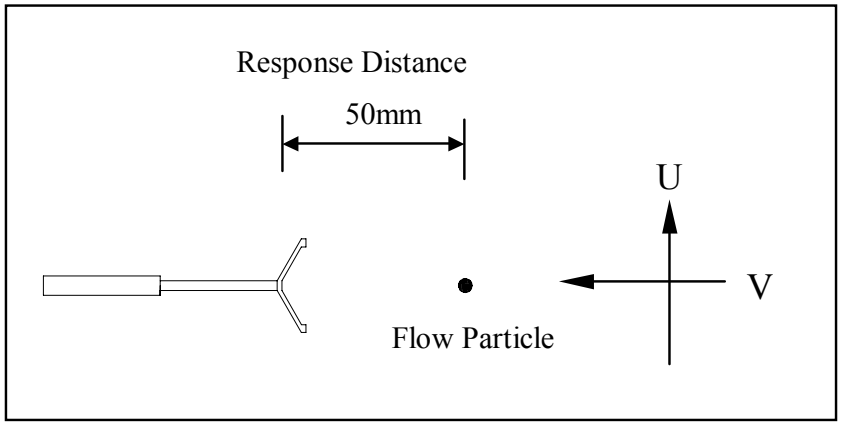

FIG 2 2-D ADV Diagram

Equipment for Elevation Measurement

An electronic point gage was designed and used to measure the increase in scour depth without interrupting the test. The point gage is designed on the principle that air, water and soil have a different electrical conductivity. In the point gage system, a close circuit is formed with a node in the soil or water and the other one in the air. Once the point gage, which is basically a needle attached to a vertical ruler, touches the surface of the scour hole (an interface between water and soil), there is a sudden change in the reading of the volt meter. The reading on the ruler marks the elevation of the scour hole at this moment. When the water is dirty and cannot be seen through, the deepest scour location needs to be searched point by point. The needle is so tiny that the damage caused by the thrust on the scour hole surface can be neglected. It takes 1 minute to take one reading and about 10 minutes to finish one set of data for a single pier scour tests. The resolution of the measurement is ±1mm.

As shown in FIG 1, the point gage and ADV are installed on a cage moving along the longitudinal direction of the flume. The hanging measurement cage is built in the 1.5m flume to decrease the distance between the reading point and the measuring point and to minimize measurement errors. In the flume tests, it was found that the presence of the piers had almost no influence on the approaching flow at a distance equal to 1 time the channel width or further, upstream of the pier. The approaching velocity and water depth are therefore measured 2.5 m upstream of the pier and in the middle of the channel. In addition, a digital camera is used to record the scour hole geometry after each test.

Soils and Soil Bed Preparation

The properties of the soil used (porcelain clay and mortar sand) are detailed in the prediction request. The porcelain clay is delivered in vacuum extruded blocks with dimensions of 250mm x 180mm x 180mm and sealed in plastic bags. The blocks are installed in the soil tank as shown in FIG 3. After one layer is finished, compaction is conducted using a 20 lbs concrete brick to minimize voids and holes between blocks. Careful compaction is performed on the clay in the vicinity of the pier where the scour hole develops. Once the soil tank is filled, the soil surface is leveled with a straightedge spatula. After each test, the scoured area is cleaned and new clay blocks are installed for the next experiments. The installation of the sand consisted of placing the sand in layers and compacting them in place. During the installation, water was added to the dry sand so that the sand could be compacted more tightly.

FIG 3 Preparation of the Clay Soil Tank

Experimental Procedure

All the pier scour tests were conducted according to the following seven steps:

1. Prepare soil bed and install pier as described in the above section;
2. Measure the initial soil surface elevation around the pier with the point gage;
3. Install the ADV at the middle of the channel and 2.5m upstream of the second pier, and set the node of the ADV at a height of 0.4 times the expected water depth (0.375m in the current tests) above the false bottom; (it should be noted that the velocity measured at this point is regarded as the mean approach velocity);
4. Set the water depth and the velocity in the flume by adjusting the flow of the mini pump and of the main pump;
5. Record the scour depth at necessary intervals,
6. Set the pump rate, water depth and mean velocity according to Step 3-4 when a hydrographic flood is simulated in the flume;
7. After the scheduled time, stop the pump, empty the water in the flume, record the shape of the scour hole with a digital camera and finish the test.

In Step 5, the recorded scour depth is the deepest scour depth at the time of the measurement. The point gage is used to measure the scour depth at different locations around the pier to find the location of the deepest scour depth.

Experimental Results and Observations

Table 1 Schedule of Flume Tests

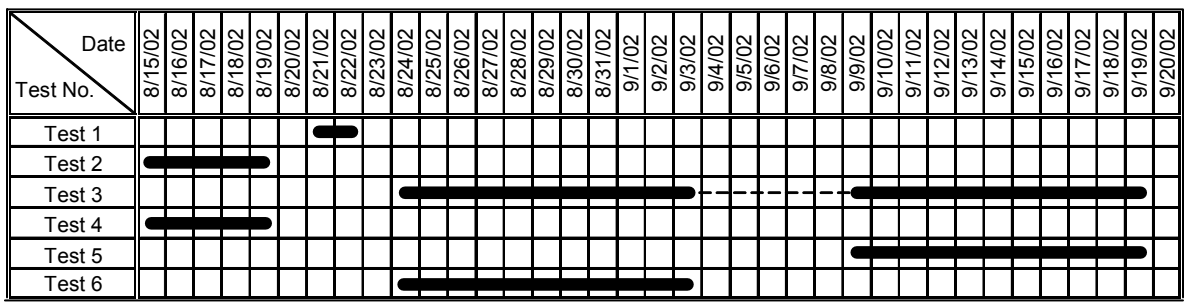

As shown in Table 1, the flume tests for the prediction event were performed in 4 groups. Most of the time, the two tanks as shown in FIG 1 were used simultaneously to save experimental time. The interval between tests represents the time to clean up the previous tests and to prepare the next ones. The duration of Test 3 was cut from 30 days as planed in the prediction request to 20 days. The measured results as shown in a later section indicate that after 20 days the maximum scour depth was close to being reached. Test 3 was conducted in two separated phases, accompanied by Test 6 in the first 10 days and Test 5 in the second 10 days.

Flume Test 1

In Flume Test 1, a 160 mm diameter circular pier was placed in a clean sand deposit and subjected to a constant velocity of 350mm/s over a period of one day. It was conducted in the upstream tank 1 in FIG 1, starting at15:35, August 21, 2002 to 15:35, August 22, 2002. The measured maximum scour depth as a function of time is given in Table 2 and plotted in FIG 4. The scour hole geometry when the test was terminated is shown in FIG 5. For pier scour in sand, the location of deepest point was in front of the pier. The sand that was eroded from the vicinity of the pier was deposited downstream.

Table 2 Measured Scour Depth as a Function of Time in Flume Test 1

Time (Hr)	Scour (mm)	Velocity (mm/s)
0.00	0	350
0.50	63	
1.00	110	
1.33	113	
2.00	127	
4.75	147	
7.75	160	
9.42	163	
11.33	168	
24.00	183	

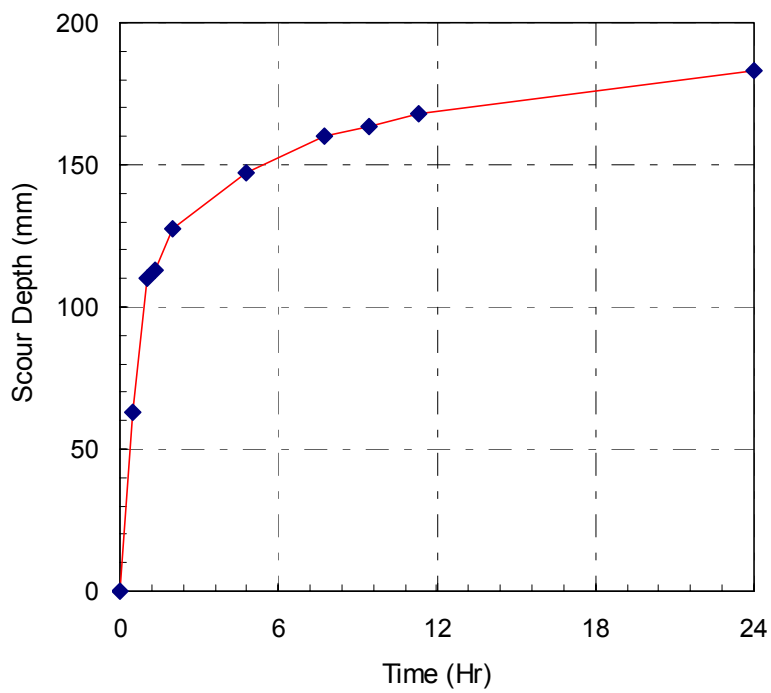

FIG 4 Measured Scour Depth as a Function of Time in Flume Test 1

FIG 5 Scour Hole Geometry for Flume Test 1

Flume Test 2

In Flume Test 2, a 160 mm diameter circular pier was placed in a clean sand deposit and subjected to a multi-velocity hydrograph as shown in FIG 6 over a period of 4 days. Test 2 was conducted in the upstream tank in FIG 1, from 21:45, August 15, 2002 to 21:45, August 19, 2002. The measured maximum scour depth as a function of time is given in Table 3 and plotted in FIG 7. It shows that scour in sand develops very fast and that the scour depth can reach a stable value in a very short time under constant flow. When the second and bigger flood comes in, there is clear jump in scour depth. After the first two days, the scour depth is already fully developed, and the next two days of flow do not bring any significant increment in scour depth.

The scour hole geometry when the test was terminated is shown in FIG 8. As shown in FIG 9, coarse particles deposit behind the pier in an armoring process.

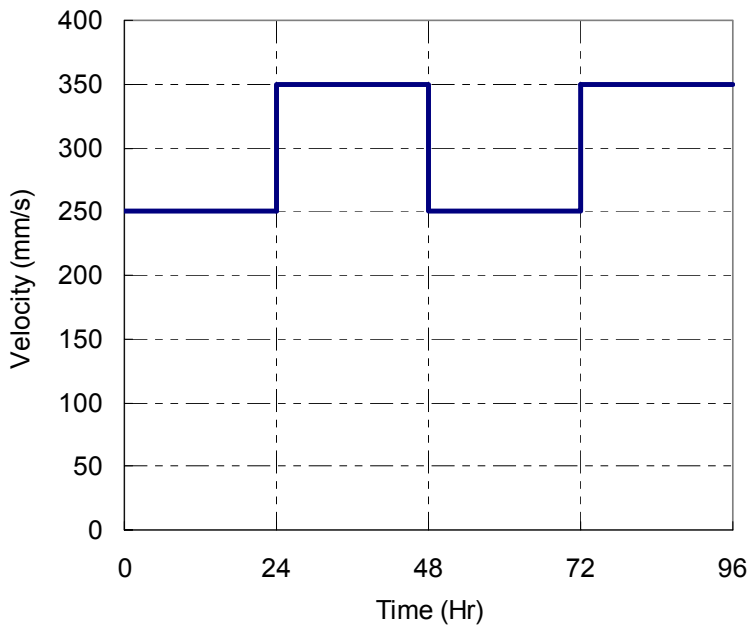

FIG 6 Multi-velocity Hydrograph for Flume Test 2 and Flume Test 4

Time (Hr)	Scour (mm)	Velocity (mm/s)
0.00	0.00	250
0.50	21.26	
0.83	45.72	
1.17	53.16	
1.92	69.11	
2.92	80.80	
6.17	93.56	
8.00	98.88	
9.67	104.20	
24.00	113.76	
24.33	143.53	350
24.50	145.66	
25.00	148.85	
26.50	156.29	
30.42	165.86	
35.17	171.18	
48.00	176.49	
52.00	177.56	250
58.42	178.62	
72.00	178.62	
72.50	180.75	350
82.17	180.75	
96.00	185.00	

Table 3 Measured Scour Depth as a Function of Time in Test 2

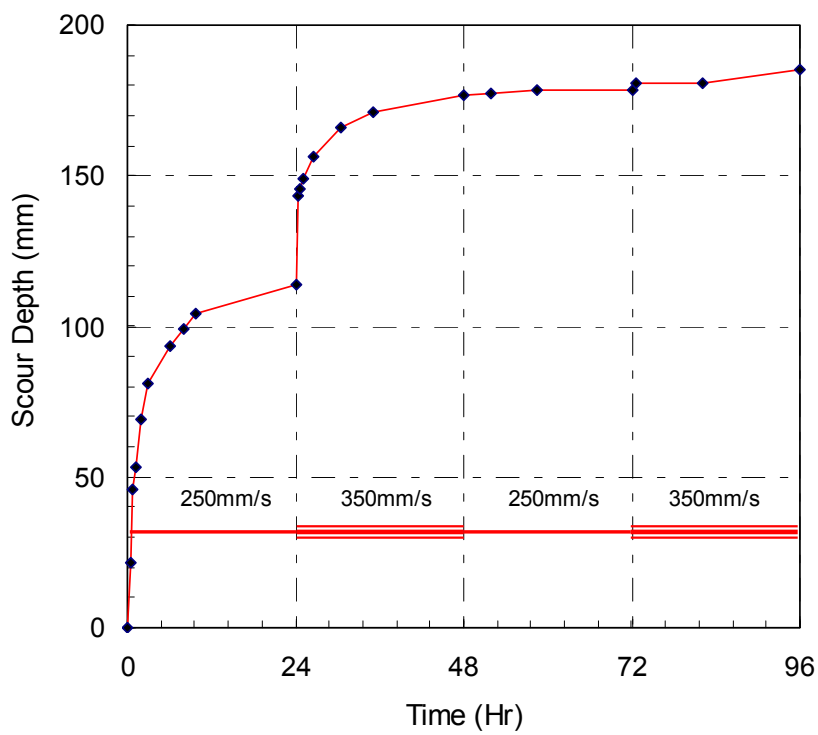

FIG 7 Measured Scour Depth as a Function of Time in Test 2

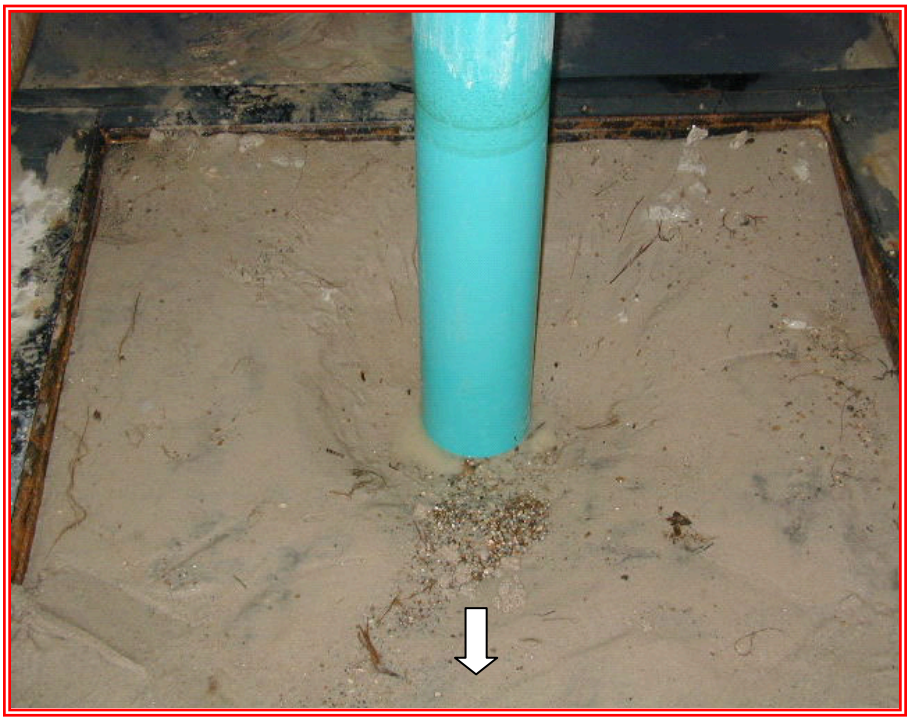

FIG 8 Back View of Scour Hole for Test 2

FIG 9 Coarse Particle Deposition in Test 2

Flume Test 3

In Flume Test 3, a 160 mm diameter circular pier was placed in a clay deposit and subjected to a constant velocity of 350mm/s over a period of 20 days. The test is conducted in the downstream tank in FIG 1, with Test 5 and 6 conducted in the upstream tank consecutively. As shown in Table 1, the duration of Test 3 is broken into two periods, accompanied by Test 6 from 14:40, August 24, 2002 to 14:40, September 3, 2002 and accompanied by Test 5 from 12:45, September 9, 2002 to 12:45, September 19, 2002. During the interval, the scour hole was kept under water to void soil desiccation. The measured maximum scour depth as a function of time is presented in Table 4 and FIG 10. It can be seen on FIG 10 that within 144 hours (about 6 days or 30% of the total scour duration) the scour depth in the clay has reached 150mm, or 93% of the final scour depth of 161mm. FIG 11 shows the scour hole geometry when the test was terminated. The deepest scour hole in this clay is generated on the side of the pier, instead of the front of the pier as in sand.

Time (Hr)	Scour (mm)	Velocity (mm/s)
0.00	0	350
6.17	12	
9.67	26	
23.92	56	
34.33	70	
47.08	98	
71.50	115	
82.50	130	
98.67	130	
105.33	138	
128.50	145	
152.33	150	
200.92	154	
240.00	156	
336.42	156	
387.25	160	
480.00	161	

Table 4 Measured Scour Depth as a Function of Time in Test 3

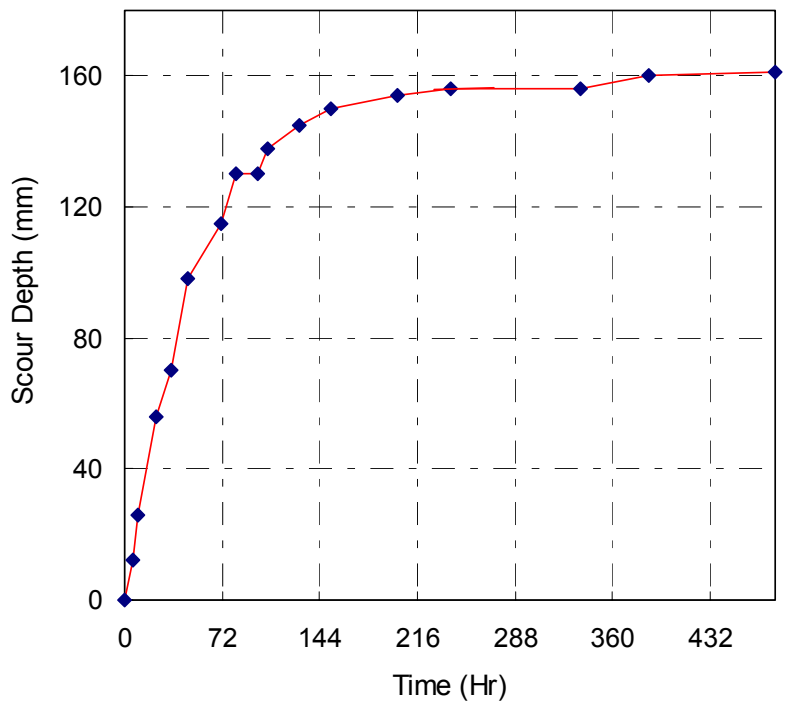

FIG 10 Measured Scour Depth as a Function of Time in Test 3

FIG 11 Scour Hole Geometry for Test 3

Flume Test 4

In Flume Test 4, a 160 mm diameter circular pier was placed in a uniform clay deposit and subjected to a multi-velocity hydrograph as shown in FIG 4 over a period of 4 days. Test 4 was conducted in the downstream tank in FIG 1, with Test 2 conducted in the upstream tank simultaneously. Test 4 is same as Test 2 except that the soil is clay instead of sand. Their comparison can be used to illustrate the difference between scour in sand and in clay. The measured maximum scour depth as a function of time is presented in Table 5 and FIG 12. It shows that there is a change in scour rate associated with the change in velocity. However, this change is not as drastic as in sand (compare FIG 12 and FIG 7).

The scour hole geometry when the test was terminated is shown in FIG 13. As shown in the figure, there is no erosion on the soil in the soil tank except the vicinity around the pier. The scour hole is relatively localized compared to the scour hole in sand. The deepest scour depth is formed at the side of the pier as marked in FIG 14.

Time (Hr)	Scour (mm)	Velocity (mm/s)
0.00	0.00	250
6.08	21.26	
11.67	45.72	
24.00	53.16	
25.00	69.11	350
26.50	80.80	
30.42	93.56	
35.17	98.88	
48.00	104.20	
52.00	113.76	250
58.42	143.53	
72.00	145.66	
96.00	148.85	350

Table 5 Measured Scour Depth as a Function of Time in Test 4

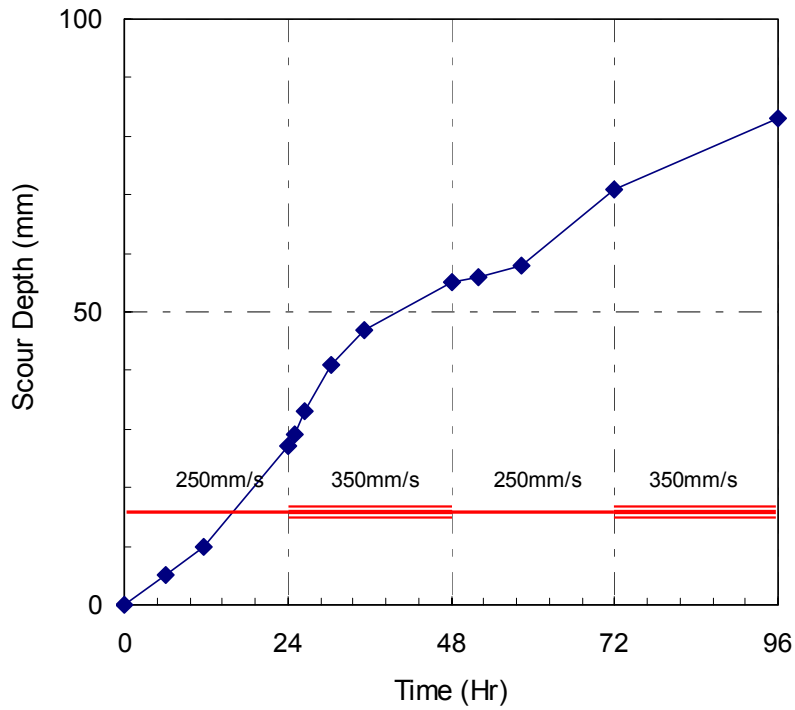

FIG 12 Measured Scour Depth as a Function of Time in Test 4

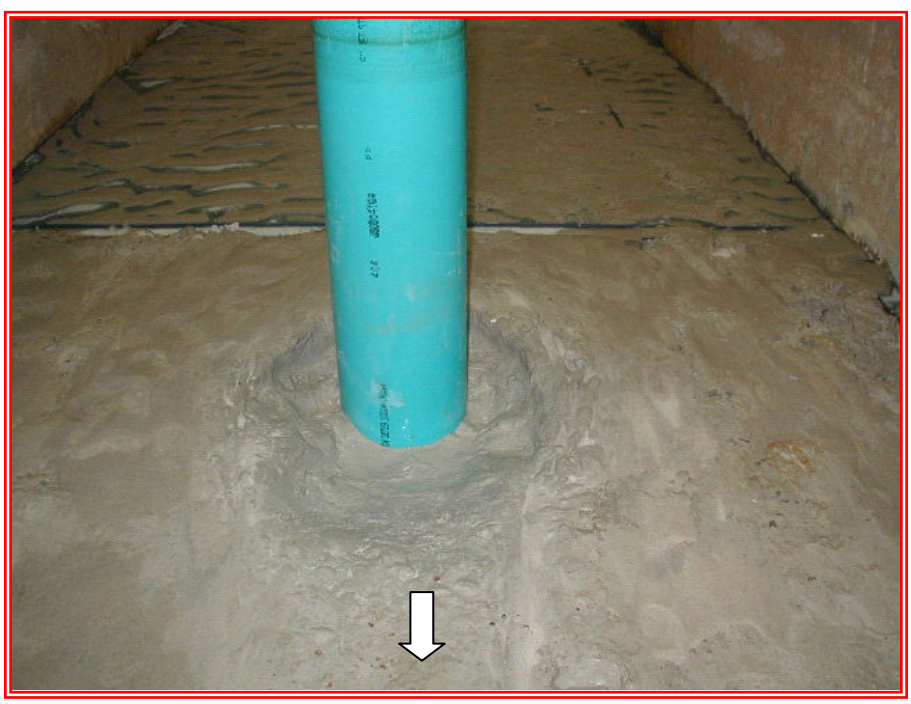

FIG 13 Back View of Scour Hole for Test 4

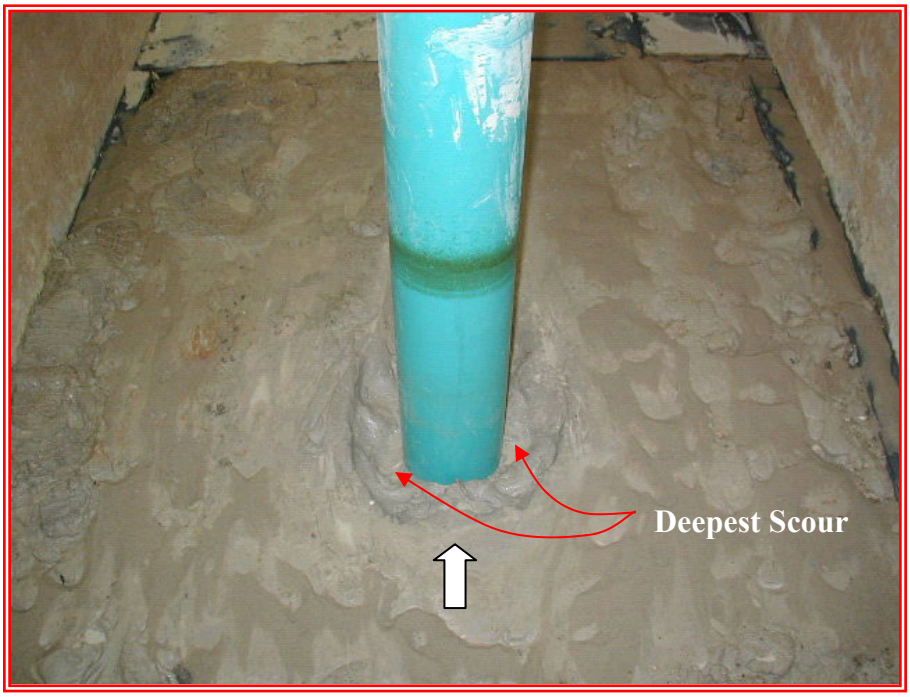

FIG 14 Front View of Scour Hole for Test 4

Flume Test 5

In Flume Test 5, a 160 mm diameter circular pier was placed in a sand over clay layered soil and subjected to a constant velocity flow of 350mm/s over a period of 10 days. The thickness of the top sand layer was 80mm. The measured maximum scour depth as a function of time is presented in Table 6 and FIG 15. FIG 16 shows the scour hole geometry when the test was terminated. It indicates that when the scour penetrates the top sand layer and touches the bottom clay layer, the scour rate drops suddenly, but there is still further scour developing in the clay layer over a long duration. The sand around the scour hole is swept into the scour hole and eroded way. As shown in FIG 16, only a relatively small scour hole exists in the clay layer. As the scour hole develops from the sand layer to the clay layer, the deepest scour location moves from the front of the pier to the side of the pier.

Time (Hr)	Scour (mm)	Velocity (mm/s)
0.00	0	
0.50	30	
1.00	60	
1.50	76	
2.00	80	
3.00	80	
5.92	81	
8.83	83	
20.00	106	
31.92	118	350
35.92	120	
48.42	128	
71.67	144	
96.42	146	
123.25	147	
147.25	147	
169.25	150	
191.25	150	
240.00	152	

Table 6 Measured Scour Depth as a Function of Time in Test 5

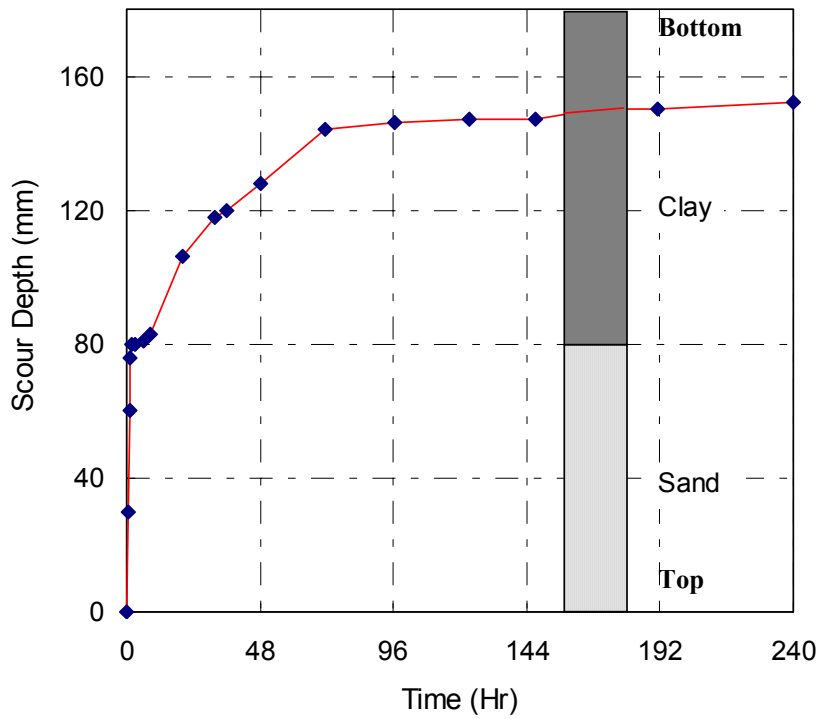

FIG 15 Measured Scour Depth as a Function of Time in Test 5

FIG 16 Scour Hole Geometry for Test 5

Flume Test 6

In Flume Test 6, a 160 mm diameter circular pier was placed in a clay over sand layered soil and subjected to a constant velocity flow of 350mm/s over a period of 10 days. The top clay layer is 80mm thick. The measured maximum scour depth as a function of time is presented in Table 7 and FIG 17. FIG 18 to FIG 21 show the scour hole geometry when the test was terminated.

Several interesting phenomena are observed in this test. First, the scour development curve (FIG 17) indicates that the scour rate does not suddenly increase as expected when the scour touches the bottom sand layer. Instead, the scour rate remains approximately equal to the rate in the clay. This rate continues until the scour depth reaches 100mm and then the scour rate begins to increase compared to the scour rate in uniform clay at the same depth. It was found that when the scour depth first touches the sand layer, the deepest part of the scour hole in clay is so concentrated that only a very tiny area touches the sand layer. Under this condition, the sand cannot be effectively eroded away and the scour process consumes most of its energy to enlarge the scour hole horizontally but not to increase the scour depth. At this stage, the scour generation is mostly dominated by the characteristics of a scour hole in clay. After finishing the enlargement of the scour hole, the scour hole works like a scour hole in uniform sand and the scour begins to show a larger scour rate. Meanwhile, the deepest scour location moves from the side of the pier to the front of the pier just where it usually is in uniform sand.

FIG 18 and 19 demonstrate that the scour hole for a clay over sand layered soil is wider and larger than the scour hole developed in uniform clay but smaller than that scour in uniform sand. Another important aspect of the scour hole is its edge slope. FIG 20 indicates that slopes with angles larger than 90º exist in the top clay layer. FIG 21 clearly illustrates that during the scour development in the bottom sand layer, the flow will dig underneath the top clay layer, which will fail in blocks into the scour hole; this is another mechanism in the scour hole development.

Time (Hr)	Scour (mm)	Velocity (mm/s)
0.00	0	350
6.17	16	
9.67	19	
23.92	52	
34.33	72	
47.08	94	
57.58	100	
71.50	120	
82.50	120	
98.67	135	
105.33	151	
128.50	162	
152.33	164	
200.92	170	
240.00	177	

Table 7 Measured Scour Depth as a Function of Time in Test 6

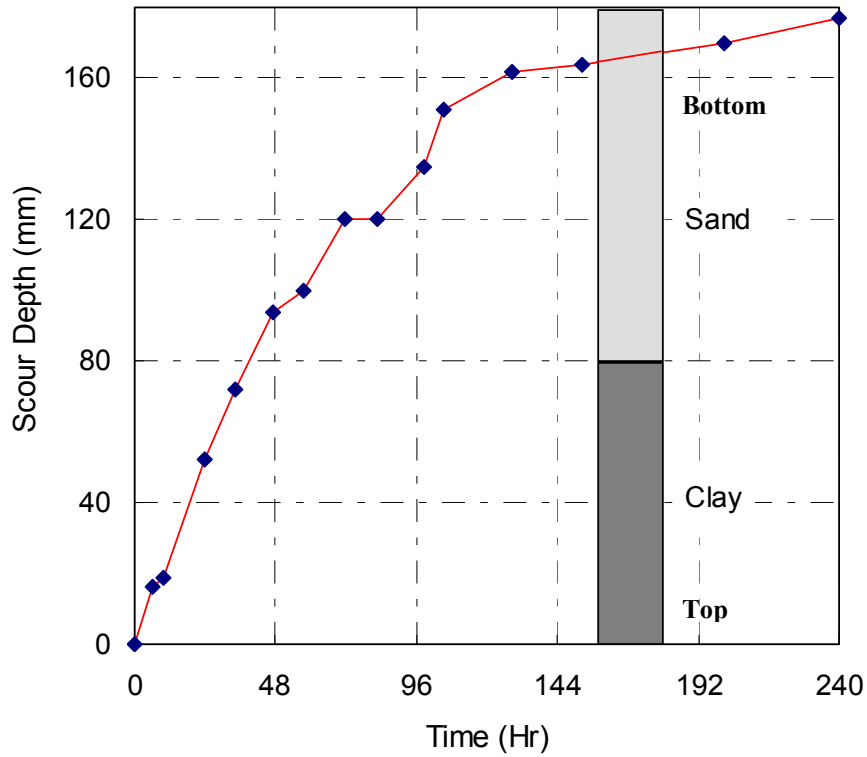

FIG 17 Measured Scour Depth as a Function of Time in Test 6

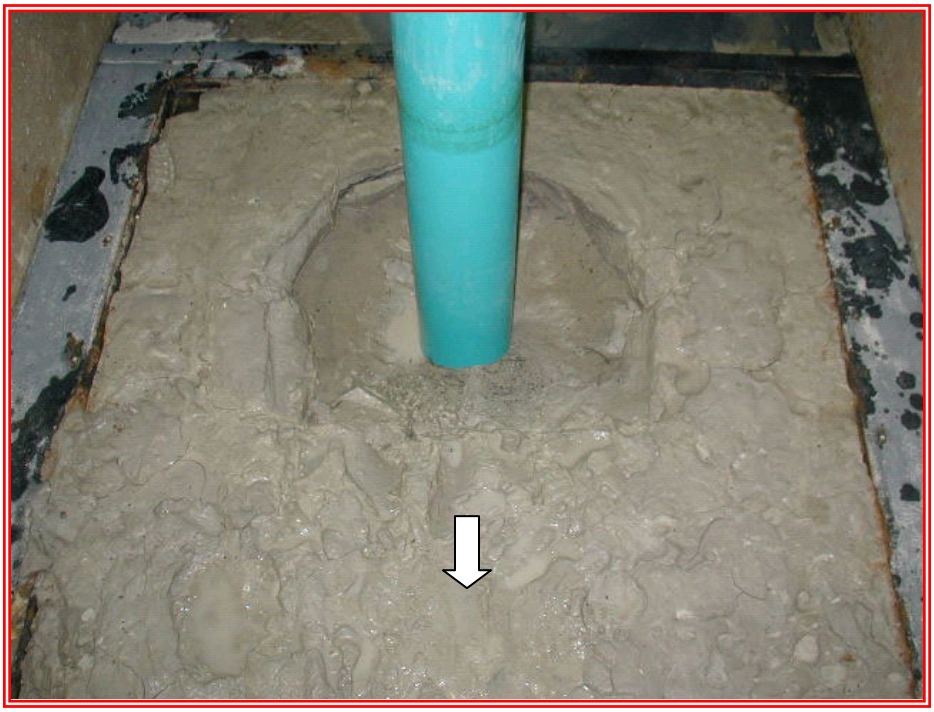

FIG 18 Back View: Scour Hole Geometry for Test 6

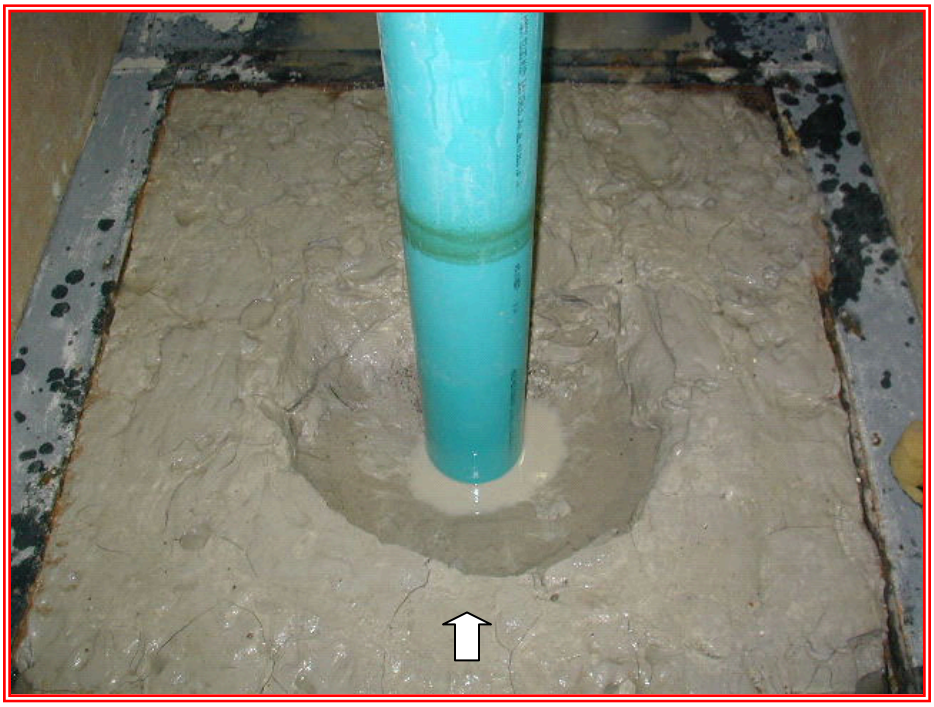

FIG 19 Front View: Scour Hole Geometry for Test 6

FIG 20 Steep Slope of the Scour Hole in Test 6

FIG 21 Falling Clay Block in the Scour Hole for Test 6

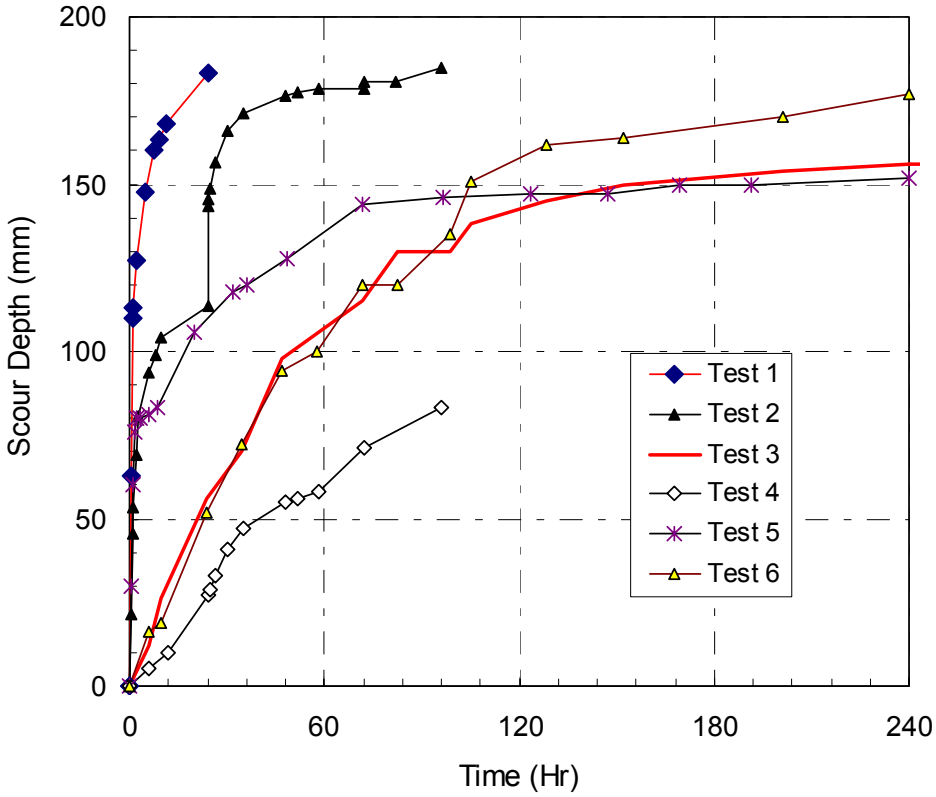

FIG 22 Comparison between Flume Test Results

Evaluation of Flume Test Results

The scour development curves are plotted in FIG 22 for all the 6 flume tests. Similarities exist among the flume tests, which can be used to check the validity of the flume tests.

Because the scour depth is a function of time, the final scour depth measured in the flume tests only represents the instantaneous scour depth when the test is stopped. A hyperbolic extrapolation model (Briaud et al, 1999) is used to predict the ultimate scour depth $Z_{max.}$ Examples of the hyperbolic regression fit are shown in FIG 23 and FIG 24 and the predicted ultimate scour depths are listed in Table 8. It can be seen that the order of the magnitude of the ultimate scour depth is: clay over sand > sand> clay >sand over clay.

Table 8 Instant scour depth Z and ultimate scour depth Z_{max} for the Flume Tests

Test No.	Test 1	Test 2	Test 3	Test 4	Test 5	Test 6
Z(mm)	183	185	161	83	152	177
Z_{max} (mm)	189	---	172	---	159	238

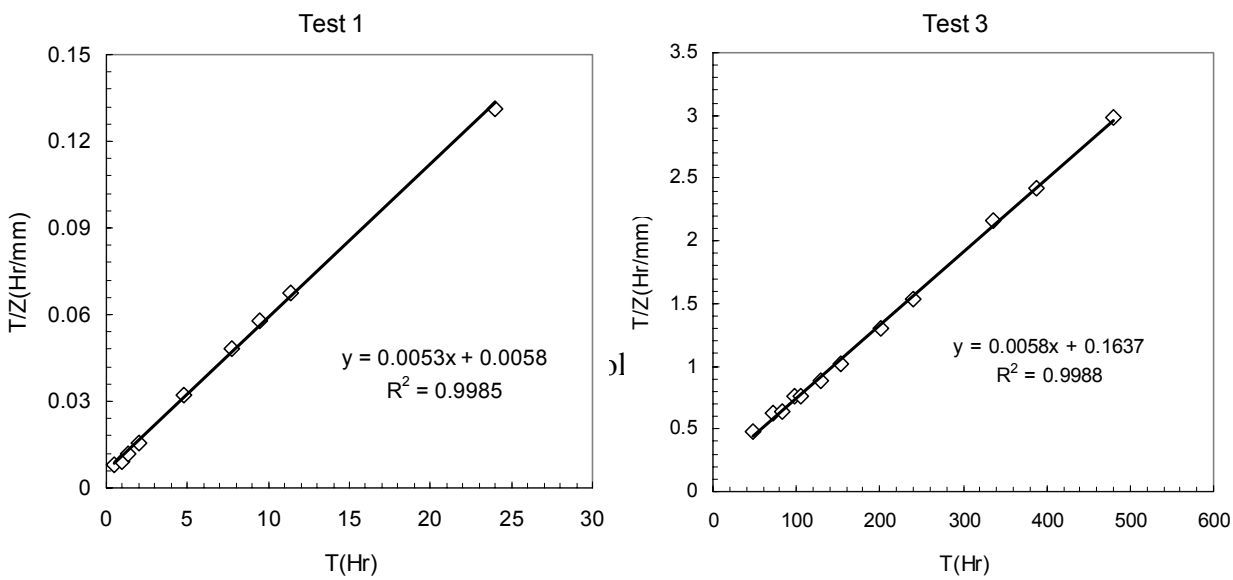

FIG 23 Linear Regression for Flume Test 1 3 by Hyperbola Model

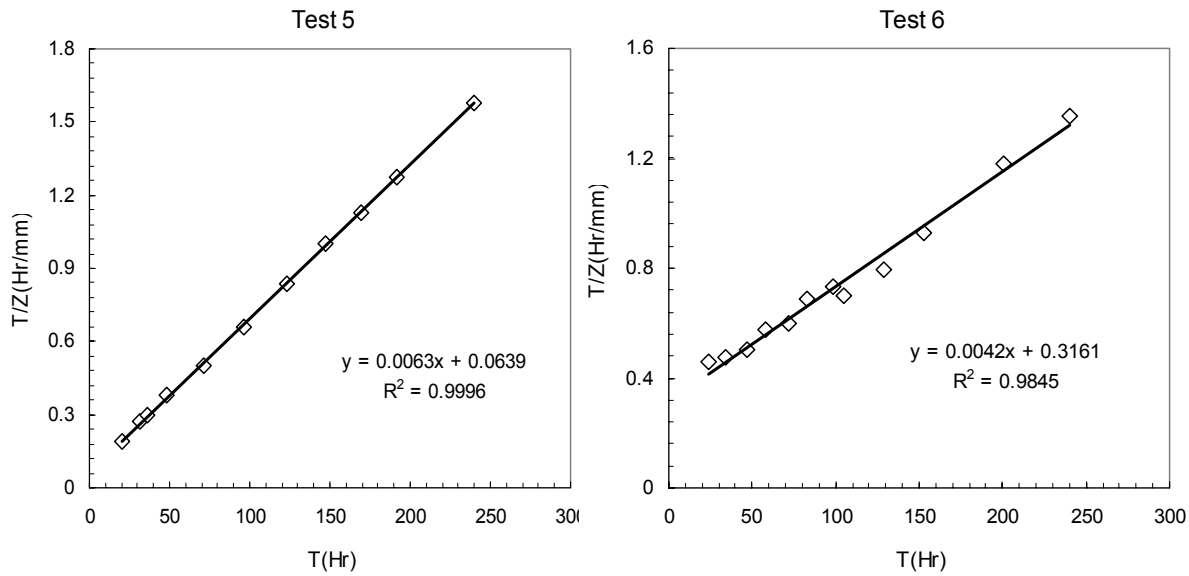

FIG 24 Linear Regression for Flume Test 5 6 by Hyperbola Model

REFERENCE:

1. Briaud, J.-L., Ting, F., Chen, H.C., Gudavalli, R., Perugu, S., Wei, G.S., "SRICOS: Prediction of Scour Rate in Cohesive Soils at Bridge Piers", ASCE Journal of Geotechnical Engineering, Vol 125, No.41999, pp.237-246.

Comparison Between Predictions and Measurements

Ya Li[1], Jun Wang[1], Wei Wang[1], Jean-Louis Briaud[1], Hamn-Ching Chen[1]

Results from Prediction Response

The Prediction Request lead to 5 responses, dealing with some or all 8 prediction cases. The prediction results are compared with the measurements from the flume tests or the field data in Table 1. The methods used by the predictors are described briefly in the following.

Table 1 Results from Prediction Response

Scour Case	Measurement	1	2	3	4	5
		Ferrando	Link	Piepers	Wu	Jia
Case 1 (mm)	183		150	230	182	323
Case 2 (mm)	185		170	233	205	
Case 3 (mm)	161			182.6		
Case 4 (mm)	83			109.2		
Case 5 (mm)	152			233.3		
Case 6 (mm)	177			281		
Case 7 (m)	7.1	10.72 (8/3/93 Flood)	10.06 (8/3/93 Flood)	7.3		
Case 8 (m)	1.25	5.42	1.76 (5/1/91 flood) 2.52 (500 years flood)	1.0-1.3		

Ferrando and Cian predicted Bridge Case 7 and 8 based on the HEC-18 equation for constant velocity. In the calculation, the scour depths for uniform cylindrical and non-uniform cylindrical pier cases are compared and the larger one is selected. Link and Zanke calculated the pier scour depth in non-cohesive soils by using a semi-empirical approach for hydrographic flood. In their approach, the maximum scour depth is calculated by HEC-18 equation and the time effect of scour development is evaluated by the method developed by Zanke. Piepers used Breussers's, Teramoto's and the SRICOS method separately to predict the scour depth; the largest value from the three methods is shown in Table 1. Wu and Wang conducted a numerical simulation by CCHE2D to predict the scour depth for Flume Case 1 and 2. Jia, Xu, and Wang conducted a numerical simulation by CCHE3D to predict the scour depth for Flume Case 1.

1. Dept. of Civil Engineering, Texas A&M Univ., College Station, TX 77843-3136

Results from Commonly Used Equation

Commonly used equations for pier scour are summarized in Table 2. The symbols used in the equations are defined in Table 3. The scour depth predicted by these equations is the ultimate scour depthfor a pier subjected to a constant velocity. The results are summarized in Table 4. For Bridge Case 7 and 8, the selected parameters are defined in Table 5, 6 and 7.

Table 3 Definitions of the Symbols Used in the Scour Equations

B:	Pier projection width
B1:	Approaching flow width
Comp:	Soil compact ratio
D_{50}:	Median diameter of the bed material
Fr:	Flow Froude Number directly upstream of the pier = $V/\sqrt{gH}$
Fr_c:	Critical Froude Number of the bed material = $V_c/\sqrt{gH}$
g:	Acceleration of gravity
H:	Flow depth directly upstream of the pier
IWC:	Initial water content
K:	Correction factors for specific conditions.
q:	Unit flow rate
Su	Undrained shear strengthof soil
V:	Mean velocity of flow directly upstream of the pier
V_c:	Critical velocity of the bed material
Z_{max}:	Ultimate scour depth
ρ_f:	Flow density
γ_s:	Unit weight of bed material

Table 4 Prediction Results from Commonly Used Equations

Equations	Case 1 (mm)	Case 2 (mm)	Case 3 (mm)	Case 4 (mm)	Case 5 (mm)	Case 6 (mm)	Case 7 (m)	Case 8 (m)	Case 8* (m)
6	539.2						26.2		
7	309.9						12.7	9.6	10.6
8	190.7						1.52	1.6	1.6
9	191.2						5.7	4.0	5.3
10	249.8						12.3	6.6	9.2
11	265.6						3.8	4.1	4.1
12	583.8						45.2	14.5	22.6
13	148						3.54	0.33	1.2
14	228.2						9.2	6.2	7.9
15	384						13.3	15	15
16	225.4						12.8		
17		51.4							
18		180.6							
19		125.3							
20	185.9	186	163.3	94.3	153.2	186.3	7.3	3.6	5.5
Measured	183	185	161	83	152	177	7.1	1.25	----

Table 2 Commonly Used Equation for Pier Scour

Number	Reference	Equation
6	Inglis (1949)	$\frac{Z_{\max}}{B} = 2.32 \cdot \left(\frac{q^{2/3}}{B}\right)^{0.78}$
7	Laursen and Toch (1956)	$\frac{Z_{\max}}{B} = 1.5\left(\frac{H}{B}\right)^{0.3}$
8	Basak, et al (1975)	$Z_{\max} = 0.558 \cdot B^{0.586} (meter)$
9	Shen, Schneider, and Karaki (1969)	$Z_{\max} = 0.00022 \cdot \mathrm{Re}^{0.619}$
10	Jain and Fisher (1979)	$\left\langle \begin{array}{l} Z_{\max} = 2.0B\left(Fr - Fr_c\right)^{0.25}\left(\frac{H}{B}\right)^{0.5} \\ Fr - Fr_c > 0.2 \end{array}\right.$ $\left\langle \begin{array}{l} Z_{\max} = 1.85B \times Fr_c^{0.25}\left(\frac{H}{B}\right)^{0.5} \\ Fr - Fr_c < 0 \end{array}\right.$
11	Larras (1963)	$Z_{\max} = 1.05 \cdot B^{0.75}$
12	Froehlich (1987)	$\frac{Z_{\max}}{H} = 0.32K_*\left(\frac{B'}{B}\right)^{0.62}\left(\frac{H}{B}\right)^{0.46} Fr^{0.2}\left(\frac{B}{D_{50}}\right)^{0.08} + 1$ $K_* = 1.0$ for round-nosed pier
13	Abdou (1993)	$Z_{\max} = 144.5H \times F_r^{3.47}$
14	HEC-18 (1996)	$\frac{Z_{\max}}{H} = 2.0K_1K_2K_3K_4\left(\frac{B}{H}\right)^{0.35} F_r^{0.43}$
15	Melville and Sutherland (1988)	$Z_{\max} = 2.4K_sK_\theta B$
16	Kothyari, Garde, et al (1992)	$\frac{Z_{\max}}{B} = 0.66\left(\frac{B}{D_{50}}\right)^{-0.25}\left(\frac{H}{B}\right)^{0.16}\left(\frac{V^2 - V_c^2}{D_{50} \times \left(\Delta\gamma_s / \rho_f\right)}\right)^{0.4}\left(\frac{B1 - B}{B1}\right)^{-0.3}$
17	Hosny (1995)	$Z_{\max} = 0.9B\left(IWC\right)^{-2/3} \cdot Fr^{3/2} \cdot Comp^{-2}$
18	Molinas *et al*. (1999)	$\frac{z_{\max}}{B^{0.66}H^{1.13}} = \begin{cases} 0 & \begin{pmatrix} Fr \le 0.2 \\ Comp \ge 0.85 \end{pmatrix} \\ 45.95\left(IWC\right)^{-0.36} Fr^{1.92}Comp^{1.62} & \begin{pmatrix} Fr \le 0.2 \\ Comp < 0.85 \\ Fr > 0.2 \end{pmatrix} \end{cases}$
19	Ivarson (1998)	$\frac{Z_{\max}}{H} = 2.0K_1K_2K_3K_4\left(\frac{B}{H}\right)^{0.35} F_r^{0.43}$ $K_4 = 0.677\log\left(500\frac{B}{S_u}\right)$
20	SRICOS-EFA	See details below

Table 5: Parameters for Bridge Case 7

Velocity (m/s)	2.43
Average Pier Width (m)	4.63
Average Pier Length (m)	13.41
Skew Angle (°)	4
Q (m^3/sec)	26561.2
Critical Velocity (m/s)	1.07
Water Depth (m)	22.52
Fr	0.163
Fr_c	0.072

Table 6: Parameters for Bridge Case 8 and for the 5/1/91 flood

Velocity (m/s)	1.2
Pier Width (m)	3.05
Equivalent Pier Length (m)	8.23
Skew Angle (°)	25
Q (m^3/sec)	1410.2
Vc (m/s)	0.66
Water Depth (m)	6.9
Fr	0.15
Frc	0.08

Table 7: Parameters for Bridge Case 8 and for the 500-year flood

Velocity (m/s)	1.9
Pier Width (m)	3.05
Equivalent Pier Length (m)	8.23
Skew Angle (°)	25
Q (m^3/sec)	4190.9
Vc (m/s)	0.7
Water Depth (m)	9.6
Fr	0.2
Frc	0.07

Result from SRICOS-EFA Method

The SRICOS-EFA method (Briaud, 2002) was developed at Texas A&M University on the basis of flume tests, numerical simulation, and laboratory testing of the soil erodibility. This method predicts the scour depth as a function of time for a given hydrograph. The maximum scour depth for pier scour is calculated by using an empirical equation based on flume test results:

$$Z_{\max}(m) = 0.00018 \cdot K \cdot \mathrm{Re}^{0.635}\,(\mathrm{m}) \tag{1}$$

Where Re is the pier Reynolds Number, and K denotes the correction factors for different pier installation cases. The scour depth is a function of the scouring time t, and for a constant velocity and a uniform soil, it is given by the Hyperbola model:

$$z(t) = \frac{t}{\dfrac{t}{Z_{\max}} + \dfrac{1}{\dot{z}_i}} \tag{2}$$

where $\dot{z}_i$ is the initial scour rate corresponding to the initial shear stress $\tau_{\max}$ when scour starts. The initial scour rate $\dot{z}_i$ is obtained from the erosion function of the bed soil (measured with the Erosion Function Apparatus (EFA)) at the value corresponding to the initial shear stress $\tau_{\max}$. The initial shear stress $\tau_{\max}$ is given by the following equation based on a series of numerical simulations:

$$\tau_{\max} = 0.094\rho V^2 \cdot k \cdot \left(\frac{1}{\log(\mathrm{Re})} - 0.1 \right) \tag{3}$$

where k represents the correction factors for shear stress caused by different pier installation cases.

For scour under a complex hydrograph and for a layered soil system, the scour depth vs. time curve can be calculated by accumulating the individual hyperbolas generated by incremental single floods and uniform soils. For more details on the SRICOS –EFA method refer to Briaud et al (1999, 2001a, 2002)

Based on the SRICOS-EFA method, the time histories of the scour development for the flume cases 3, 4, 5, and 6 are predicted in FIG 1, 2, 3 and 4 respectively. Because the maximum scour depth in sand can be developed in a very short time, the time histories for Case 1 and 2 are not presented here. For Bridge Case 7 and 8, because the EFA curves are not available, only the ultimate scour depths according to equation (1) are calculated with the parameters specified in Table 5-7. The scour depths given by SRICOS-EFA method are also listed in Table 4 on Line 14.

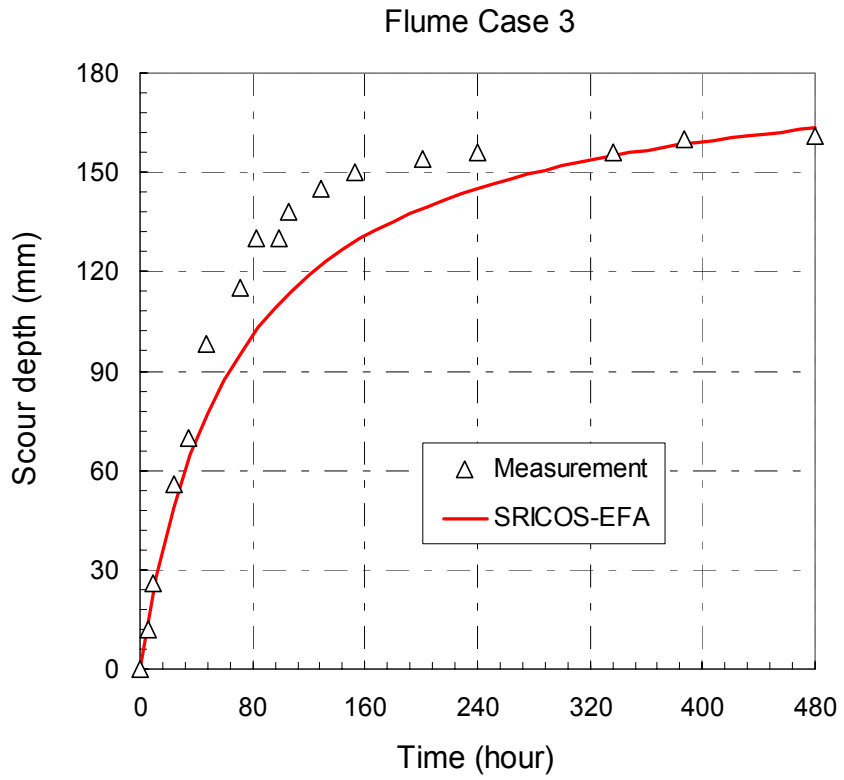

FIG 1 Comparison Between SRICOS –EFA Method and Measurement for Flume Case 3

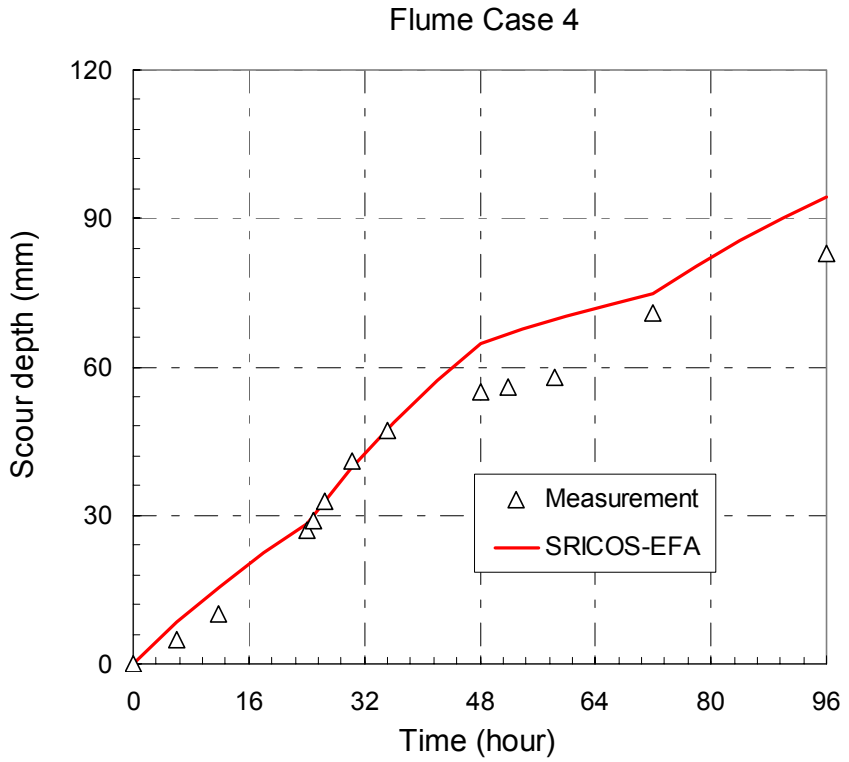

FIG 2 Comparison Between SRICOS –EFA Method and Measurement for Flume Case 4

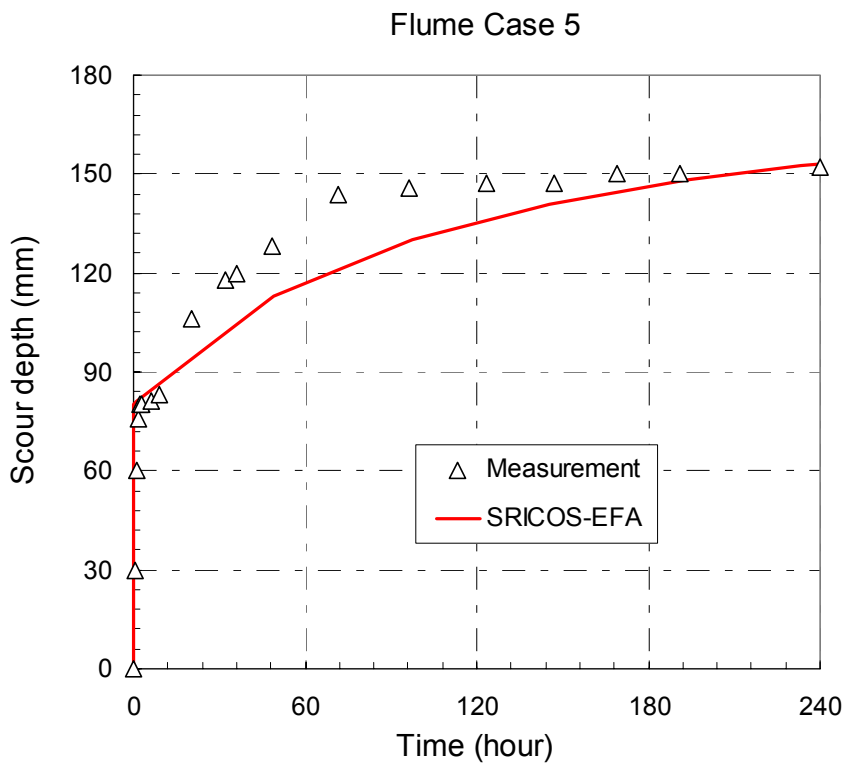

FIG 3 Comparison Between SRICOS –EFA Method and Measurement for Flume Case 5

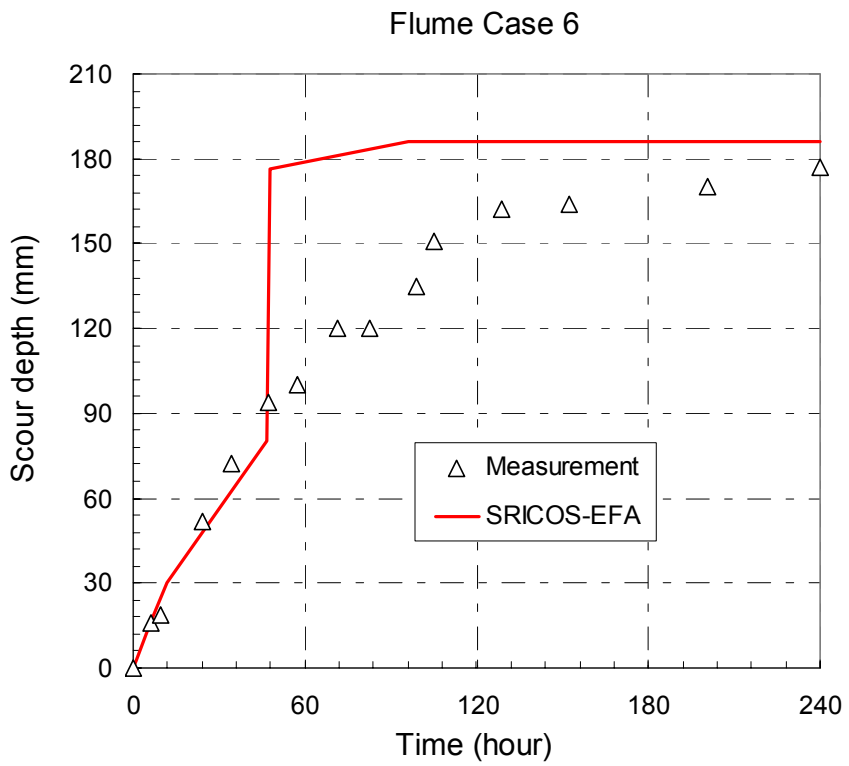

FIG 4 Comparison Between SRICOS –EFA Method and Measurement for Flume Case 6

Prediction Comparison and Conclusion

For comparison purposes, the 5 responses to the prediction request as well as the 15 predictions according to the equations of Table 2 are given in Tables 1 and 2. FIG 5-13 compare the measured scour depths and the predicted scour depths for the 20 methods. The following conclusions can be reached:

1. Pier scour in a uniform sand and subjected to a constant velocity can be well predicted by a variety of equations.
2. Only several approaches are available to handle pier installed in uniform sand but subjected to a changing velocity. The predictions by these approaches are satisfactory.
3. Very few approaches deal with pier scour developed in clay or layered soil systems and with the influence of time.
4. For the bridge case histories, when the case is limited to uniform sand and constant velocity, most predictions give a relatively conservative result.

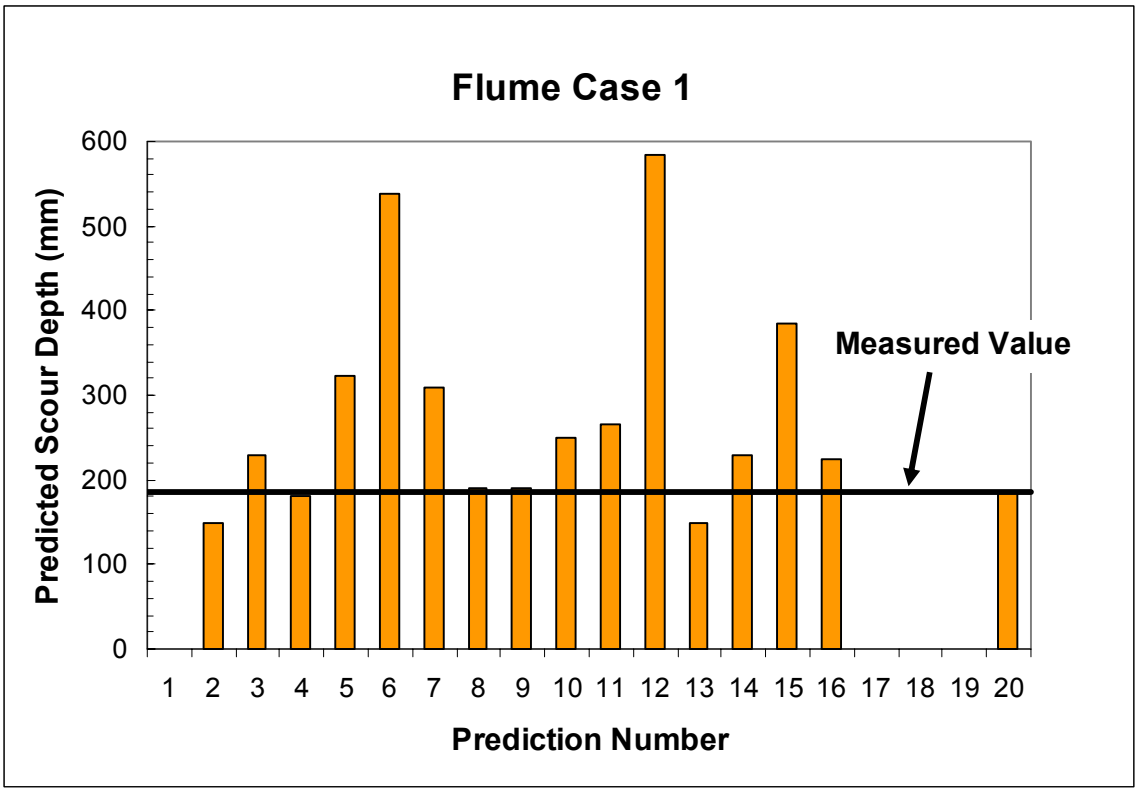

FIG 5 Comparison for Flume Test Case 1

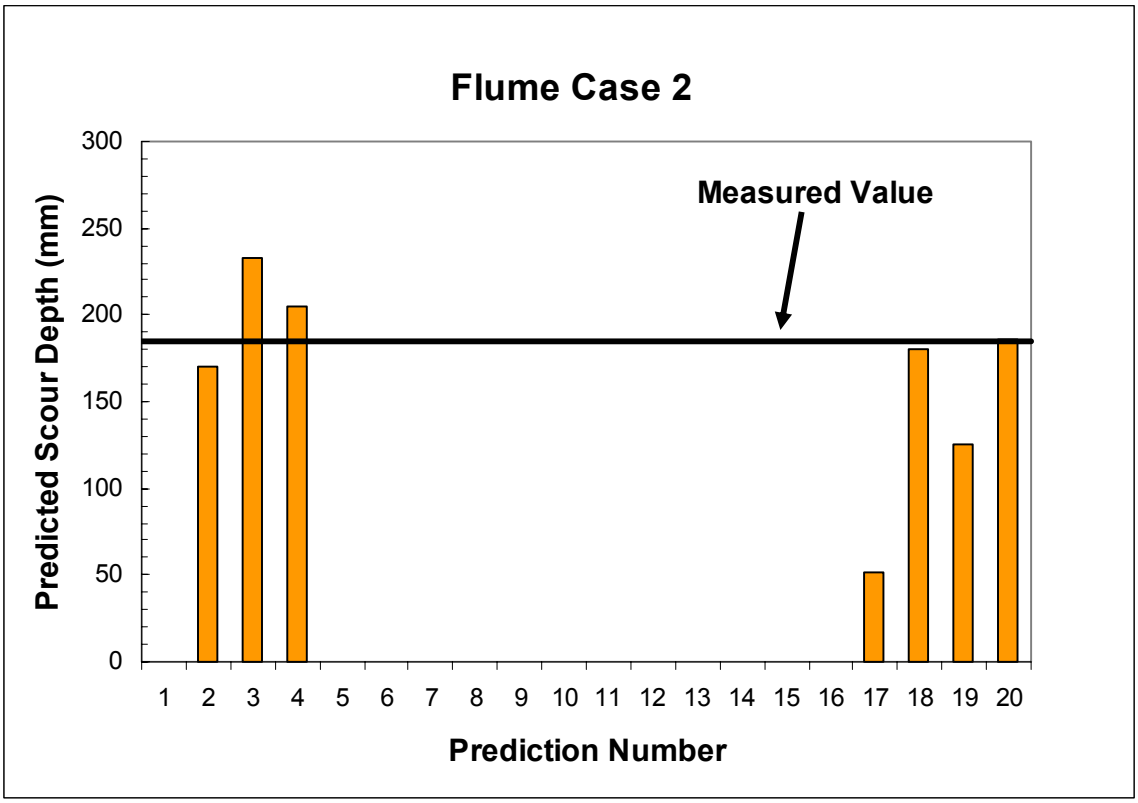

FIG 6 Comparison for Flume Test Case 2

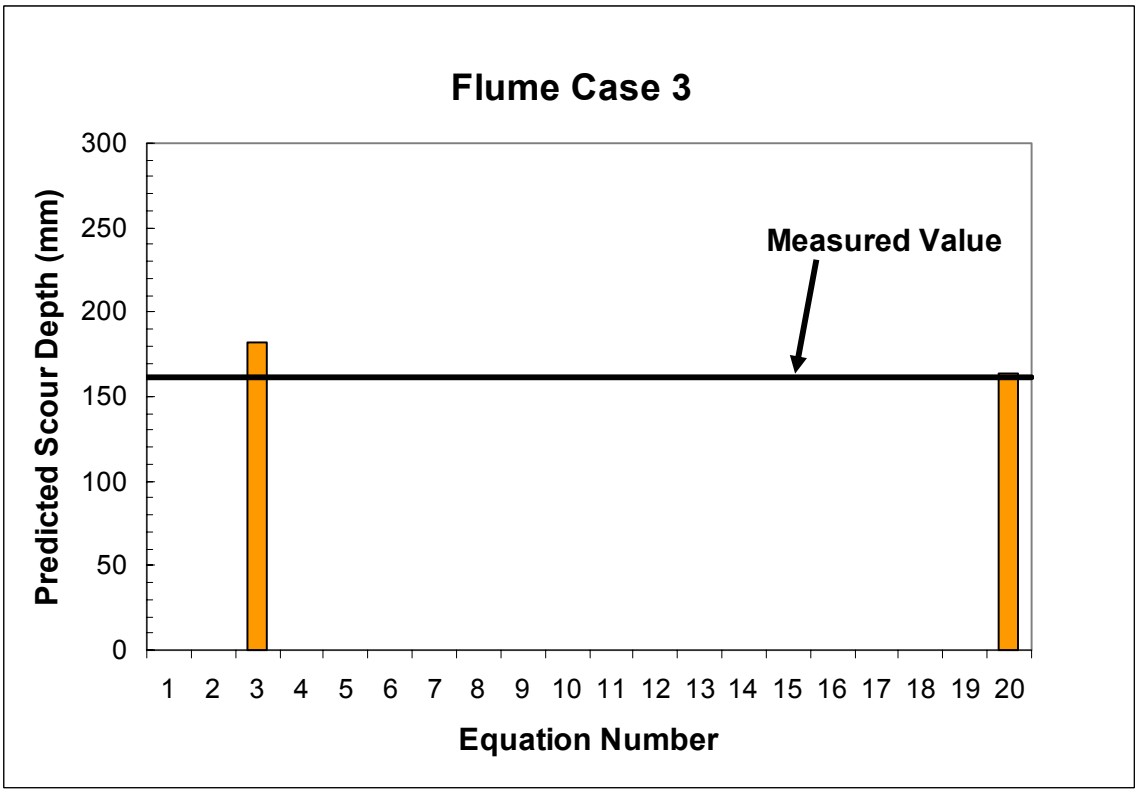

FIG 7 Comparison for Flume Test Case 3

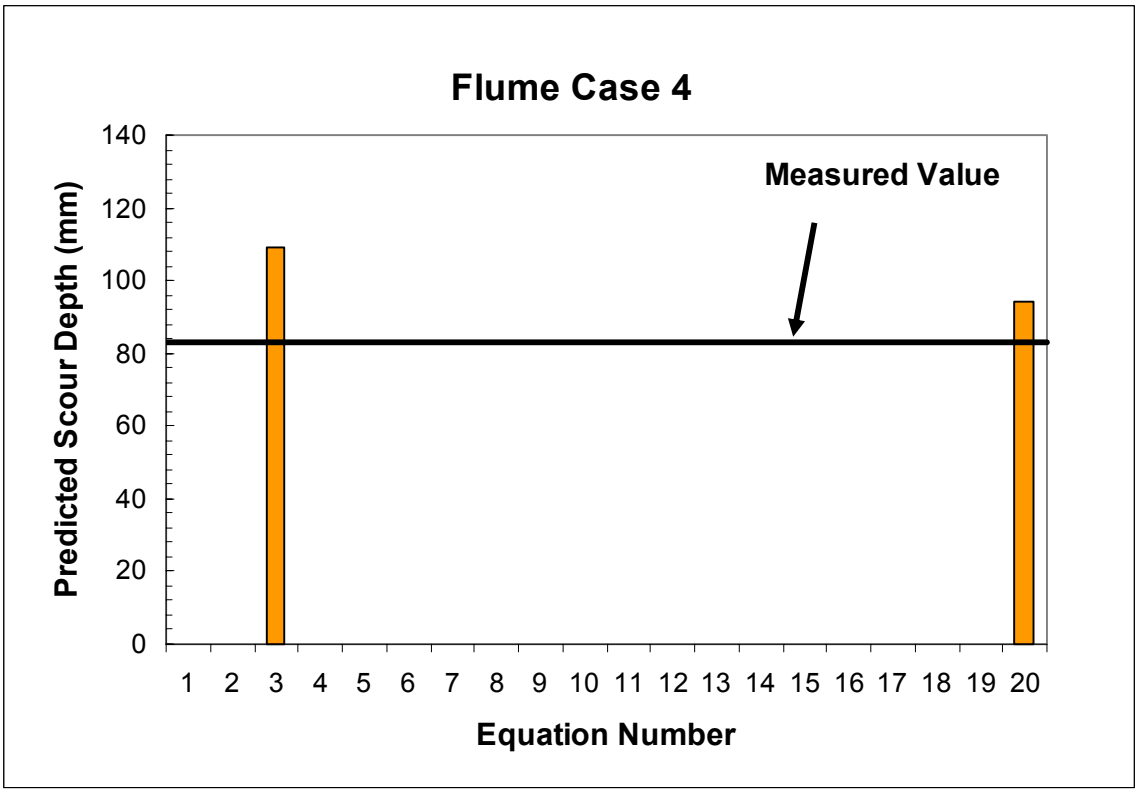

FIG 8 Comparison for Flume Test Case 4

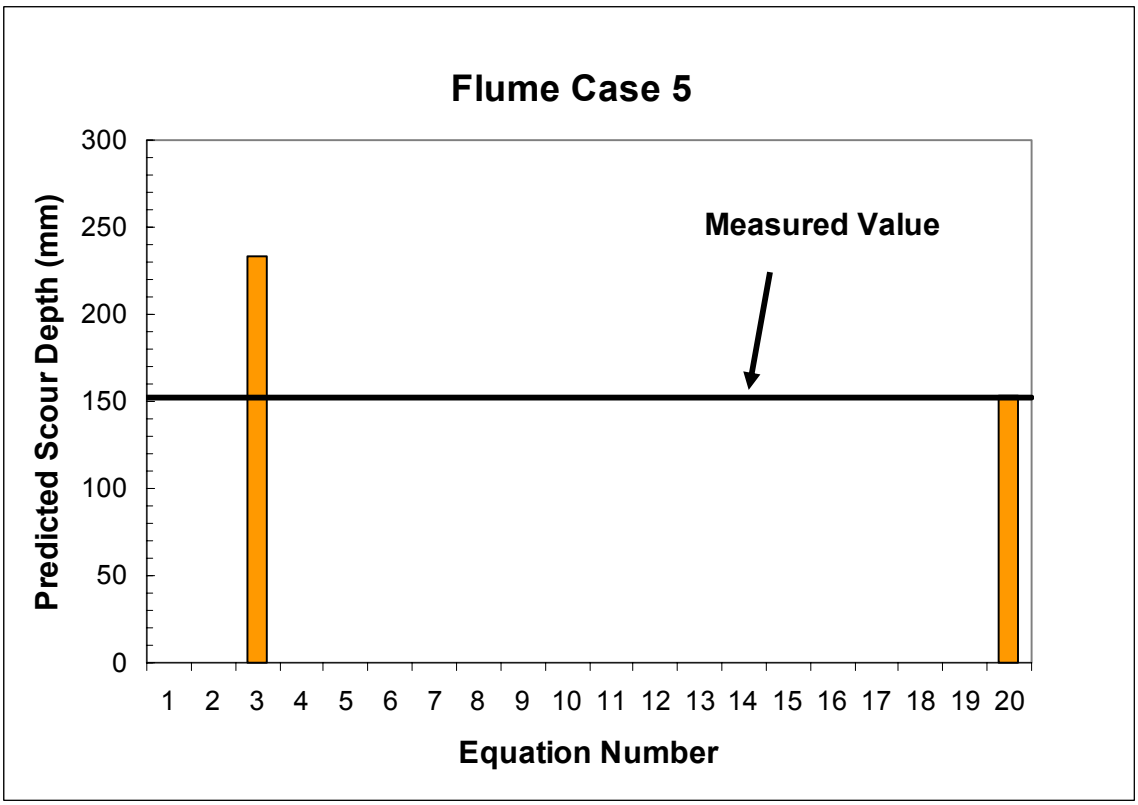

FIG 9 Comparison for Flume Test Case 5

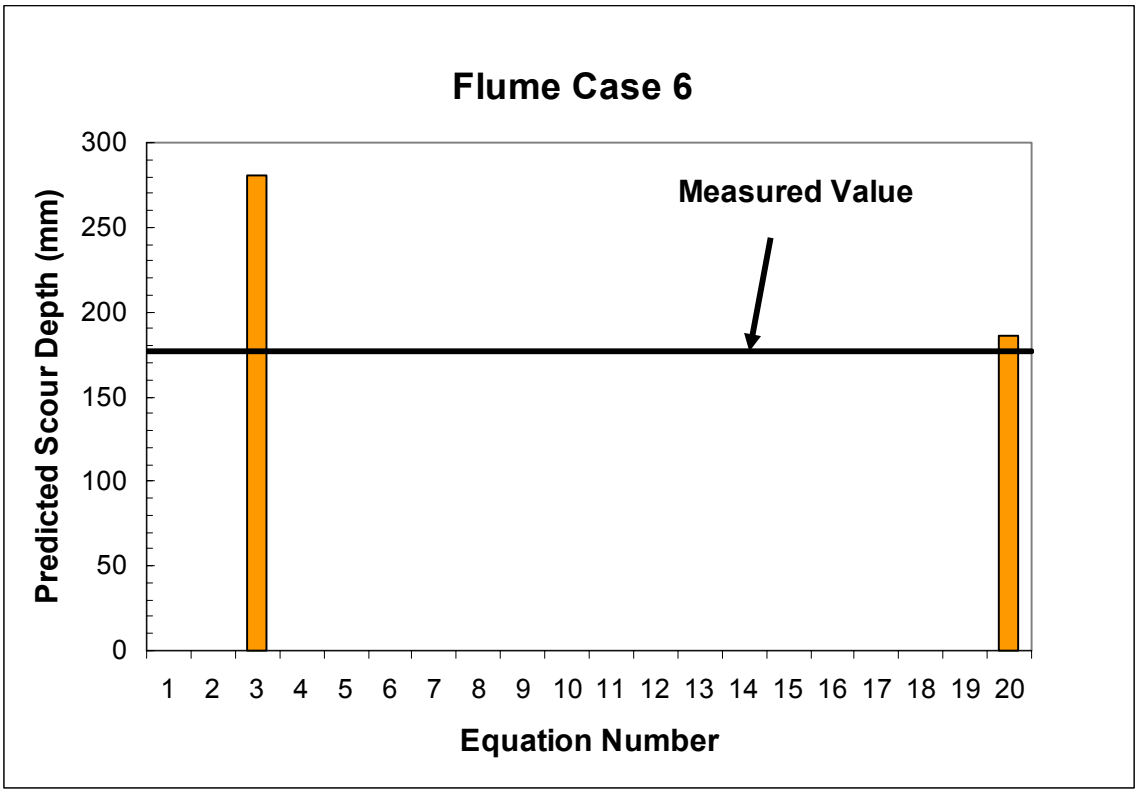

FIG 10 Comparison for Flume Test Case 6

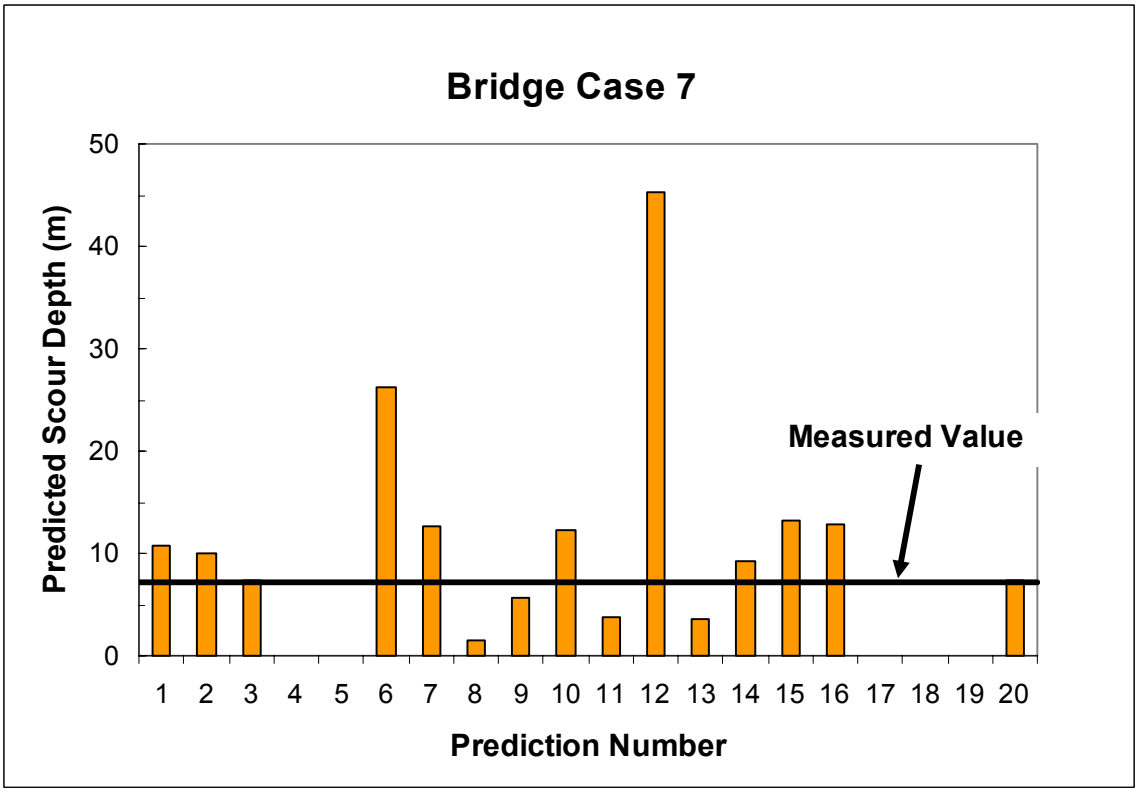

FIG 11 Comparison for Bridge Case 7

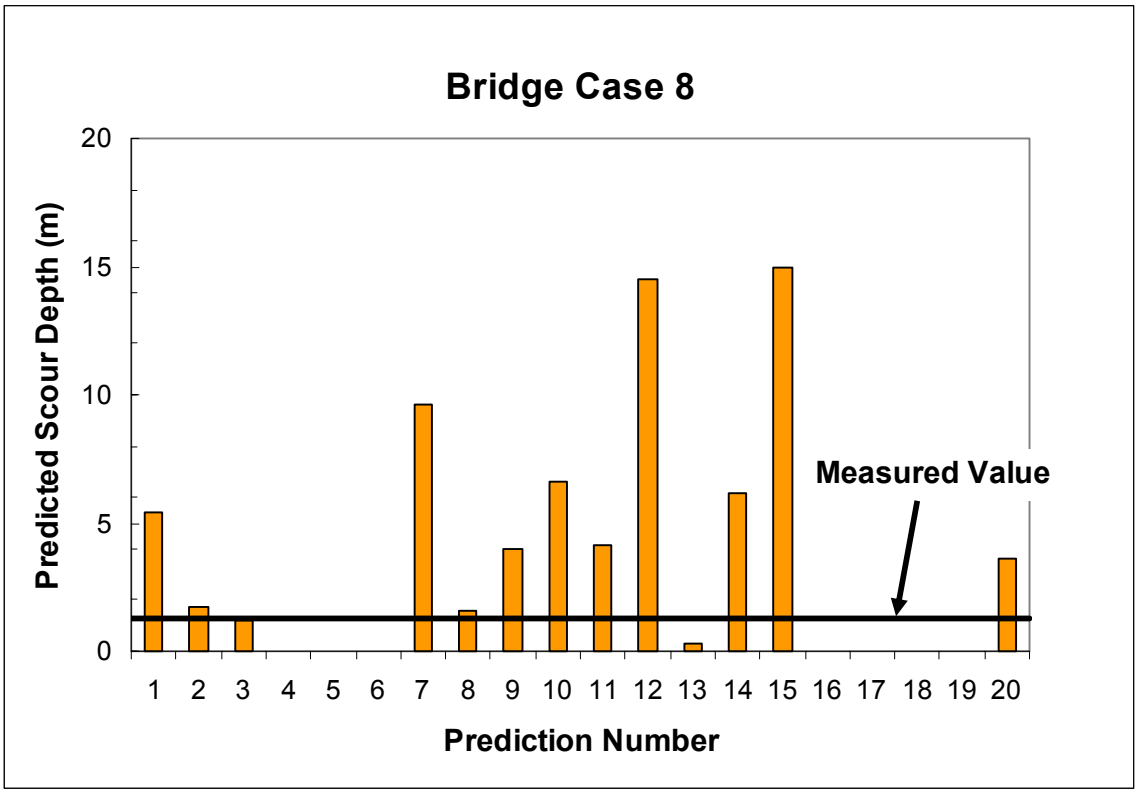

FIG 12 Comparison for Bridge Case 8 and the 5/1/91 Flood

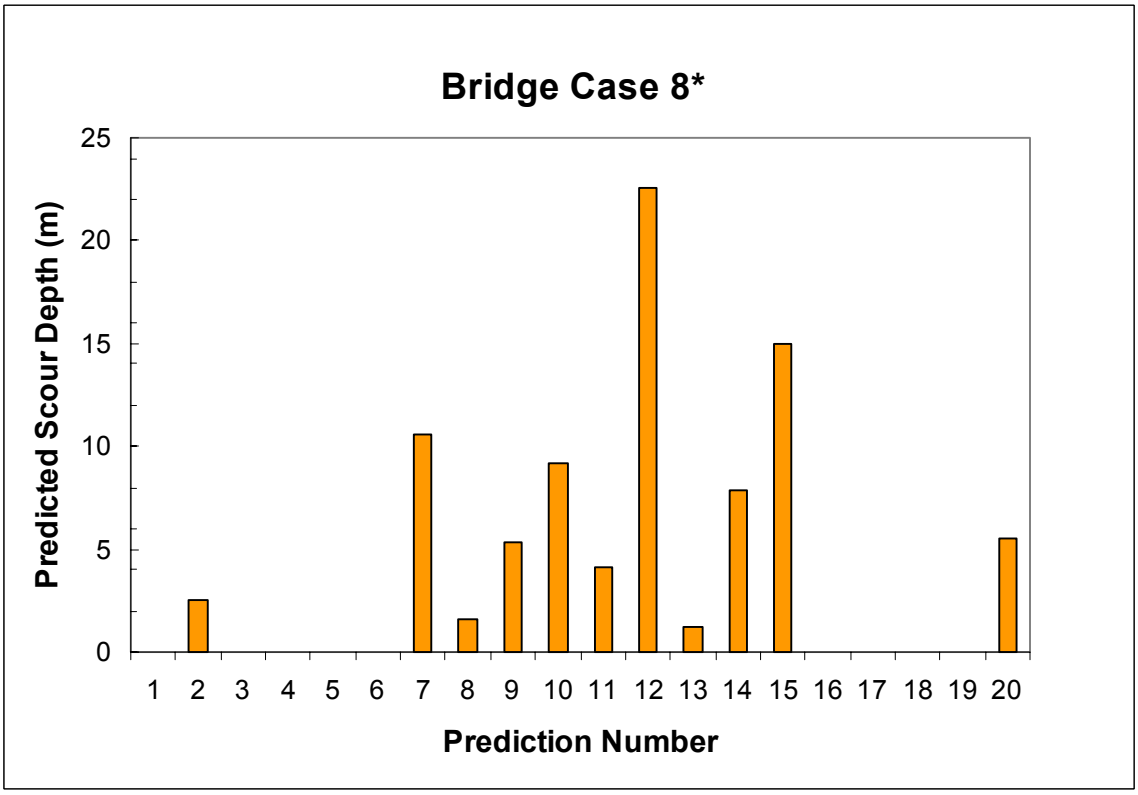

FIG 13 Comparison for Bridge Case 8 and the 500-Year Flood

REFERENCE:

1. Abdou, M.I., (1993), "Effect of sediment gradation and coarse material fraction on clear water scour around bridge piers", Ph.D. Dissertation, Civil Engineering Department, Colorado State University, Fort Collins, Co. USA.
2. Basak, V., Basamisli, Y., and Ergun, O., (1975), :Maximum equilibrium scour depth around liner-axis square cross-section pier groups", Report No. 583, Devlet su isteri genel mudurlugu, Ankara, Turkey (in Turkish).
3. Briaud, J.-L., (2002), "The SRICOS-EFA Method", Proceedings of the First International Conference on Scour of Foundations, Texas Transportation Institute, Texas A&M University System, College Station, Texas, USA.
4. Briaud, J.-L., Ting, F., Chen, H.C., Gudavalli, R., Perugu, S., Wei, G.S., "SRICOS: Prediction of Scour Rate in Cohesive Soils at Bridge Piers", ASCE Journal of Geotechnical Engineering, Vol 125, No.4, 1999, pp.237-246.
5. Briaud, J.-L., Ting, F., Chen, H.C., Cao, Y., Han, S.W., Kwak, K.W., "Erosion Function Apparatus for Scour Rate Predictions", ASCE Journal of Geotechnical Engineering, Vol 127, No.2, 2001a, pp.105-113.
6. Briaud, J.-L., Chen, H.C., Kwak K., Han, S.W., Ting, F.C.K., "Multiflood and Multilayer Method for Scour Rate Predictions at Bridge Piers", ASCE Journal of Geotechnical Engineering, Vol 127, No.2, 2001b, pp.105-113.
7. Froehlich, D.C., (1988), "Analysis of onsite measurements of scour at piers", Proc., National Hydraulic Engineering Conference, ASCE, Colorado Spring, Co., USA.
8. Hosny, H.M., (1995), "Experimental study of local scour around circular bridge piers in cohesive soils", Ph.D. Dissertation, Civil Engineering Department, Colorado State University, Fort Collins, Co. USA.
9. Inglis, C.C., (1949), "The behavior and control of rivers and channels", Research Publication No. 13, C.W.I.&N., Research Station, Poona, India.
10. Ivarson, W.R., (1998), "Scour and erosion in clay soils", ASCE Compendium of Conference Scour Papers (1991to 1998), Reston, VA, USA, 104-119.
11. Jain, S.C., and Fisher, E.E., (1979), "Scour around bridge piers at high Froude numbers", Rep. No. FHWA-RD-79-104, Federal Highway Administration, Washington D.C., USA.
12. Kothyari, U.C., Garde, R.J., and Ranga Raju, K.G., (1992), "Temporal variation of scour around bridge piers", Journal of the Hydraulics Division, ASCE, 118(8), 1091-1106.
13. Larras, J., (1963), "Profondeurs maximales d'erosion des fonds mobiles autour des piles de ponts", Proc. 14th IAHR Congress, Paris, France, 299-313 (in French).
14. Laursen, E.M., and Toch, A., (1956), " Scour around bridge piers and abutments", Bulletin No.4, Iowa Highway Research Board, Ames, IA, USA.
15. Melville, B.W., and Sutherland, A.J., (1988), 'Design method for local scour at bridge piers", Journal of the Hydraulics Division, ASCE, 114(10), 1210-1226.
16. Molinas, A., Jones, S., and Hosny, H.M., (1999), "Effect of cohesive material properties on local scour around piers", Transportation Research Board, 78th Annual Meeting, Washington D.C., USA.
17. Shen, H.W., Schneider, V.R., and Karaki, S., (1969), "Local scour around bridges piers", Proceedings, ASCE, 95(HY6), 1919-1940.

18. Sheppard, D.M, Zhao, G., and Ontowirjo, B., (1998), “Local scour near single piles in steady currents”, ASCE Compendium of Conference Scour Papers (1991to 1998), Reston, VA, USA, 371-376.

AUTHOR INDEX

Author	Page
Abghari, A.	684
Adams, J. P.	954
Alonso, C.	349, 734
Anglin, C. D.	582, 978
Annandale, G. W.	449
Awad, M. A.	471
Baig, S. M.	1111
Barkdoll, B.	734
Bermudez, H.	719
Bettencourt, B.	842
Bettess, R.	162
Bixler, M.	918
Boehm, D. W.	609
Bollaert, E.	449
Bos, K. J.	567
Bozo, L.	884
Briaud, J-L.	57, 156, 227, 242, 272, 373, 459, 1061, 1188, 1208
Cao, Y.	227, 459
Casado, J. M.	34
Chang, K-A.	869
Chen, H-C.	14, 156, 242, 373, 459, 1061, 1188,1208
Cheng, L.	175
Chiew, Y-M.	70, 707
Chin, C-O.	968
Chiu, P-H.	869
Choi, S-U.	206
Chung, M-K.	227
Cian, C.	1152,1155
Coleman, S.	749
Curry, J. E.	292
D'Odorico, P.	272
Davies, E. B.	1019
Davis, S.	227
Dennett, K. E.	642, 1008
Dhiman, R. K.	560, 896
Di Stasi, J. M.	516
Ding, D.	540
Dumas, C. E.	112
Edelmann, J.	842
Edgers, L.	842
Escarameia, M.	320
Ettema, R.	364, 383, 734
Farrag, K.	283
Ferrando, G.	1152, 1155
Fredsoe, J.	795
Fricthel, P.	642, 1008
Fukui, J.	47, 410
Gardner, R. W.	623
Guven, O.	292
Hager, W. H.	774
Heibaum, M. H.	1
Ho, C. L.	516
Ho, T-C.	869
Hoe, D.	749
Hoffmans, G.	92
Huessin, M.	918
Hunt, B.	227
Islam, M. S.	684
Itamunoala, F.	582
Jeon, E. J.	272
Jeong, S.	854
Jia, Y.	349, 1181
Johnson, P. A.	678
Jones, J. S.	140, 485, 810
Jung, B-S.	437
Kajima, R.	421
Kandaris, P. M.	954
Kanno, Y.	307
Kant, G.	567, 656
Khan, M. A.	1111
Kim, H.	437
Kirshen, P.	842
Kitsunai, S.	910
Kobayashi, N.	910
Kondziolka, R. E.	954
Krolack, J.	112
Kruisbrink, A. C. H.	567
Kuhnle, R.	349, 734
Kumar, A. V.	500
Kusakabe, O.	1081
Kwak, K.	227
Lachhab, A.	364
Lagasse, P.	1051
Lauchlan, C.	184
Lewandowski, E.	842
Li, W.	968

Author	Page
Li, Y.	156, 242, 373, 459, 1188, 1208
Lim, S-Y.	395, 785
Lin, C.	869
Lindo, M. H.	656
Lindsey, W. B.	699
Link, O.	1160
Lopardo, M. C.	34
Lopardo, R. A.	34
Maeno, S.	218
Martinez, E.	364
Masahiko, S.	337
May, R. W. P.	184, 320
McDonald, J. A.	1019
Melville, B.	120, 734, 749
Melville, J. G.	292
Mercado, E. J.	1019
Mia, F.	218
Michelsen, J.	795
Millen, G.	582
Miller, Jr., W.	827
Mishra, S. K.	699
Mohapatra, D. K.	560
Molinas, A.	485
Morvant, M.	283
Muceku, Y.	884
Mueller, D. S.	257, 1096
Muraishi, H.	337
Murakami, S.	307
Nago, H.	218
Nairn, R. B.	978
Nakajima, D.	337
Nakato, T.	528
Neelamani, S.	500
Nevels, Jr., J. B.	764
Ng, S.	1042
Nishimura, T.	1081
Nishitani, M.	47
Nurtjahyo, P.	156, 242, 373, 459
O'Neill, M. W.	1019
Ogihara, K.	337
Oh, B. C.	437
Oliveto, G.	774
Olson, L. D.	929
Otuka, M.	410
Pagan-Ortiz, J. E.	636
Parchure, T.	734
Park, S.	1061
Parola, A.	734
Percher, M.	842
Phillips, R.	719
Piepers , T	1166
Price, G. R.	1032
Punrattanasin, P.	1081
Rao, S. N.	500
Rausche, F.	918
Razdan, K. K.	896
Rees, P.	516
Richards, D. L.	670
Richardson, E. V.	810, 993
Roulund, A.	795
Sainz, J. A.	597
Sakakiyama, T.	421
Salgado, R.	597
Sassa., S.	546
Schaefer, K. J.	623
Schall, J. D.	1032
Schleiss, A.	449
Sheppard, D. M.	198, 810, 827
Shimamura, M.	910, 945
Siddharthan, R.	642, 1008
Singh, R.	896
Soltani, A.	642, 1008
Spaan, G. B. H.	656
Spitz, W.	1051
Subjarassang, A.	1081
Suh, J.	854
Sultan, N.	719
Sumer, B. M.	795
Suzuki, H.	945
Tan, S-K.	785
Unger, J.	774
Verheij, H. J.	92, 567
Wagner, C. R.	257, 1096
Wang , S. Y	1176, 1181
Wang, J.	156, 242, 373, 459, 1188, 1208
Wang, W.	1188, 1208
Won, J.	854
Wu, Z.	307
Wu,W.	1176
Xu, Y.	1181
Yang, W.	206
Yasuhara, K.	307
Youn, S-Z	437
Yu, G.	395, 785
Zanke, U.	1160
Zarriello, J. J.	1111
Zevenbergen, L.	1051
Zha, J.	684
Zhang, L.	540
Zhou, W.	540